2008

ENDOTHELIAL CELL DYSFUNCTION BY ENVIRONMENTAL CONTAMINANTS

Elizabeth Grace Oesterling
University of Kentucky, bethoesterling@uky.edu

ABSTRACT OF DISSERTATION

Elizabeth Oesterling

The Graduate School

University of Kentucky

2008

ENDOTHELIAL CELL DYSFUNCTION BY ENVIRONMENTAL CONTAMINANTS

ABSTRACT OF DISSERTATION

A dissertation submitted in partial fulfillment of the
requirements for the degree of Doctor of Philosophy in the
College of Medicine, Graduate Center for Toxicology
at the University of Kentucky

By

Elizabeth Grace Oesterling

Lexington, Kentucky

Director: Dr. Bernhard Hennig, Professor of Animal Sciences

Lexington, Kentucky

2008

ABSTRACT OF DISSERTATION

ENDOTHELIAL CELL DYSFUNCTION BY ENVIRONMENTAL CONTAMINANTS

Within the last few decades, epidemiological evidence has linked exposure to air pollution, both its particles and its organic components, with cardiovascular disease (CVD) progression. CVD is a life long disease with the disruption of the endothelium being the inaugural event in this inflammatory process. The vascular endothelium is extremely susceptible to environmental insults given its tremendous surface area and that it is in constant contact with blood and components circulating within the blood, including xenobiotics. The endothelium is important as a barrier from blood constituents however, dysfunction of this barrier leads to the influx of lymphocytes and granulocytes that lead to the fatty build-up characteristic of atherosclerosis.

The studies presented in this dissertation tested the hypothesis that two unique environmental contaminants, alumina nanoparticles and benzo[a]pyrene (B[a]P), lead to increased endothelial cell dysfunction, characterized by increased adhesion molecule expression. Alumina nanoparticles induced vascular cell adhesion molecule-1 (VCAM-1), intercellular adhesion molecule-1 (ICAM-1), and E-selectin (ELAM-1), as well as increased monocyte adhesion to activated endothelium. Polystyrene nanoparticles did not elicit this response. B[a]P induced ICAM-1 expression, but only after toxification by aryl hydrocarbon receptor (AhR) controlled enzymes. Silencing of either AhR or the membrane microdomains called caveolae attenuated the B[a]P-induced ICAM-1 response. It was also shown that the induction of ICAM-1 occurred by signaling through MEK, p-38 MAPK, and activator protein-1 (AP-1). These data provide a novel mechanism by which air pollutants like B[a]P may cause increased atherosclerosis and describe a new toxicant, alumina nanoparticles, as a possible threat for the development of inflammatory diseases, such as atherosclerosis.

Little is known about dietary interventions capable of alleviating xenobiotic-induced toxicity. Nutrition is an obtainable and inexpensive means of possible preventative therapy. With this in mind, it was also hypothesized that plant polyphenols, such as flavonoids, can down-regulate B[a]P-induced ICAM-1. Selective flavonoids, containing both a 4’ B-ring hydroxyl

substitution and a 2-3 C-ring double bond, protected against B[a]P-induced ICAM-1 activation, however this protection did not correlate with the flavonoid's antioxidant capacity.

KEYWORDS: manufactured nanoparticles; endothelium; adhesion molecules; cardiovascular disease; polycyclic aromatic hydrocarbons

ENDOTHELIAL CELL DYSFUNCTION BY ENVIRONMENTAL CONTAMINANTS

By

Elizabeth Grace Oesterling

Bernhard Hennig

Director of Dissertation

David K. Orren

Director of Graduate Studies

7/17/2008

Date

RULES FOR THE USE OF DISSERTATIONS

Unpublished dissertations submitted for the Doctor's degree and deposited in the University of Kentucky Library are as a rule open for inspection, but are to be used only with due regard to the rights of the authors. Bibliographical references may be noted, but quotations or summaries of parts may be published only with the permission of the author, and with the usual scholarly acknowledgements.

Extensive copying or publication of the dissertation in whole or in part also requires the consent of the Dean of the Graduate School of the University of Kentucky.

A library that borrows this dissertation for use by its patrons is expected to secure the signature of each user.

Name	Date

DISSERTATION

Elizabeth Grace Oesterling

The Graduate School
University of Kentucky
2008

ENDOTHELIAL CELL DYSFUNCTION BY ENVIRONMENTAL CONTAMINANTS

DISSERTATION

A dissertation submitted in partial fulfillment of the
requirements for the degree of Doctor of Philosophy in the
College of Medicine, Graduate Center for Toxicology
at the University of Kentucky

By

Elizabeth Grace Oesterling

Lexington, Kentucky

Director: Dr. Bernhard Hennig, Professor of Animal Sciences

Lexington, Kentucky

2008

ACKNOWLEDGMENTS

The following dissertation, while an individual work, benefited from the insights, direction, and support of several people. First, I would like to thank my mentor, Dr. Bernhard Hennig, for his acceptance of me into his laboratory and the consequences of that decision for the next four years. He has taught me to be a better investigator and better communicator. He has pushed me to be independent and yet still a team player. He has allowed me the opportunity to travel to conferences and meet other scientists, domestic and internationally. This dissertation would not be possible without his support.

I would also like to thank the other members of my committee, Dr. Mary Vore, Dr. Michal Toborek, and Dr. Daniel Noonan, for their continued comments and encouragement over this period of study. I would also like to thank Dr. Ming Gong, my outside examiner, who was willing to take this extra responsibility. I appreciate all of their time and energy put into making this the finest dissertation possible and me the finest investigator possible.

No projects are conducted in a vacuum. I would like to thank the members of my laboratory for their continued conversation and suggestions. Thanks to Dr. Gudrun Reiterer, Dr. Lei Wang, Dr. Xabier Arzuaga, Dr. Huiyun Shen, Zuzana Majkova, YuanYuan Zheng, Dr. Yean Jung Choi, Dr. Eun Jin Lim, and Dr. Sung Gu Han. Also, thank you to the members of the Toborek laboratory for their assistance, especially Dr. Sung Yung Eum. Thank you to Dr. Leonidas Bachas for his nanoparticle expertise and directions. Also

thank you to Dr. Nitin Chopra for his help with the nanoparticle characterization. Thank you to Dr. Thomas Curry for walking me down to Labor & Delivery dozens of times to obtain human umbilical cords. Thank you to the Flow Cytometry Core Facility for their swift analysis of my data and troubleshooting along the way.

I would like to thank the organizations that made funding for these projects possible: the American Heart Association (0613216B), the NIEHS Toxicology Department Training Grant (T32ES07266), the NIEHS Superfund Basic Research Program (P42ES07380), and the University of Kentucky.

Finally, I would like to thank my family, especially my mother, my father, Chris and Phil, for their continued support. I am who I am because of them. They taught me to strive to be the best, while having a good time along the way. They instilled in me a love for science and the determination to work towards a goal. They have allowed me to be who I want to be and make mistakes along the way. Thank you for all you have done. I love you very much.

TABLE OF CONTENTS

LIST OF TABLES

LIST OF FIGURES

LIST OF FILES

Chapter One. Introduction

Cardiovascular disease is currently the leading cause of death worldwide, accounting for 12% of all global deaths, and is projected to maintain this status through the year 2030 [1]. Atherosclerosis, leading to heart attack and stroke, has been attributed to cause approximately 75% of these deaths [2]. Atherosclerosis is a progressive disease of the vasculature, which initiates in the first decade of life [3]. It is characterized by the accumulation of lipids and fibrous elements in the large arteries. Initially, atherosclerosis was thought to be a lipid disease based largely on the correlation between hypercholesterolemia and atheroma formation [4]. However, only 50% of patients with atherosclerosis actually manifest hyperlipidemia. More recently, focus has changed to the role of inflammation in atherosclerosis [5, 6]. Inflammatory cells, such as monocytes and lymphocytes, are recruited to the site of disease by inflammatory mediators such as cytokines and chemokines. These cells form a chronic inflammatory state by interacting with modified lipoproteins thus converting into factories for cytokine release [7].

Disruption of the endothelial homeostasis is still considered the initiating event in the development of atherosclerosis. Endothelial cells form the interior lining of the arterial wall, protecting the vessel from circulating factors. The endothelium plays a number of regulatory roles that maintain vascular hemodynamics, vascular remodeling, inflammation, growth, and anti-thrombogenic processes [8]. The definition presented as to its dysfunction demonstrates the shear number of critical roles the endothelium plays. Endothelial cell dysfunction is characterized by "disturbances in the barrier function of the vascular endothelium; its impaired anti-thrombogenic properties; perturbed angiogenic competence; inappropriate regulation of vascular smooth muscle tonicity, proliferative capacity, and migratory properties; and perturbed synthetic function and deterrence of neutrophils and monocytes from diapedesis" [8]. More concisely, the four main elements include: adhesiveness, permeability, proliferation, and thrombogenesis.

Under normal physiological conditions, the vascular endothelium resists adherence to circulating immune effector cells. However, after insult or injury endothelial cells up-regulate various adhesion molecules, such as intercellular adhesion molecule-1 (ICAM-1, CD54), vascular cellular adhesion molecule-1 (VCAM-1, CD106), and platelet-endothelial cell adhesion molecule-1 (PECAM-1, CD31), integrins, and L, E, and P-selectins. These molecules are responsible for leukocyte recruitment and trafficking through vessels during periods of inflammation. Their recruitment serves as a protective means of clearing cytotoxic and pro-inflammatory oxidized

low density lipoproteins (oxLDL) and apoptotic cells, however their accumulation and differentiation eventually leads to development of atherosclerotic lesions. Monocytes are attracted to the endothelium by chemokines such as monocyte chemotactic protein-1 (MCP-1), which is released by activated endothelial cells [9, 10]. MCP-1 is localized to macrophage rich areas of atherosclerotic plaques [11]. Deletion of this chemokine reduces development of atherosclerosis in hyperlipidemic mice [12, 13].

Initially, the selectins bind sialylated and fucosylated carbohydrate ligands presented on immune cells, thus mediating initial tethering and rolling along the endothelium. E-selectin binds CD44, P-selectin glycoprotein ligand-1 (PSGL-1), and E-selectin ligand-1 (ESL-1) on myeloid cells such as monocytes and neutrophils and CD43 on T-helper 1 lymphocytes [14]. E-selectin is inducible by a number of inflammatory mediators such as tumor necrosis factor-α (TNF-α) [15], interferon-γ [16], and interleukin-1 [17]. E-selectin was shown to be present in endothelial cells of both fibrous and lipid-containing human atherosclerotic plaques [18]. Mice lacking both P- and E-selectins develop delayed onset, smaller, and less calcified lesions in a hyperlipidemic environment [19]. A human polymorphism has been discovered in the E-selectin gene that leads to an increased risk for the development of atherosclerosis, again linking the selectin with the disease [20]. The interaction of selectins with their ligands triggers tighter adhesion via integrin-adhesion molecule binding and clustering.

Integrins are cell-surface receptors expressed on immune cells and form αβ heterodimers. The main integrins participating in leukocyte tight binding are β_2 and α_4 integrins, namely LFA-1 (CD11a/CD18 or $\alpha_L\beta_2$), Mac-1 (CD11b/CD18, or $\alpha_M\beta_2$), and VLA-4 (CD49d/CD29 or $\alpha_4\beta_1$). Knockdown of CD18, the β_2 integrin, leads to decreased lesion formation in mice fed an atherogenic diet [21]. Also, neutralizing monoclonal antibodies against the integrin VLA-4 or the α_4 subunit has been shown to decrease neutrophil and macrophage recruitment to the vessel wall [22, 23]. LFA-1 and Mac-1 bind ICAM-1 and -2 [24, 25], while VLA-4 binds VCAM-1 [26].

VCAM-1 and ICAM-1 are both members of the immunoglobulin (Ig) supergene family of proteins, since they contain more than one common Ig-like sequence repeat characterized by two cysteines separated by 55 to 75 amino acids [27]. ICAM-1 contains five Ig-like domains, while VCAM-1 contains six or seven [28]. VCAM-1 was the first adhesion molecule implicated in having a role in macrophage recruitment to the endothelium. VCAM-1 was found in areas of early lesion formation and expressed on the surface of activated endothelium in atherogenic rabbit models [29]. Likewise, increased expression of VCAM-1 and ICAM-1 was seen in

endothelial cells of human plaques, similar to E-selectin [18]. The deletion of VCAM-1 is embryonically lethal, however deletion of the fourth Ig domain, which is responsible for integrin binding, is viable and reduces VCAM-1 mRNA and protein to 2-8% of controls [30]. These mice, when crossed on a hyperlipidemic mouse background, had significantly reduced early atherosclerotic lesion area compared to wild-type controls. Heterozygous VCAM-1-domain four deficient mice had an intermediate, yet still markedly reduced arterial VCAM-1 expression, monocyte adherence in the aortic root, and fatty streak formation [31]. Antibodies have been used to block both VCAM-1 and ICAM-1 in mouse endothelia. Blocking of either adhesion molecule causes decreased monocyte rolling velocity, homing, and adhesion of macrophages to the endothelium [23, 32]. ICAM-1 deficient animals are viable, and when fed an atherogenic diet, these mice have a reduction in aortic lesion size, similar to VCAM-1 and E-selectin [21]. Clearly, the selectins, integrins, and adhesion molecules lead to monocyte recruitment and attachment to the endothelial vessel layer.

The endothelium also plays a part in the transendothelial migration, or diapedesis, of the leukocytes through the endothelial monolayer to the intimal layer of the vessel [33]. Endothelial release of chemokines, such as MCP-1, not only recruits monocytes to the endothelium, but also recruits leukocytes into the arterial intima. Evidence has been presented that leukocytes not only migrate through endothelial junctions (paracellularly), but also can migrate in non-junctional locations (transcellularly) [34-36]. Leukocytes actively migrate to the intimal layer of the vessel in an amoeboid fashion through transmigratory cup structures. The adhesion molecules ICAM-1 and VCAM-1 form docking structures enriched with F-actin, moesin and ezrin, and actin binding proteins, which surround adherent leukocytes [34, 37, 38]. The integrins are interconnected to actin filaments by adaptor proteins such as talin [38]. After binding of adhesion molecules to integrins, there is a rapid cytoskeletal remodeling, leading to a transient uncoupling of integrins from the actin cytoskeleton, which induces clustering. It has been shown that ICAM-1 forms ring-like structures that colocalize with LFA-1 at the site of leukocyte migration [39].

Once the monocytes enter the interstitum, they undergo a series of changes causing them to differentiate into macrophages. Growth factors, such as macrophage colony-stimulating factor (M-CSF) and granulocyte-macrophage colony-stimulating factor (GM-CSF), aid in the transition from monocyte to macrophage. Mice that lack M-CSF are deficient in tissue macrophages, revealing the need for monocyte differentiation in tissue migration [40]. The

monocytes increase expression of scavenger receptors like scavenger receptor-A (SR-A) and CD36, which allows the accumulation of massive amounts of cholesterol esters mediated by the uptake of oxidized LDL (oxLDL) [41]. Hyperlipidemic mice lacking M-CSF, SR-A, or CD36 develop significantly less atherosclerosis compared to controls [42-44]. The increased permeability of the endothelium allows for the passage of oxLDL into the intimal space. Modified LDL has been shown to be pro-inflammatory, leading to the activation of both macrophages and endothelium [45]. Macrophages that phagocytose this antigenic LDL convert into "foam cells", the hallmark of the atherogenic fatty streak, which appear foamy under the microscope due to accumulation of cytoplasmic lipid droplets [46-48].

The macrophage foam cells act as immune mediators in both innate and adaptive immune responses by producing oxygen radicals, proteases, complement factors, and cytokines and by presenting foreign antigens to T cells in the subendothelial space, respectively, thus amplifying the local inflammatory response in the lesion [40]. The initial lesion evolves into a mature, complex lesion, which is typically the point of clinical manifestations. The endothelium, like the foam cells, functions in an endocrine manner and produces growth factors that promote vascular smooth muscle cell (SMC) proliferation and migration, fibroblast-mediated collagen synthesis and matrix deposition, fibrous cap production, and platelet and immune cell recruitment and activation [6]. SMC migrate from the medial layer of the artery past the internal elastic lamina and into the subendothelial space, where they produce extracellular matrix proteins such as collagen that lead to the development of the fibrous cap and take up lipid to become SMC foam cells [49]. The buildup of SMC, extracellular matrix, macrophages, and other immune cells lead to a narrowing of the vessel; however this is not usually the reason for clinical manifestations. Plaque rupture or thrombosis is the cause of the majority of acute coronary events such as myocardial infarction and stroke [50]. The fibrous cap can become thin and weakened by increased accumulation of cells or increased blood pressure. Fissure of the cap allows coagulation factors contact with tissue factor released by macrophages, creating a pro-thrombotic stimulus. Plaque disruption may also occur through endothelial desquamation or shedding, which leads to platelet thrombosis as endothelial collagen and von Willebrand factor is uncovered, promoting platelet adhesion and activation as a function of normal wound healing [5].

It is obvious that the endothelium plays a large role in the initiation as well as progression of cardiovascular diseases such as atherosclerosis. Thus, it is important to maintain

a stable endothelial environment. Minute changes in endothelial cell function can be amplified leading to extraordinary systemic complications. Unfortunately, the endothelium's large surface area is uniquely susceptible to physiological insult as it is in constant contact with blood and circulating xenobiotics. As previously described, a number of factors can lead to endothelial dysfunction, such as endogenous inflammatory mediators like cytokines. Other risk factors not mentioned are exogenous environmental factors such as pollution, chemical insult, and nutrition. One group of pollutants that elicits detrimental effects on the vasculature is air pollution.

Annually, over 2 million people die prematurely due to effects from indoor and outdoor urban air pollution [51]. Early studies on the link between air pollution episodes and human health effects were due to severe mortal and morbid episodes in places such as Meuse Valley, Belgium, in 1930; Donora, Pennsylvania, in 1948; and London, England, in 1952 [52]. Urban air pollution is primarily derived from fossil fuel combustion processes; natural and anthropogenic, industrial and automobile derived. To avoid such devastating episodes of air pollution related disease, the United States enacted the National Ambient Air Quality Standards (NAAQS), the Clean Air Act in 1963, the Clean Air Act Amendments of 1970, and the creation of the Environmental Protection Agency (EPA) in 1970. The NAAQS monitors levels of six criteria air pollutants, ozone, lead (Pb), nitrogen oxides (NO_x), sulfur oxides (SO_x), carbon monoxide (CO), and particulate matter (PM). Particulate matter is broken down into two groups: $PM_{2.5}$ or fine particles, which are particles that are less than 2.5 μm in aerodynamic diameter, and PM_{10} or coarse particles, which are particles that are between 10 and 2.5 μm in aerodynamic diameter. A third group of particles exist that are unregulated, deemed ultrafine particles (UFP) or $PM_{0.1}$, which are particles that are less than 100 nm in aerodynamic diameter. Numerous studies have linked these pollutants with severe health effects, however particulate matter has gained mass attention in the last decade as being responsible largely for respiratory and cardiovascular related health effects.

There have been a number of epidemiological studies linking both short-term and long-term particulate matter exposure with population health impacts [53-58]. Modeling of data from 20 U.S. cities, between 1987-1994, concluded that the dose-response relationship between PM_{10} and cardiovascular and respiratory mortality is linear with no threshold value [57]. The National Morbidity, Mortality, and Air Pollution Study (NMMAPS) evaluated time-series analysis of PM_{10} effects on U.S. emergency hospital admissions [58]. They found a strong association

between acute PM_{10} exposure and daily mortality, 1 day later; that the association is strongest for respiratory and cardiovascular causes of death; and the association cannot be attributed to other air pollutants. Even low ambient concentrations of PM have positive correlations with mortality occurring concurrently or within 1-5 days after the event with cardiovascular disease as the main cause [59, 60]. Short-term increase of 10 $\mu g/m^3$ of $PM_{2.5}$ is associated with a 1.8% increase in mortality and a 1.4% increase in cardiovascular mortality [56]. Studies have not only linked increased PM with increased death but also increased hospitalizations for cardiovascular complications [61-63], especially ischemic heart disease events [55, 61]. Long-term exposure to increased $PM_{2.5}$ was associated with a 4% increase risk of mortality overall and 6% for cardiopulmonary disease [64].

The mechanisms suggested for these long-term exposure increases are varied, but they likely include: systemic inflammation, accelerated formation of atherosclerosis, and altered cardiac autonomic functions [52, 53]. Endothelial dysfunction has also been suggested as a possible reason for increased cardiovascular mortality due to PM exposure [65]. Correlations between increased inflammatory acute phase proteins, such as C-reactive protein (CRP) and PM exposure, have been seen in a number of studies [66-69]. Increased circulating cytokines IL-6 and IL-1β, as well as increased ICAM-1 and VCAM-1 expression, also have been shown [70, 71].

Fewer studies have been conducted on UFP, even though the concentration of these particles increase dramatically during high pollution episodes and can account for more than 40% of the total particle number concentration [72]. The major sources of unintentional UFP are road transport (60%) and combustion processes (23%) [73]. UFP are identified differently depending on the field of study; for instance, atmospheric scientists call them Aitken mode or nucleation mode particles, where as material scientists call them nanostructured materials. No matter the label assigned, these are nanosized particles (NP) and they confer a number of characteristics that support their potential importance. These particles are extremely small in size, thus have an increased surface area and reactivity, which may predict a greater biologic activity, per given mass, compared to larger particles [74]. NP have a high pulmonary deposition efficiency and long-term retention [75]. These particles also can have unique chemical composition, structure, shape, and aggregation [76]. The unique properties of these materials are being exploited by industry and the exploding nanotechnology field. It is estimated that by 2015, nanotechnology will be a $1 trillion market [76] and that rates of production could increase to 58,000 metric tons produced per year [77]. Currently, NP are being used

commercially in cosmetics, sunscreens, tires, stain-resistant clothing, electronics, and pigments. They are being tested as targeted drug-delivery devices and as environmental remediation strategies. According to the National Nanotechnology Initiative, thousands of tons of silica, alumina, and ceria NP are used each year as polishing mixtures for semiconductor wafers, making it the largest volume of NP produced in 2004 [73]. Alumina or aluminum oxide accounts for approximately 20% of the 2005 world market of nanoparticles [78]. Due to the large volume of particles produced and the lack of toxicity testing on nano-scale materials, concerns have been raised as to the adverse effects NP may have on biological systems [73, 74, 79, 80].

Nanotoxicology is a rapidly developing field looking at the safety of nanotechnology for manufacturing and marketing. Studies have already linked NP exposure and cardiovascular disease endpoints. Alumina NP initiate inflammatory events in macrophages, including secretion of pro-inflammatory cytokines and interaction with neighboring cell types [81, 82], which could lead to activation of the endothelium. Other metal oxide NP, including yttrium oxide (Y_2O_3) and zinc oxide (ZnO), increased expression of ICAM-1, IL-8, and MCP-1 in human endothelial cells and these particles were internalized into the cells [83]. Rats intratracheally instilled with titanium dioxide particles were found to have increased leukocyte rolling and adhesion of polymorphonuclear leukocytes, and increased vascular oxidative stress [84]. NP, such as UFP, can carry organic air toxics such as polycyclic aromatic hydrocarbons (PAHs) and volatile carbon compounds. Many particles that are produced unintentionally by combustion sources, such as diesel exhaust particles, are bound with organic compounds, transition metals, and oxidant gases that are also released by these processes [85, 86]. The combination of these absorbed or condensed particles on the surface of the core particle sometimes leads to synergistic effects on human health. For example, simultaneous exposure to PAH and iron oxides are considered one of the main factors leading to lung cancer in mine workers [87, 88]. The iron oxide particles act as a delivery system, increasing lung retention, and allowing for greater availability and metabolism of PAHs. The same theory is relevant for a number of other particles and compounds [85, 86].

The most commonly bound organic compounds studied are PAHs. PAHs are hundreds of chemically similar compounds that are ubiquitous environmental contaminants [89, 90]. They are produced as byproducts of incomplete combustion events, including: forest fires, volcanic eruptions, burning of coal and other fossil fuels, cigarette smoking, and cooking. PAHs enter the body via ingestion, inhalation, and transdermally, and will accumulate and

bioconcentrate to toxic levels in a number of species, including humans [91]. Benzo[a]pyrene (B[a]P) is a PAH with a five-membered ring structure and has been widely studied as a prototypical PAH. DNA adducts of B[a]P metabolites have been found in human atherosclerotic lesions and vascular endothelial cells, implying the transport of B[a]P through the systemic circulation [92, 93]. The main route of PAH exposure, except in smokers and coal and tar industry workers, is ingestion as a result of food chain bioaccumulation and deposition on vegetation, accounting for approximately 97% of exposure [94, 95]. PAHs have been reported as neuro-, hepato-, renal, developmental, carcinogenic, immuno-, cardio-, and reproductive toxicants [96].

B[a]P has been widely studied as a carcinogenic agent, however B[a]P is only mutagenic after metabolic activation. B[a]P is extensively metabolized by both Phase I and Phase II metabolizing enzymes, including the cytochrome P450 mixed function oxidases (CYPs) and epoxide hydrolases, as well as glutathione transferases, sulfotransferases, and UDP-glucuronyl transferases, respectively [94, 97, 98]. Three principal pathways of B[a]P metabolism have been proposed which ultimately form diol epoxides, radical cations, and *o*-quinones [97] (Figure 1.1). The formation of electrophilic diol epoxides is heavily studied as the pathway leading to DNA adducts and mutagenic events. B[a]P undergoes initial epoxidation by cytochrome P450 enzymes, CYP1A1 and CYP1B1. CYPs function as a detoxification method, making lipophilic compounds more water soluble, thus more easily excreted by the body. The B[a]P epoxide is hydrolyzed by epoxide hydrolase, and then CYPs act again to produce the ultimate carcinogen, (±)-anti-7β,8α-dihydroxy-9α,10α-epoxy-7,8,9,10-tetrahydrobenzo[a]pyrene (anti-BPDE) [97]. BPDE forms deoxyguanosine adducts within DNA, accounting for a large part of B[a]P tumorigenicity. The radical cations, produced by the induction of P450 peroxidase enzymes, produce depurinating adducts in the DNA, however this pathway is thought to contribute less to the carcinogenicity of B[a]P. The third pathway catalyzed by dihydrodiol dehydrogenase (DD) leads to the production of *o*-quinones, which can redox cycle between catechols, semiquinones, and quinones. DD oxidizes the diol produced after P450 and epoxide hydrolase activity to form a ketol which spontaneously rearranges to form the catechol. The unstable catechol goes through two one-electron oxidation reactions to form a quinone and both hydrogen peroxide and superoxide radicals in the process. The quinone can go through reduction to re-form the catechol, thus creating a redundant redox cycling reaction where large amounts of reactive oxygen species can be produced [97].

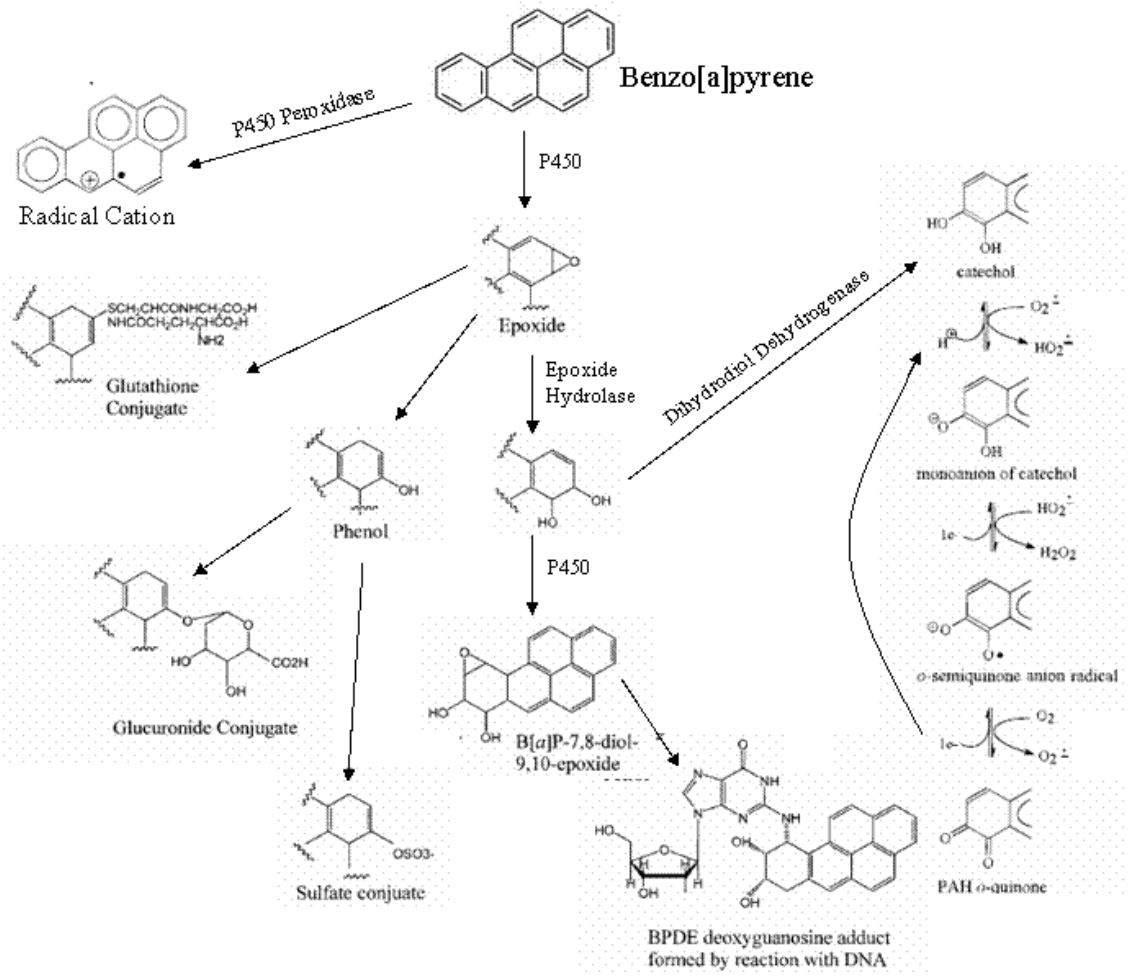

Figure 1.1: B[a]P Metabolism. Adapted from [97, 98].

The CYP enzymes play a large role in the metabolism of B[a]P, specifically CYP1A1 and CYP1B1 [99, 100]. The transcription of these xenobiotic metabolizing enzymes is controlled by the aryl hydrocarbon receptor (AhR). AhR is a ligand-activated member of the basic-helix-loop-helix/Per-ARNT-Sim family of nuclear receptors [101, 102]. AhR is well conserved from invertebrates to vertebrates suggesting its importance in development and survival [103]. In the absence of ligand, AhR is located in the cytoplasm complexed to two 90 kDa heat shock proteins (HSP90), the co-chaperone p23, and a protein variably called AhR inhibitory protein (AIP), XAP2,

and ARA9. These chaperone proteins function to keep AhR in a high affinity ligand binding conformation and prevent AhR from moving into the nucleus. The AhR binding pocket accepts planar compounds such as PAHs, polychlorinated biphenyls (PCBs), and 2',3',7',8'-tetrachlorodibenzo-*p*-dioxin (TCDD). When ligand binds to AhR, the enzyme goes through a conformational change causing HSP90, AIP, and p23 to dissociate, revealing a nuclear localization sequence (NLS) [104]. Once AhR translocates into the nucleus, it heterodimerizes with aryl hydrocarbon receptor nuclear translocator (ARNT) and the complex goes on to bind to a specific DNA sequence, GCGTG, located in regulatory DNA elements called xenobiotic response elements (XRE) (also known as dioxin response elements (DRE) and aryl hydrocarbon response elements (AhRE)). XRE are located in the promoter region of a number of metabolizing enzymes including CYP1A1, CYP1A2, CYP1B1, GSTA1, and UGT1A6 [102]. Various coactivators are involved in the binding and activation of the AhR/ARNT complex, including SRC-1, PML, NCoA-2, p/CIP, BRG-1, Med220, and CDK8 [101]. The binding of the transcription factor Sp1 to its concensus sequence [105] and the recruitment of the HAT coactivator, P300 [106], are necessary for efficient AhR/ARNT function.

The activation of AhR and the induction of related CYPs has been studied extensively in the liver, however recent importance has been placed on the determination of extrahepatic tissue levels of AhR. AhR mRNA and protein is highly expressed in the heart of healthy human subjects [107], furthermore levels are increased two-fold in patients with dilative or ischemic cardiomyopathy [108]. Localization of AhR and the regulated CYPs varies depending on the cell type. However, porcine aortic endothelial cells and human umbilical vein endothelial cells (HUVEC) were shown to have significant induction and activation of CYP1A1 [109, 110]. Induction of CYP1A1 and 1B1 has also been shown in human aortic endothelial cells [111]. Endothelial cells have the highest induction of CYP1A1 in the vasculature of rat models, which can metabolize B[a]P [112]. B[a]P metabolite, BPDE, adducts have been found in human atherosclerotic lesions, localized mainly to the endothelium [92, 93].

Increased risk of morbidity and mortality from cardiovascular diseases has been linked with a number of jobs with high occupational exposure to PAHs like B[a]P, such as aluminum smelting [113], chimney sweeping [114, 115], waste incineration [116], toll collecting [117], and tar distillation [118]. A direct exposure-response relationship was revealed between both cumulative and average B[a]P exposure and mortality from ischemic heart disease in a cohort of male asphalt workers [119]. Animal experiments support human studies, demonstrating a link

between PAH treatment and cardiovascular disease. Chickens treated with B[a]P or another PAH, 7,12-dimetrhylbenz(a,h)anthracene (DMBA), formed more frequent and larger atherosclerotic lesions than control animals [120]. The same was seen in both atherosclerosis-susceptible and atherosclerosis-resistant pigeons [121]. More recent studies, in hyperlipidemic mice, revealed B[a]P accelerated the progression of atherosclerotic plaque formation via a local inflammatory response, evidenced by increased macrophage and T-lymphocyte plaque content [122]. It was also suggested that this effect was not due to the mutagenic properties of B[a]P, since benzo[e]pyrene, the noncarcinogenic, nonmutagenic structural isoform of B[a]P, also caused a progression of plaque formation [123]. The chemokine, MCP-1, was induced in mice acutely treated with B[a]P and the dose- and time-dependent increase in MCP-1 was paralleled by induction of CYP1A1 and 1B1 *in vitro* [124]. The induction of MCP-1 by B[a]P in human endothelial cells was blocked by AhR inhibition but not by antioxidant treatment [124]. Additional studies show that air pollution and cigarette smoke exposure, which is rich in PAHs, increase the levels of ICAM-1 in both humans and animal models [125-129].

A number of signaling pathways have been linked with B[a]P exposure as well as increased inflammatory events in the endothelium, among which are the mitogen-activated protein kinases (MAPK) and the transcription factors nuclear factor- kappa B (NF-κB) and activator protein-1 (AP-1). The MAPK family of redox sensitive signaling proteins contains serine/threonine kinases that are activated by phosphorylation [130]. This phosphorylation is catalyzed by MAPK kinases, of which MEK is a member. MAPKK are also activated by phosphorylation by MAPKK kinases. There are three MAPK that have been extensively studied, p38, extracellular-related kinase (ERK), and Jun amino-terminal kinase (JNK), however, others do exist [131]. It has been suggested that ERK is primarily involved in growth and cytoprotection, while JNK and p38 are activated in inflammatory and stress responses. Cytokine induced upregulation of ICAM-1, as well as eosinophil migration, is disrupted by p38 inhibition [132]. LPS induced ICAM-1 is also disrupted *in vitro* and *in vivo* by p38 inhibitors [133]. B[a]P metabolites, both the dihydrodiol and BPDE, activated p38 in an AhR-dependent manner [134-136]. Other studies have suggested that ERK is involved in B[a]P signaling [135-137].

Cloning of the human ICAM-1 gene revealed binding sites for transcription factors including specificity protein-1 (SP-1), AP-1, and NF-κB [138, 139]. AP-1 is formed of homo- or heterodimers of Jun and Fos proteins. Phosphorylation of cJun, proximal to the transactivation

domain, is required for AP-1 containing cJun to be efficiently activated [140]. BPDE increases phosphorylation of cJun [136] as well as increases the relative AP-1 activity [141].

Recent studies have related activation of MAPK and downstream transcription factors with the presence of structured lipid raft domains such as caveolae [130, 142-144]. Disruption of caveolae, by methyl-beta-cyclodextrin or caveolin-1 knockout, inhibits p38-MAPK nuclear translocation and activation [142, 144]. Caveolae are dynamic plasma membrane microdomains that are enriched in cholesterol and glycosphingolipids. They are characterized by 50-100 nm invaginations of the plasma membrane and are implicated in the regulation of transcytosis of molecules such as albumin and LDL, and in the compartmentalization of signaling molecules [145]. Caveolae are particularly abundant in endothelial cells, likely due to the high expression levels of caveolin-1 [146-148]. Caveolin-1 is the structural component of these lipid rafts, discovered as a portion of the striated coat on the cytoplasmic surface of every caveolae [149]. This integral membrane protein drives caveolae formation by oligimerization with itself and other caveolins, and interaction with cholesterol in the membrane [146, 150]. Deletion of caveolin-1 results in a complete loss of caveolae [151] and has been used experimentally to understand the physiological function of caveolae.

Caveolae have been implicated in the pathologies of cardiovascular diseases. Hyperlipidemic mice lacking the caveolin-1 protein are protected against the development of atherosclerosis [151]. As caveolae are responsible for the uptake and transcytosis of native and modified LDL [152] and localize endothelial lipid scavenger receptors such as CD36 [153], it seems plausible that caveolae play a key role in atherogenesis. It has also been published that caveolin-1 knock-out mice have a decrease in the aortic expression of VCAM-1 [151]. Another proposed function of caveolin-1 in atherogenesis is its role in the adhesion process either as a signaling platform or as a structural participant in the building of the transcytotic channel [35, 154]. It has been recognized that ICAM-1 is translocated to lipid rafts once activated [155, 156] and that caveolae play a direct role in the transcytosis process and transmigratory cup development [35, 154].

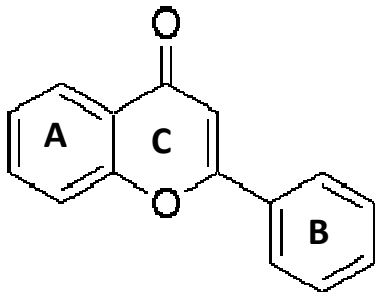

Figure 1.2: Chemical structure of the basic flavonoid compound.

Epidemiological studies have provided a clear link between the consumption of plant foods and beverages rich in polyphenols and the prevention or protection against chronic, degenerative conditions, such as cardiovascular disease [157]. Polyphenols comprise a diverse group of compounds that are secondary metabolites of plants, characterized by aromatic ring(s) bearing one or more hydroxyl substitution(s) [158]. Polyphenols are divided into at least ten different classes of compounds dependent upon chemical structure. Flavonoids are the most abundant class found in the human diet and can be recognized by the common diphenylpropane structure (C6-C3-C6), consisting of two aromatic rings linked through three carbons that usually form an oxygenated heterocycle (Figure 1.2) [158, 159]. Flavonoids are further divided into six major subclasses of compounds based on the degree of oxidation in the heterocyclic C-ring: flavones, flavonols, flavanols, flavanones, anthocyanidins, and isoflavones (Table 1.1). Various foods are abundant sources of flavonoids, however the formation of these compounds in plants is influenced by a number of factors including degree of ripeness, plant genetics, and processing and storage [159].

Flavonoids have been extensively studied for their ability to protect against damage to cells and tissues in disease processes. High intake of flavonoids is repeatedly associated with a decrease in the risk of coronary heart disease with studies on men and women with a reported relative risks between 0.62 and 0.47 [157, 160-163]. However, studies have also found no significant association [164] or even a higher risk of heart disease [165] after elevated ingestion of flavonoids. Flavonoid consumption in animal experiments has led to a reduction of atherosclerotic lesions [166-168]. The data are controversial; still, the mechanisms of action of the majority of these compounds are more uncertain. One hypothesis is that certain flavonoids

decrease plasma cholesterol and LDL concentrations, seen in subjects fed a parsley enriched diet and in animal and cell experiments [169-171].

Table 1.1: Flavonoid food sources and examples divided by subclassification. Adapted from [159]

FLAVONOID SUBCLASS	EXAMPLES	FOOD SOURCES
Flavone	Apigenin, Luteolin	Celery, Parsley
Flavonol	Quercetin, Kaempferol	Onions, Apples, Wine
Flavanol	Epicatechin, Gallocatechin	Tea, Cocoa
Flavanone	Hesperidin, Naringenin	Oranges, Citrus
Anthocyanidin	Cyanidin, Malvidin	Cherries, Grapes
Isoflavone	Genistein, Daidzein	Soy, Legumes

A heavily studied theory is that the antioxidant ability of certain groups of flavonoids is responsible for the protective effects elicited. The structure of the compound influences the flavonoid's antioxidant ability. The number of free phenolic hydroxyl substitutions, able to scavenge free radicals, significantly enhances the antioxidant capacity of each flavonoid [172, 173]. Many flavonoids have been shown to scavenge peroxyl, alkyl peroxyl, superoxide hydroxyl, and peroxynitrite radicals; however the radical scavenging abilities of the flavonoids are not the only characteristics that make them effective antioxidants. Flavonoids also chelate transition metal ions responsible for reactive oxygen species (ROS) generation [174], as well as increase the activity of endogenous antioxidant defense systems including GST, glutathione reductase, catalase, and superoxide dismutase [175, 176]. Conversely, studies showing beneficial effects of flavonoids do not always correspond with the antioxidant properties of these chemicals. For instance, red wine polyphenols will decrease lipid deposition in high-fat fed mice, however there were no changes in markers of lipid peroxidation [168]. The direct ROS scavenging properties of flavonoids are unlikely the key to their actions, as the plasma concentrations of endogenous antioxidants such as uric acid (150-450 μM) are much higher than plasma concentrations of polyphenols (<10 μM) [166].

Studies have also been conducted looking at the benefit of polyphenols to endothelial cell function. Multiple groups have used flavonoids to block the adhesion of monocytes to the

cytokine or endotoxin activated endothelium [177-180]. Reduction of adhesion molecules has also been reported [172, 177, 180]. One group suggested a correlation between the number of hydroxyl substitutions on the B ring and the prevention of cell adhesion, similar to the relationship seen with the reducing ability [178]. However, the same relationship did not exist for prevention of adhesion molecule expression. It has been suggested that inhibition of adhesion molecule expression is dependent upon the presence of 5,7-dihydroxyl substitution of the A-ring and C-ring 2,3 unsaturation and 4-keto group [172]. These structural elements were also found to be important for the competitive binding of flavonoids to ATP-binding sites of ATP-dependent enzymes such as protein tyrosine kinases [172].

Flavonoids also interact with receptors such as AhR, eliciting some of their behaviors through agonist or antagonist activities. In this manner, flavonoids can influence the metabolism and toxification of chemicals. The flavonol, resveratrol inhibits TCDD-induced AhR DNA binding and the expression of CYP1A1 and 1B1 [181]. This inhibition was able to block the formation of redox active catechol estrogens formed from the oxidation of β-estradiol, known to cause human mammary cancer. Kaempferol and two methoxylated flavonoids attenuated B[a]P induced DNA binding by reducing CYP1A1 production [182]. Kaempferol has also been shown to be protective against cigarette smoke condensate-induced lung cancer cell growth [183]. These actions were linked to the inhibition of TCDD binding to AhR, formation of the AhR/ARNT DNA binding complex, CYP1A1 promoter activity, and CYP1A1 protein expression. Studies have looked at the structural relationship between flavonoids and the antagonism of AhR [183-185]. Substitution at 4'-position of the B-ring is necessary for the ability of the flavonoids to interact with the AhR binding pocket and antagonize the receptor. It is possible that substitution at this position allows for the creation of an electron-rich center and for the compound to fit the approximate van der Waals dimensions (14 x 12 x 5 Å) for AhR ligands [184]. These characteristics contribute to the formation of an external hydrogen bond between the flavonoid and the amino acid residues of AhR [183].

This dissertation intends to describe and elucidate two new environmental risk factors for endothelial cell dysfunction, leading to atherosclerosis: alumina nanoparticles and B[a]P. Alumina nanoparticles have been shown to be pro-inflammatory in other cell types. Also, other metal oxide nanoparticles lead to increased vascular adhesion. It is hypothesized that NP, such as alumina, lead to increased endothelial cell dysfunction, evidenced by increased inflammatory processes. Epidemiolgical evidence links environmental exposure to air pollution and the

carried organic compounds with increased risk for cardiovascular diseases. Mechanisms of action are controversial and unclear. It is hypothesized that B[a]P augments cardiovascular disease by inducing adhesion molecule expression and that this event is due to metabolism by AhR mediated enzymes, as well as signaling through caveolae. This dissertation also intends to provide a possible strategy to protect against B[a]P-induced toxicity. Nutrition is a sensible means of providing a possible primary prevention strategy against toxicity associated with environmental contaminants. It is hypothesized that flavonoids will protect vascular endothelial cells against B[a]P-induced ICAM-1 induction and add to the current knowledge of the biological actions of polyphenols.

Chapter Two. Manufactured Alumina Nanoparticles Induce Expression of Endothelial Cell Adhesion Molecules

2.1 Synopsis

Nanotechnology is a rapidly growing industry that has elicited much concern because of the lack of available toxicity data. Exposure to ultrafine particles may be a risk for the development of vascular diseases due to dysfunction of the vascular endothelium. Increased endothelial adhesiveness is a critical first step in the development of vascular diseases, such as atherosclerosis. The hypothesis that alumina nanoparticles increase inflammatory markers of the endothelium, measured by the induction of adhesion molecules as well as the adhesion of monocytes to the endothelial monolayer, was tested. Following characterization of alumina nanoparticles by TEM, electron diffraction, and particle size distribution analysis, endothelial cells were exposed to alumina at various concentrations and times. Both porcine pulmonary artery endothelial cells and human umbilical vein endothelial cells showed increased mRNA and protein expression of VCAM-1, ICAM-1, and ELAM-1. Furthermore, human endothelial cells treated with alumina particles showed increased adhesion of activated monocytes. The alumina particles tended to agglomerate at physiological pH in serum-containing media, which led to a range of particle sizes from nano to micron size during treatment conditions. These data show that alumina nanoparticles can elicit a pro-inflammatory response and thus present a cardiovascular disease risk.

2.2 Introduction

Nanotechnology is a fast growing industry with seemingly limitless applications from cosmetics and skin care products to abrasives and polishers to drug delivery devices. Manufactured nanoparticles (MNP), materials created in the diameter range of <100 nm, display unique physicochemical characteristics due in part to their smaller size, large surface-to-volume ratio, and increased reactivity. These changes in characteristics could cause a generally bioinert material to behave differently at the nanoscale. Alumina, or aluminum oxide, is among the most abundantly produced nanosized particles, estimated to account for approximately 20% of the 2005 world market of nanoparticles [78]. Because of the extreme potential of MNP and their increased usage, occupational and public exposure will dramatically increase in the future.

Future estimates of engineered nanoparticle production rates anticipate that by the year 2011, rates could increase to 58,000 metric tons produced per year [77]. With this in mind, there has been a recent emergence of concern dealing with the potential for toxicity and the lack of data to substantiate or dismiss these concerns [73, 74, 79, 80].

It has been shown that inhaled nanosized particles can travel into the bloodstream, possibly through the "gap fenestration pathway" at the air-blood barrier where gaps from 0.03 to 3 μm between alveolar epithelial cells have been visualized [186], thus allowing for particle interaction with luminal cell types, such as the vascular endothelium, and entering into extrapulmonary tissues [187-189]. Inflammation or dysfunction of the endothelial layer is considered to be an initiating event for the development of vascular diseases, such as atherosclerosis [5, 190, 191]. Increased adhesiveness of the endothelium leads to the recruitment and extravasation of leukocytes from the lumen into the vessel intima, where the leukocytes could engulf oxidized lipid particles and develop into inflammatory foam cells. These processes can be monitored *in vitro* by measuring inflammatory markers such as vascular cellular adhesion molecule-1 (VCAM-1), intercellular adhesion molecule-1 (ICAM-1), and P- and E-selectins (ELAM-1). Nanoparticles may play a role in exacerbating or accelerating this critical first step toward vascular disease. It has been shown that after intratracheal instillation in rats, treatment with TiO_2 particles caused increased rolling and adhesion of polymorphonuclear leukocytes to the luminal surface of systemic venules [84]. Further, alumina nanoparticles have been shown to initiate inflammatory events in macrophages, including secretion of pro-inflammatory cytokines and interaction with neighboring cell types [81, 82] that could also lead to activation of the endothelium. The development of endothelial adhesiveness is mediated by a number of adhesion molecules, such as VCAM-1 [29], ICAM-1 [192], and ELAM-1 [19]. A recent study demonstrated that metal oxide nanoparticles can lead to dysfunction of the endothelium, but that this process was dependent upon the particle composition [83]. Iron oxide (Fe_2O_3), yttrium oxide (Y_2O_3), and zinc oxide (ZnO) were all internalized into human aortic endothelial cells, but only Y_2O_3 and ZnO were able to induce the expression of ICAM-1, interleukin-8, or monocyte chemotactic protein-1.

It was hypothesized that MNP, such as alumina, lead to increased endothelial cell dysfunction, evidenced by increased inflammatory processes. This was tested in both human umbilical vein endothelial cells and primary porcine pulmonary artery endothelial cells. Cells

were exposed to commercially bought alumina for up to 24 h, and various measures of cellular adhesion were analyzed.

2.3 Materials and Methods

Materials

Antibodies used were anti-VCAM-1 (clone 1.G11B1, Millipore, Billercia, MA), anti-ICAM-1 (clone RR1/1, Invitrogen, Carlsbad, CA), anti-ELAM-1 (clone 1.2B6, Chemicon International, CA), and anti-GAPDH (Santa Cruz Biotechnology, Santa Cruz, CA). Anti-rabbit, anti-mouse, and anti-goat secondary antibodies were purchased from Santa Cruz Biotechnology (Santa Cruz, CA). Alexafluor 488 and 546 conjugated secondary antibodies were purchased from Invitrogen (Molecular Probes, Carlsbad, CA).

Nanoparticle Characterization

The alumina nanoparticles used in this study were obtained from Alfa Aesar (Ward Hill, MA; Alumina Oxide, γ-α, 99.98% purity, 10-20 nm, stock# 10459, Lot# I20G14). The polystyrene nanoparticles were obtained from Spherotech (Lake Forest, IL; PP-008, 0.05-0.1 μm). Alumina particles were weighed and autoclaved for 15 min at 121 °C. Experimental media were added, and the nanoparticle dispersion was characterized by using a particle size distribution analyzer (PSD), transmission electron microscopy (TEM), and electron diffraction. There were no changes in the structural and physical characteristics of alumina nanoparticles after autoclaving. This was confirmed by TEM and electron diffraction studies before and after this process. The latter also revealed the presence of similar phases (α, γ, and κ– Al_2O_3) in the autoclaved and non-autoclaved nanoparticles. In addition, high resolution TEM indicated no change in the lattice of the autoclaved and non-autoclaved nanoparticles.

For the PSD, nanoparticles were dispersed in the media and vortexed. Subsequently, 5 ml of the dispersion was added to a quartz cuvette, and placed in the Brookhaven 90Plus Nanoparticle size analyzer (Brookhaven Instruments, Holtsville, NY). Fluctuations of the scattered light due to the random motion of the particles were measured and converted into particle diameter. The scattering angle in the experiments was set at 90^{o}, particle refractive index was 1.761, and the viscosity of the solution was assumed to be 1.2 cP. It has been previously reported that the viscosity of 10% fetal bovine serum (FBS) is close to that of ethanol, which is 1.2 cP [193, 194].

The experiment was allowed to run for 90 min, and the software automatically generated the diameter distribution in a multimodal mode.

For the TEM, a drop of the nanoparticle suspension was placed on a 200 mesh Cu-lacy carbon TEM grid (EM Sciences, Hatfield, PA). The droplet on the grid was allowed to dry overnight in a vacuum oven at room temperature. After evaporation, the alumina nanoparticles were dispersed on the TEM grid. TEM measurements were performed in a JEOL 2010f instrument (JEOL, Tokyo, Japan) with operating voltage of 200 kV. The electron diffraction experiment was performed on the same sample used for TEM. The diffraction pattern and indexing was obtained using DigitalMicrograph imaging software (Gatan, Pleasanton, CA) interfaced with the microscope. The indexed rings and the alumina phases were further confirmed with the standard Joint Committee on Powder Diffraction International Centre for Diffraction Data (JCPDS-ICCD).

Cell Culture

Both primary porcine arterial endothelial cells (PECs) and primary human umbilical vein endothelial cells (HUVECs) were used in these experiments as models to evaluate inflammatory cardiovascular disease. Cells were isolated from porcine pulmonary arteries and human umbilical cord veins, respectively, as explained previously [195]. Human umbilical cords were obtained from the University of Kentucky Labor and Delivery unit. Porcine endothelial cells were cultured in M199 (GIBCO Laboratories, Grant Island, NY), supplemented with 10% FBS (Hyclone Laboratories, Logan, UT). HUVECs were cultured in M199 supplemented with 20% FBS as described previously [195].

Experimental Conditions

Cells were supplemented with autoclaved alumina particles or polystyrene particles at a concentration of 1.0 – 250 μg/ml, and then events of endothelial cell dysfunction were measured. One of the hallmarks of endothelial cell dysfunction is increases in endothelial cell adhesiveness. The experimental media for PECs and HUVECs contained 1% or 10% FBS, respectively. Alumina exposure is also represented as mass per culture dish surface area to more accurately represent the experimental conditions. Conversion of treatment groups to mass per culture dish surface area corresponds to treatments of 1.4 – 350 ng/mm^2.

Western Blotting

Whole-cell lysates were prepared with a lysis buffer containing 50 mM Tris-HCl (pH 8.0), 200 mM NaCl, 20 mM EDTA, 1% SDS, 0.5% Na-deoxycholic acid, 0.01% NP-40, 200 mM sodium orthovanadate, and 100 mM phenylmethylsulfonyl fluoride. Equal amounts of protein (40 μg) were fractionated by SDS-polyacrylamide gel electrophoresis and transferred to nitrocellulose membranes. The membrane was blocked at room temperature with 5% nonfat milk in Tris-buffered saline (TBS, pH 7.6) containing 0.05% Tween 20, and then washed with TBS-Tween. VCAM-1, ICAM-1, and GAPDH antibodies were incubated at 4 °C overnight at a 1:1000 dilution in 5% bovine serum albumin in TBS-Tween. Horseradish peroxidase-conjugated secondary antibodies were incubated for 1 h at a 1:3000 dilution. Bands were visualized by using ECL immunoblotting detection reagents (Amersham Biosciences, Buckinghamshire, England). Bands were quantified using UN-SCAN-IT gel Version 5.1 (Silk Scientific, Orem, UT) and normalized to GAPDH protein expression.

Immunofluorescence

Confluent endothelial cells were grown on glass culture slides and incubated with or without alumina (100 μg/ml) or with TNF-α (10 ng/ml; Sigma) for 24 h. After three washes in phosphate-buffered saline (PBS), cells were treated with 50:50 acetone:methanol for 30 min. After 45 min of blocking of nonspecific binding with PBS containing 1% bovine serum albumin (BSA), cells were incubated with VCAM-1, ICAM-1, or ELAM-1 primary antibodies (for 30 min at 37 °C, dilution of 1:50) and were washed twice in PBS. Then, they were incubated simultaneously with Alexafluor 546 or 488-labeled secondary antibody (15 min at 37 °C, dilution of 1:200). Three negative controls were prepared by incubation of the cells with secondary antibody species-specific IgG, no primary antibody added, or no primary and secondary antibody added. The cells were washed twice in PBS and stained with Hoechst 33342 dye (for 5-10 min at 37 °C, concentration 1μg/ml). The stained slides were mounted in aqueous mounting medium before being visualized and captured using an Olympus BX61WI confocal microscope and FluoView software.

Real Time PCR

Porcine endothelial cells were treated with alumina (100 μg/ml) for 4 and 8 h. Total RNA was extracted from cells using Trizol reagent (Invitrogen, Carlsbad, CA, USA) according to

the manufacturer's instructions and then reverse transcribed into cDNA using the Reverse Transcription System (Promega, Madison, WI, USA). VCAM-1 and ELAM-1 gene expression changes were analyzed using quantitative real-time PCR and SYBR Green technology (ABI 7300, Applied Biosystems, Foster City, CA, USA). Real-time PCR was conducted using 100 ng cDNA, 12.5 µl 2x SYBR Green PCR Master Mix (Applied Biosystems), and 150 pmol of forward and reverse primers (Integrated DNA Technologies, Coralville, IA, USA) in a total volume of 25 µl. The sequences of primer pairs used were as follows: porcine VCAM-1 (sense, 5'-ACACCACCCCAGTCACCATATC-3'; antisense, 5'-TGGAAAGACATGGCTGCCTAT-3'), porcine ELAM-1 (sense, 5'-TGATCTTCCTGATTCCAATCCA-3'; antisense, 5'- ACACATCTGGTCGCAATTCAAA-3'), and porcine β-actin, used as an internal control (sense, 5'-TCATCACCATCGGCAACT-3'; antisense, 5'-TTCCTGATGTCCACGTCGC-3'). The following thermocycling conditions were used: 50 °C for 2 min, 95 °C for 10 min, followed by 95 °C for 15 s and 60 °C for 60 s for 40 cycles. The standard curve was generated by plotting the threshold cycle (Ct) versus the log concentration of the serial dilutions of one specific cDNA sample, which served as a calibrator. All samples were prepared in duplicate; their concentrations were calculated based on the standard curve and normalized to β-actin mRNA expression.

Monocyte Adhesion

Human THP-1 monocytes (50,000 cells) were activated with TNF-α (10 min) and loaded with the fluorescent probe calcein (Molecular Probes, Carlsbad, CA). HUVECs were treated with 14 ng/mm^2 or 140 ng/mm^2 alumina particles for 8 h. Monocytes were added to treated endothelial cell monolayers and incubated (30 min), allowing for monocyte adhesion. Unbound monocytes were washed away, and the monolayer was fixed with 1% glutaraldehyde. Attached fluorescent monocytes were counted using a fluorescent microscope (Olympus IX70, Center Valley, PA).

Statistical Analysis

Values are reported as means ± standard error of the mean (SEM) of at least three independent groups. Comparisons between treatments were made by one-way analysis of variance followed by Holm-Sidak multiple comparison tests using SigmaStat 3.0 software (Systat Software, San Jose, CA). Statistical probability of $p<0.05$ was considered significant.

2.4 Results

Alumina nanoparticle characterization and stability

The alumina particles were characterized by TEM and electron diffraction. The diameter of particles was observed in TEM images and the size distribution was found to be comparable to the size reported by the manufacturer of 10 – 20 nm (Figure 2.1A). The TEM images show alumina nanoparticles in both agglomerated and non-agglomerated states (data not shown). Dynamic light scattering experiments confirmed the presence of particle agglomerates greater than 500 nm in diameter in the presence of FBS media; nevertheless, a significant portion of alumina was still present as non-agglomerated nanoparticles of less than 100 nm in size. Electron diffraction indicated the presence of α, γ, and κ– Al_2O_3 (Figure 2.1B). Alumina can exist in many forms, α, χ, η, δ, κ, θ, γ, ρ; these arise during the heat treatment of aluminum hydroxide or aluminum oxy hydroxide during the synthesis of alumina nanoparticles. The most thermodynamically stable form is α-Al_2O_3.

Alumina increases endothelial adhesion molecule expression

Alumina particles induced protein expression of VCAM-1 (Figure 2.2A) and ICAM-1 (Figure 2.2B) in a time dependent manner in both HUVECs and porcine endothelial cells (data not shown) treated with 140 ng/mm^2 alumina. This adhesion molecule induction was also dose-dependent with significant increases in VCAM-1 after treatment with 140 ng/mm^2 alumina (Figure 2.3A) and ICAM-1 after treatment with 70 or 140 ng/mm^2 alumina (Figure 2.3B). The same up-regulation was not seen in cells treated with polystyrene particles at the same and higher concentrations (Figure 2.3). The similar concentration dependent trend was seen in additional inflammatory endpoints examined including cycloxygenase-2 (data not shown). Cytotoxicity experiments showed that concentrations of alumina particles above 1400 ng/mm^2 led to overt cell death shown by MTT assay and changes in cell morphology. For this reason further experiments were conducted at 140 ng/mm^2, where no detectable cell death occurred.

Alumina particles also induced mRNA expression of both VCAM-1 (Figure 2.4A) and ELAM-1 (Figure 2.4B) in porcine endothelial cells after 4 and 8 h of treatment at a culture dish surface area dose of 140 ng/mm^2 (1.4 g/cm^2). VCAM-1 had a higher induction after 4 h of

treatment than after 8 h once normalized to β-actin. ELAM-1 had a higher induction after 8 h, than after 4 h.

The increased adhesion molecule protein expression resulting from alumina treatment was also visualized by immunofluorescence staining (Figure 2.5). Alumina increased VCAM-1, ICAM-1, and ELAM-1 after 24 h of treatment (100 μg/ml or 250 ng/mm^2) shown in porcine endothelial cells and HUVECs, respectively, as did TNF-α, which was used as a positive control. Increased VCAM-1, ICAM-1, and ELAM-1 protein staining was visualized in both cell types.

Alumina increases monocyte adhesion to endothelium

Alumina treatment was also found to increase the adhesion of activated monocytes onto the endothelial cell monolayer (Figure 2.6). Fixed, adherent fluorescently-labeled THP-1 monocytes were counted. There was a statistically significant increase in adhered monocytes when the endothelium was treated with either 14 or 140 ng/mm^2 alumina.

A

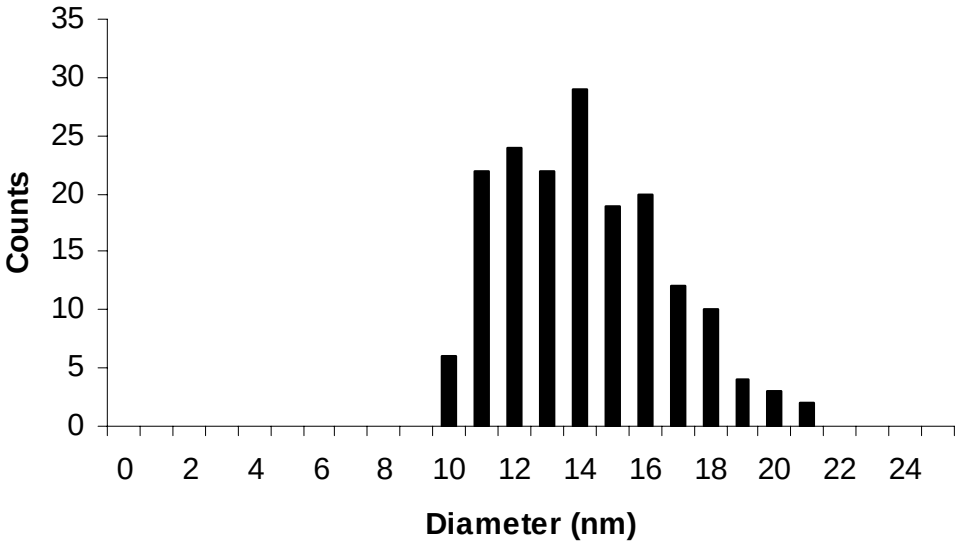

B

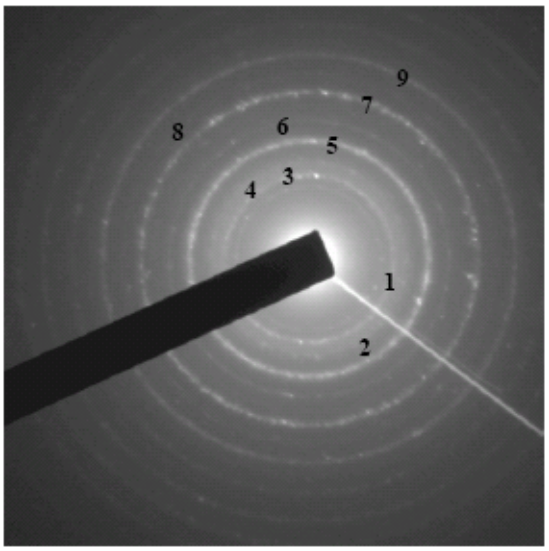

Spot#	hkl and phase
1	(111), κ phase
2	(121), κ phase
3	(013), κ phase
4	(104), γ phase
5	(212), κ phase
6	(024), γ phase
7	(144), κ phase
8	(531), α phase
9	(220), γ phase

Figure 2.1: **Diameter distribution and electron diffraction pattern of alumina nanoparticles.** Diameter distribution of TEM images indicated the size of alumina nanoparticles to be between 10 and 20 nm. (A) Electron diffraction data indicated the presence of three different phases of alumina nanoparticles. Results were verified and confirmed using standard data obtained from the International Centre for Diffraction Data (ICDD) database. (B)

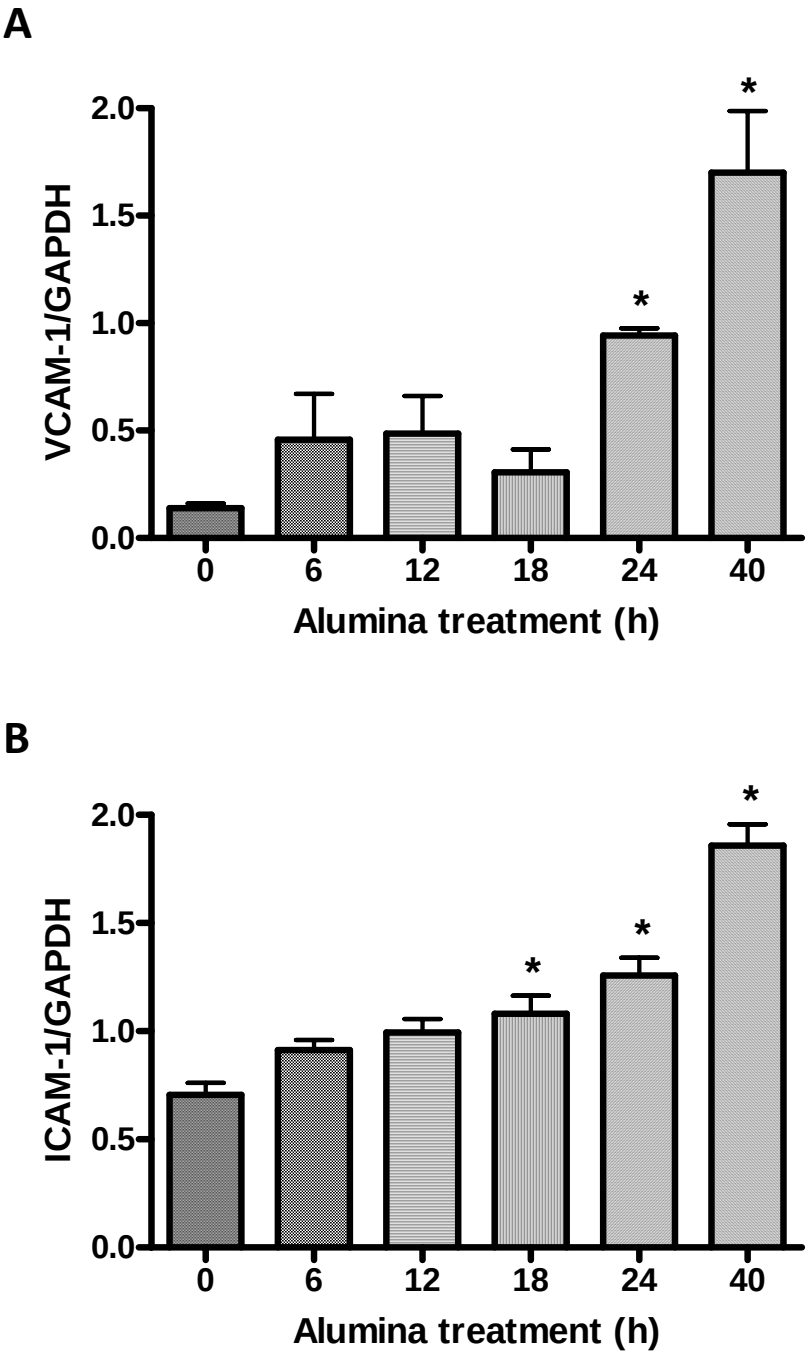

Figure 2.2: **Alumina increases VCAM-1 and ICAM-1 protein expression in a time-dependent manner.** HUVECs were treated with 140 ng/mm^2 (100 µg/mL) alumina particles for 0 – 40 h. Whole cell lysates were analyzed by immunoblot for VCAM-1 (A), ICAM-1 (B), and GAPDH. Bars represent average and SEM of at least three independent groups normalized to GAPDH. * $p<0.05$ compared to control cultures.

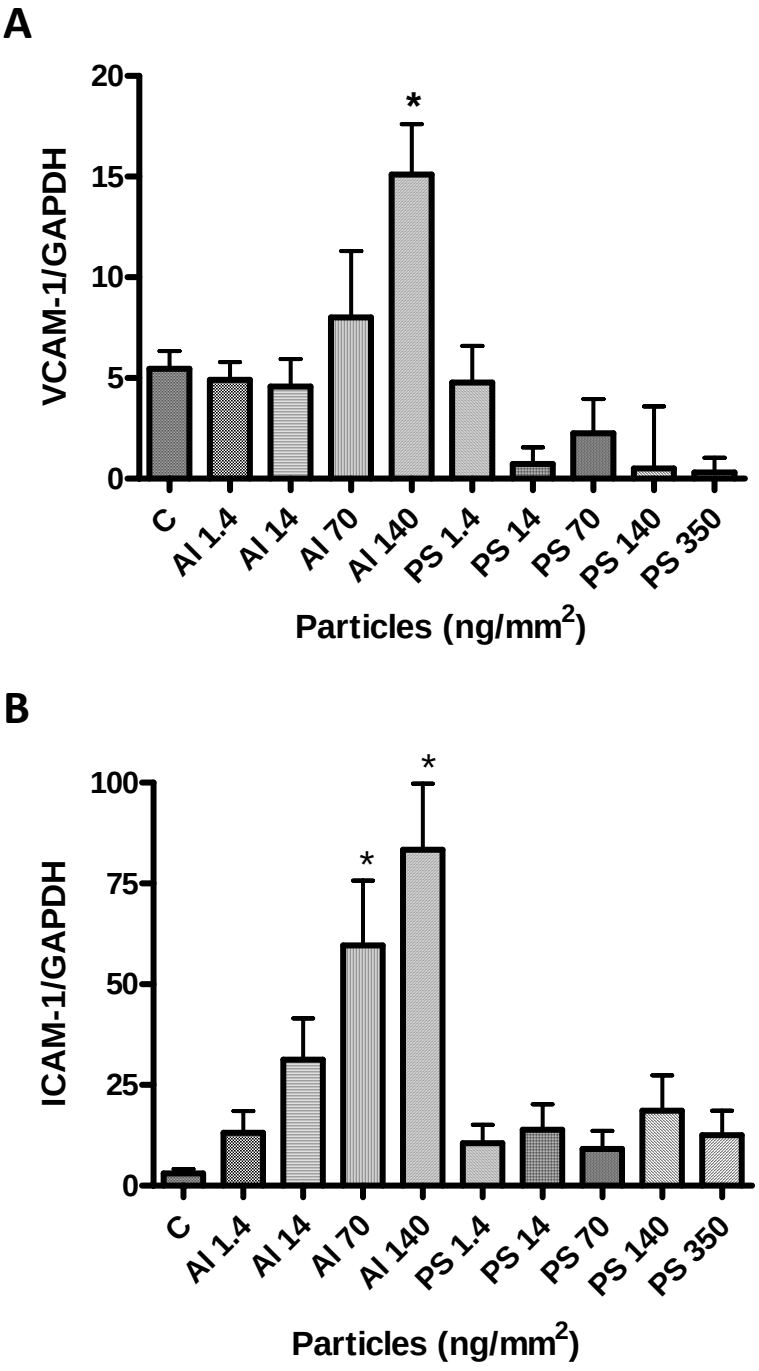

Figure 2.3: **Alumina increases VCAM-1 and ICAM-1 protein expression in a dose-dependent manner.** HUVECs were treated with alumina (Al) or polystyrene (PS) particles for 24 h, at varying concentrations (1.4-350 ng/mm^2, 1-250 µg/mL). Whole cell lysates were analyzed by immunoblot for VCAM-1 (A), ICAM-1 (B), and GAPDH. Bars represent average and SEM of at least three independent groups normalized to GAPDH. * $p<0.05$ compared to control cultures.

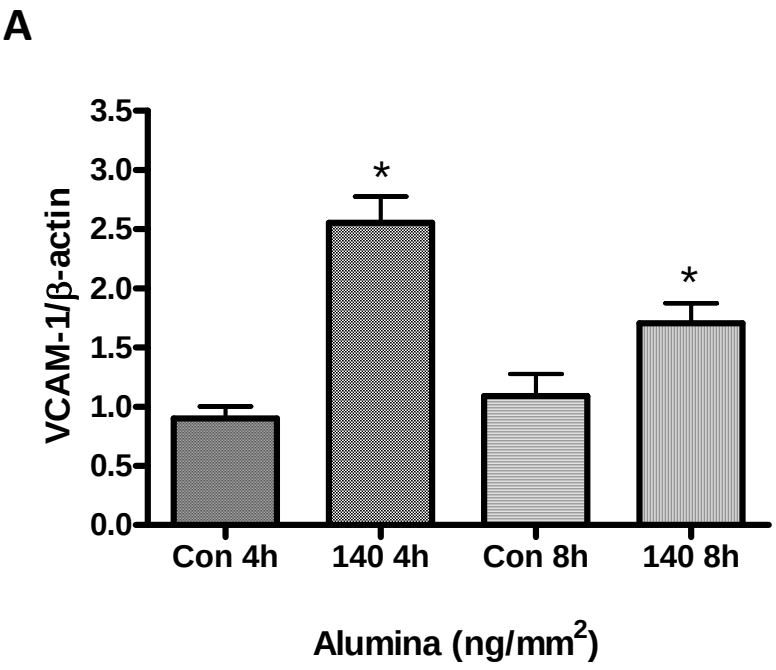

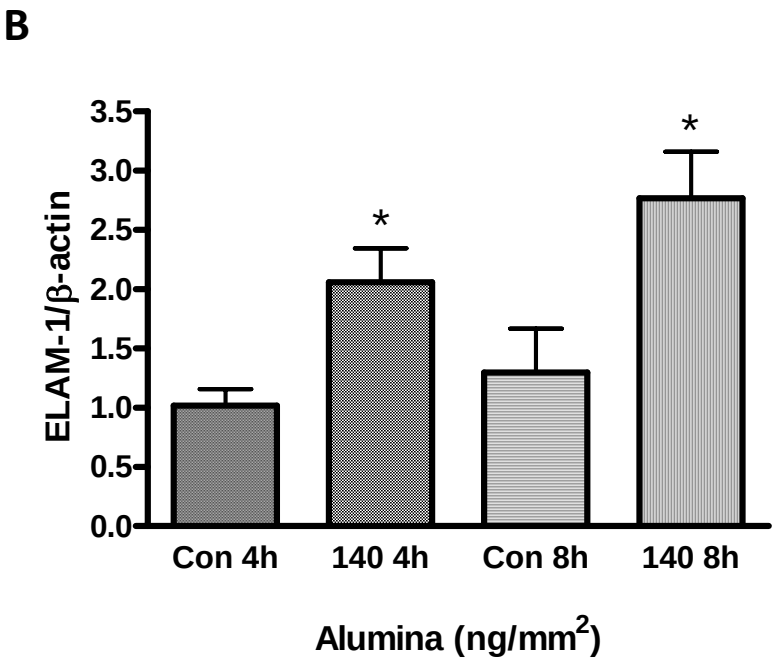

Figure 2.4: **Alumina increases ELAM-1 and VCAM-1 mRNA expression.** Porcine endothelial cells (PECs) were treated with 140 ng/mm^2 alumina particles for 4 and 8 h. VCAM-1 (A) and ELAM-1 (B) expression was analyzed using quantitative real-time PCR and SYBR Green technology. Bars represent average and SEM of at least three independent groups normalized to β-actin. * $p<0.05$ compared to corresponding time control cultures.

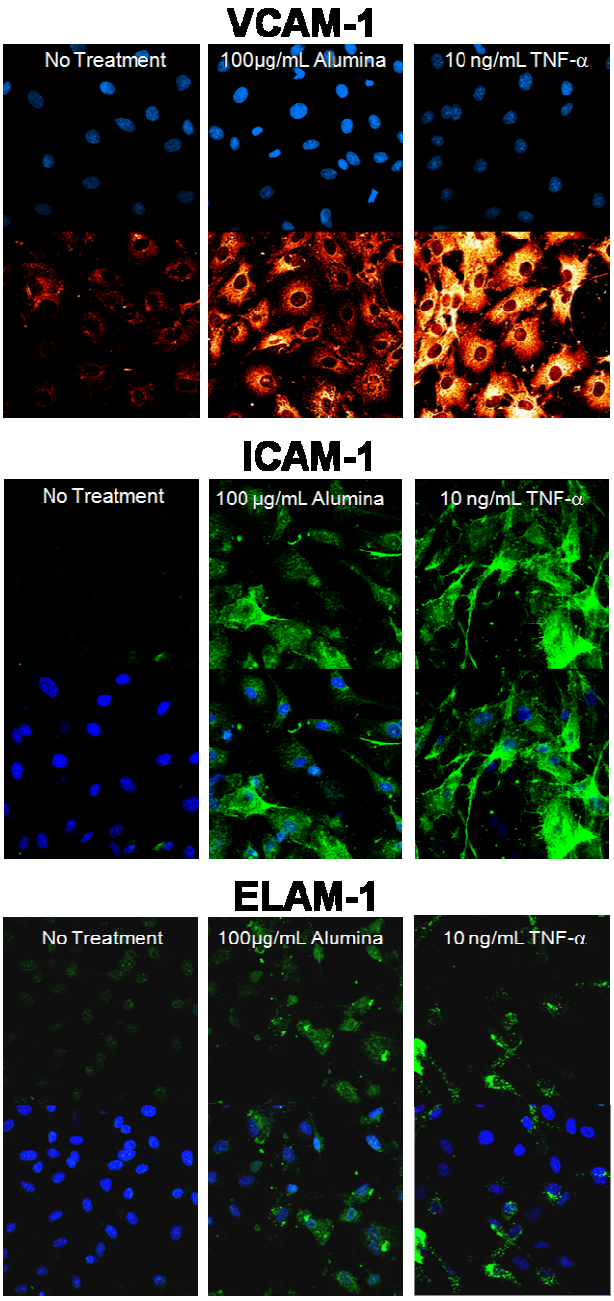

Figure 2.5: **Alumina increases adhesion molecule protein expression**. PECs and HUVECs were treated with 100 µg/mL alumina particles or 10 ng/mL TNF-α for 24 h. Cells were fixed and probed for VCAM-1 (PEC), ICAM-1 (HUVEC), or ELAM-1 (HUVEC) using AlexaFluor antibodies. VCAM-1 staining is shown as orange, ICAM-1 and ELAM-1 as green, and nuclei are stained with Hoechst 33342 in blue. Samples were visualized and captured using an Olympus BX61WI confocal microscope. Images are representative of multiple treatment groups among both cell types.

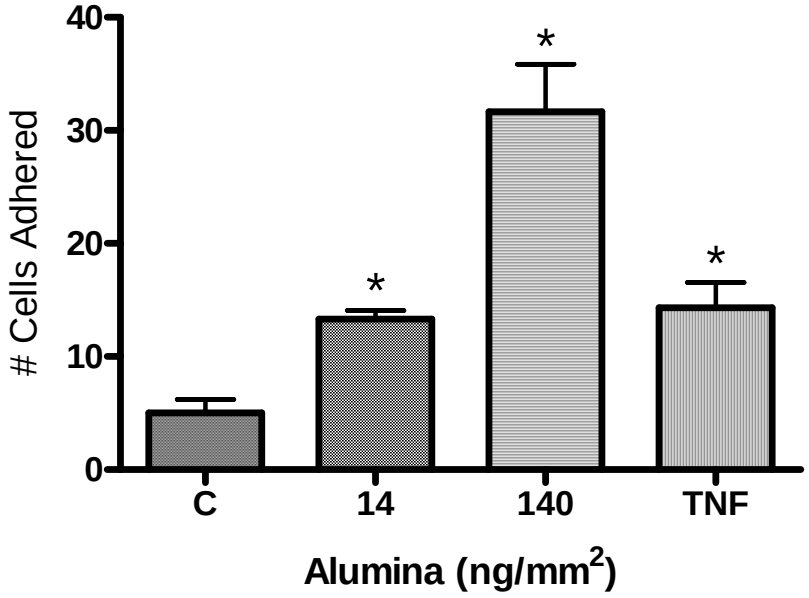

Figure 2.6: **Alumina increases monocyte adhesion to endothelial monolayers.** Human THP-1 monocytes were activated with TNF-α (10 min) and loaded with the fluorescent probe calcein. HUVECs were treated with 140 ng/mm^2 or 14 ng/mm^2 alumina particles for 8 h. Monocytes were added to treated endothelial cell monolayers, allowing for monocyte adhesion. Attached fluorescent monocytes were counted using a fluorescent microscope (Olympus IX70). * $p<0.05$ compared to control cultures.

2.5 Discussion

There is evidence suggesting that exposure to ultrafine particulate air pollution (<100 nm) is linked to increased incidence of cardiovascular diseases [196-199]. It is thus conceivable that human exposure to manufactured particulate matter in this size range also presents a risk to consumers as well as to occupational workers. The mechanisms leading to the increased cardiovascular risks have not been fully elucidated, but endothelial cell dysfunction and inflammation is a key step toward the progression of vascular diseases and has been shown to be associated with air pollution effects [127, 200, 201]. With this in mind, it was hypothesized that MNP, such as alumina, lead to increased endothelial cell dysfunction, evidenced by increased endothelial adhesiveness. Endothelial adhesion molecules are responsible for migration of leukocytes into the vessel, where the leukocytes develop into inflammatory foam cells evident in atherosclerotic fatty streaks. Results in the current study demonstrated that direct exposure of endothelial cells to alumina nanoparticles increased adhesion molecule mRNA and protein expression in a dose- and time-dependent manner as well as increased adhesion of activated monocytes to the endothelial cell monolayer. The mechanisms behind these events are not well understood.

One possibility for the induction of adhesion molecules is the production of reactive oxygen species (ROS) and the activation of redox sensitive signaling pathways. Preliminary experiments on the effects of alumina on both 4-hydroxynonenal (4-HNE) and protein carbonyl production did not reveal significant increases in ROS production (data not shown). These results are in agreement with recent studies suggesting that certain other metal oxide nanoparticles have not significantly promoted ROS upon internalization into cells [83, 202, 203]. Nuclear factor-kappa B (NF-κB) is part of one known pathway that leads to the production of inflammatory adhesion molecules like VCAM-1, ICAM-1, and ELAM-1 [204, 205]. Preliminary studies on the role of NF-κB were also conducted using the irreversible NF-κB inhibitor (E)3-[(4-t-butylphenyl)sulfonyl]-2-propenenitrile (BAY 11-7085), which acts by preventing the phosphorylation, and thus release and degradation of IκBα, the endogenous inhibitory NF-κB regulatory protein [206]. The results suggest that NF-κB inhibition did not change the magnitude of induction of VCAM-1 over control; thus, VCAM-1 induction is possibly not through the NF-κB pathway. Other signaling pathway options have not been investigated, however a number of possibilities exist, including specificity protein-1 (SP-1) [207, 208], activator protein-1

(AP-1) [209], and interferon regulatory factor (IRF-1) [210, 211], which can operate solely or in unison to promote adhesion molecule up-regulation.

Recent studies have also shown that manufactured nanoparticles may play a pro-inflammatory role once exposed to endothelial cells. Carbon black particles were shown to induce monocyte chemoattractant protein-1 (MCP-1) in human endothelial cells and reduce the expression of endothelial nitric oxide synthase, important for the contractive properties of the endothelium [212]. A recent study also showed the induction of MCP-1 along with ICAM-1 and IL-8 in endothelial cells treated with ZnO or Y_2O_3 nanoparticles [83].

The alumina particles used were measured to be around 10 - 20 nm as provided by the manufacturer data and confirmed by TEM. When added to culture media that includes serum proteins, larger agglomerates were found in addition to smaller nanoparticles as has been shown by other groups before [213]. These particles and smaller aggregates were in the size range of particles that could enter the cell through endocytosis [214]. It is likely that exposure to these larger agglomerated nanoparticle units is a physiologically relevant scenario. Indeed, many toxicity studies on nanoparticles in animals were carried out with aggregated or agglomerated particles instead of individual nanoparticles, yet still observed nanoparticle based effects [215]. Mathematical models have predicted that 10-20% of respired particles between 0.1 and 1 μm in diameter reach the alveolar regions of the lungs where they can come in contact with the circulation [74]. These models were based on singlet particle exposure; still alumina aggregates in the current study were found in this size range, suggesting again that both the aggregated and non aggregated particles may lead to toxic events and enter the circulation.

Experiments in the current study were conducted in two primary endothelial cell types. Similar results were observed in both cultures; however human cells seemed more sensitive to nanoparticle exposure compared to porcine derived cells. As these experiments were conducted *in vitro*, other elements characteristic of physiological exposure could not be modeled. For example, endothelial cells *in vivo* are constantly exposed to flow conditions, which will likely change the delivery and interactions between nanoparticles and the vascular wall [216]. Endothelial cells also work in concert with various other cell types including leukocytes and smooth muscle cells. The effects of nanosized alumina on these cell types could also cause inflammatory changes in the endothelium. Another area of interest is the concentration that actually enters the circulation and comes in contact with the endothelium.

The amount of translocation of particles from the lung into the circulation has not been fully explained. It has been shown that nanoparticles do enter the circulation and extrapulmonary tissues [187, 217, 218] with possibly up to 15% of the inhaled dose reaching the capillaries [219].

In summary, data from the current study demonstrate that alumina nanoparticles cause increased adhesiveness shown by induction of VCAM-1, ICAM-1, and ELAM-1 as well as increased monocyte adhesion to vascular endothelial cells. These data suggest that exposure to nanoparticles may be a significant risk for the development of inflammatory diseases such as atherosclerosis.

Chapter Three. Benzo[a]pyrene Induces Intercellular Adhesion Molecule-1 Through a Caveolae and Aryl Hydrocarbon Receptor Mediated Pathway

3.1 Synopsis

Toxicologic and epidemiologic studies have linked benzo[a]pyrene (B[a]P) exposure with cardiovascular diseases such as atherosclerosis. The mechanisms of action leading to these diseases have not been fully understood. One key step in the development of atherosclerosis is vascular endothelial dysfunction, which is characterized by increased adhesiveness. To determine if B[a]P could lead to increased endothelial adhesiveness, the effects of B[a]P on human endothelial cell intercellular adhesion molecule-1 (ICAM-1) expression was investigated. B[a]P was able to increase ICAM-1 protein only after pretreatment with the aryl hydrocarbon receptor (AhR) agonist β-naphthoflavone (β-NF). Knockdown of AhR by siRNA or treatment with AhR antagonist α-naphthoflavone (α-NF) eliminated the induction of ICAM-1 from B[a]P, confirming the necessity of AhR in this process. Likewise, B[a]P only increased monocyte adhesion to the vascular endothelium when cells were pretreated with β-NF. Experiments were done to define a signaling mechanism. B[a]P increased phosphorylation of MEK and p38-MAPK, and inhibitors to these proteins blunted the ICAM-1 induction. B[a]P was also able to increase AP-1 DNA binding and phosphorylation of c-Jun. Phosphorylation of c-Jun was disrupted by MEK and p38-MAPK inhibitors linking the signaling cascade. Finally, the importance of membrane microdomains, caveolae, was demonstrated by knockdown of the structural protein caveolin-1. Disruption of caveolae eliminated the B[a]P induced ICAM-1 expression. These data suggest a possible pro-inflammatory mechanism of action of B[a]P involving caveolae, leading to increased vascular endothelial adhesiveness and this inflammation may be a critical step in the development of B[a]P-induced atherosclerosis.

3.2 Introduction

A mounting interest in the correlation between air pollution and increased cardiovascular events has developed over the last few decades. Epidemiological studies have linked increased particulate matter (PM10 or PM2.5) exposure with heightened cardiovascular morbidity [220] and mortality [53, 54, 56]. Also, it has been known for years that coronary artery disease is exacerbated by cigarette smoke [221]. Both of these complex mixtures contain large amounts of polycyclic aromatic hydrocarbons (PAHs) [222-224], among which is the

probable human carcinogen B[a]P, which are formed as byproducts of incomplete combustion processes. Similar to studies on air pollution and cigarette smoke, a cohort of asphalt workers with occupational exposure to B[a]P was shown to have a positive correlation between cumulative and average B[a]P exposure and risk for ischemic heart disease [119].

B[a]P is monitored by the US Environmental Protection Agency as part of the group termed polycyclic organic matter. B[a]P augments the severity and progression of atherosclerotic plaques in animal models [120-122], which are not attributed to the mutagenic properties of the compound [123]. An alternate hypothesis is an increased inflammatory response, a key step in the development and progression of atherosclerosis. B[a]P treatment has been shown to increase the inflammatory chemokine, monocyte chemoattractant protein-1 (MCP-1) in aortic tissues of hyperlipidemic mice [124]. Interestingly, this response is attenuated by treatment with an AhR antagonist. B[a]P is metabolically activated by the AhR-induced enzymes cytochrome P450 1A1 (CYP1A1) and epoxide hydrolase, resulting in carcinogenic B[a]P-diol epoxides (BPDE), as well as the redox cycling o-quinones. Endothelial cells have the highest induction of CYP1A1 in the vasculature of rat models, and these cells have the ability to metabolize B[a]P [112].

The vascular endothelium is susceptible to physiological insult as it is in constant contact with circulating xenobiotics. B[a]P DNA adducts have been found in human atherosclerotic lesions and to a large part localized to the endothelium, thus supporting this concept [92, 93]. Vascular endothelium dysfunction is a key initiating event in numerous cardiovascular diseases such as atherosclerosis. Dysfunction of the endothelium is marked by increased adhesiveness caused by the presentation of cellular adhesion molecules, such as ICAM-1 (CD54) and vascular cell adhesion molecule-1 (VCAM-1, CD106). ICAM-1, a member of the immunoglobulin superfamily that binds to β2 integrins, causes adhesion of circulating leukocytes to the vascular wall, leading to diapedesis through the vessel wall and accumulation in the intimal layer. Studies have established the importance of ICAM to the development of cardiovascular disease. Pretreatment of hyperlipidemic mice with antibodies against ICAM-1 reduced macrophage homing to aortas [23], and *Icam1-/-* mice fed a western diet have decreased lesion size compared to controls [21]. Studies also demonstrate that air pollution and cigarette exposure increase the levels of ICAM-1 in both humans and animal models [125-129].

The human ICAM-1 gene was cloned and found to contain binding sites for transcription factors including specificity protein-1 (SP-1), activator protein-1 (AP-1), and nuclear factor-κB (NF-κB) [138, 139]. These transcription factors are activated by a number of upstream kinases such as the MAP kinase (MAPK) family of proteins, including p38 MAPK, extracellular signal-regulated kinase (ERK), and c-Jun N-terminal kinase (JNK). MAPK are serine/threonine kinases that are activated by phosphorylation by MAPKK, such as MEK. These signaling cascades have been shown to be redox sensitive and elicit a large amount of crosstalk between the MAPK members [130]. More recent literature suggests caveolae play a role in some MAPK signaling cascades [130, 142-144]. Caveolae are plasma membrane microdomains enriched in cholesterol and glycosphingolipids, and function in cellular trafficking as well as act as signaling platforms for a range of cascades. Caveolae are characterized by the presence of caveolins, the structural component of these lipid rafts, and are particularly abundant in endothelial cells [145, 147, 148].

It has been shown that B[a]P induces atherosclerosis in hyperlipidemic mouse models and epidemiological studies support this finding. However, mechanisms involved in these events are not fully understood. We hypothesized that B[a]P augments cardiovascular disease by inducing adhesion molecule expression and that this event is due to metabolism by AhR mediated enzymes, as well as signaling through caveolae.

3.3 Materials and Methods

Materials

Antibodies used were anti-ICAM-1 (clone RR1/1, Invitrogen, Carlsbad, CA), anti-caveolin-1 (Affinity Bioreagents, Golden, CO), anti-p38 (Cell Signaling Technology, Danvers, MA), anti-phospho-p38 (Thr180/Tyr182) (Cell Signaling Technology), anti-MEK (Santa Cruz Biotechnology, Santa Cruz, CA), anti-phospho-MEK1/2 (Ser217/221) (Cell Signaling Technology), anti-cJun (Zymed, San Francisco, CA), anti-phospho-cJun (Ser73) (Upstate, Lake Placid, NY), anti-AhR (clone RPT1, Abcam, Cambridge, MA), anti-actin (Sigma Aldrich, St. Louis, MO), and anti-GAPDH (Santa Cruz Biotechnology). Anti-rabbit, anti-goat, and anti-mouse secondary antibodies were purchased from Cell Signaling Technology. AlexaFluor 488 conjugated secondary antibody was purchased from Invitrogen. The inhibitors SB203580 and PD98059 were purchased from Calbiochem (EMD Chemicals, Gibbstown, NJ) and dissolved in endotoxin-free DMSO (Sigma Aldrich, St. Louis, MO). Fluoranthene was purchased from Accustandard (New Haven, CT).

Human TNF-α, B[a]P, β-NF, α-NF, and propidium iodide were purchased from Sigma Aldrich (St. Louis, MO).

Cell Culture

Primary human umbilical vein endothelial cells (HUVEC) were used in these experiments as models for inflammatory cardiovascular disease. Cells were isolated from human umbilical cord veins as explained previously [195]. Human umbilical cords were obtained from the University of Kentucky Labor and Delivery unit. HUVEC were cultured in M199 media (GIBCO Laboratories, Grant Island, NY) supplemented with 20% FBS (Hyclone Laboratories, Logan, UT) as described previously [195]. The experimental media contained 10% FBS. B[a]P, β-NF, α-NF, and inhibitors were dissolved in DMSO. The final concentration of DMSO in the culture media did not exceed 0.03%. All vehicle controls and treated cultures contained the same amount of DMSO.

Cytochrome P4501A1 Activity

HUVEC grown on white-walled 96 well plates were treated with β-NF (1 μM) for 16 h. Both β-NF and α-NF have been shown to alter HUVEC CYP1A1 expression and AhR function at this concentration [225, 226]. Cytrochrome P4501A1 activity was measured by increased luminescence due to the conversion of Luciferin-CEE to Luciferin via P450-Glo Assay (Promega, Madison, WI) in accordance with manufacturer's instructions. CYP1A1 activity was normalized to cell number. Cell number was determined using the Cell-Titer Glo Assay (Promega) as directed by the manufacturer's instructions.

Western Blotting

Whole-cell lysates were prepared with a lysis buffer containing 50 mM Tris-HCl (pH 8.0), 200 mM NaCl, 20 mM EDTA, 1% SDS, 0.5% Na-deoxycholic acid, 0.01% NP-40, 200 mM sodium orthovanadate, and 100 mM phenylmethylsulfonyl fluoride. Equal amounts of protein (40 μg) were fractionated by SDS-polyacrylamide gel electrophoresis and transferred to nitrocellulose membranes. The membrane was blocked at room temperature with 5% nonfat milk in Tris-buffered saline (TBS, pH 7.6) containing 0.05% Tween 20, and then washed with TBS-Tween. Antibodies against ICAM-1, p-38, p-p38, p-MEK, p-pMEK, actin, and GAPDH were incubated at 4 °C overnight at a 1:1000 dilution in 5% bovine serum albumin in TBS-Tween. Caveolin-1

antibody was incubated at 1:10,000 dilutions in the same conditions. Horseradish peroxidase-conjugated secondary antibodies were incubated for 1 h at a 1:3000 dilution. Bands were visualized by using ECL or ECL plus immunoblotting detection reagents (Amersham Biosciences, Buckinghamshire, England). Bands were quantified using UN-SCAN-IT gel Version 5.1 (Silk Scientific, Orem, UT) and normalized to actin or GAPDH protein expression.

Monocyte Adhesion

Human THP-1 monocytes (50,000 cells) were activated with TNF-α dissolved in water (10 min) and loaded with the fluorescent probe calcein (Molecular Probes, Carlsbad, CA). HUVECs were pretreated with DMSO or β-NF for 16 h and then treated for 8 h with DMSO, B[a]P (3 or 10 μM), or TNF-α. Monocytes were added to treated endothelial cell monolayers and incubated (30 min), allowing for monocyte adhesion. Unbound monocytes were washed away, and the monolayer was fixed with 1% glutaraldehyde. Attached fluorescent monocytes were counted using a fluorescent microscope (Olympus IX70, Center Valley, PA).

Flow Cytometry

HUVEC were pretreated with β-NF for 16 h and then pretreated with inhibitors to p38 MAPK (SB203580; 10 μM) or MEK (PD98059; 20 μM) for 1 h. After pretreatment, the cells were treated with DMSO or B[a]P (10 μM) for 24 h. HUVEC were washed with PBS, and then removed with trypsin. Cells were centrifuged, washed, and then incubated in 3% bovine serum albumin containing the primary antibody for ICAM-1 (2μg/ml) for 30 min. Cells were then centrifuged, washed, and then resuspended in AlexaFluor 488 labeled secondary antibody (3μg/ml) for 20 min. HUVECs were then washed and stained with propidium iodide (2 μg/ml) for 5 min in order to gate for live cells. Cells were then analyzed by the University of Kentucky Flow Cytometry Facility using a Becton-Dickinson FacsCalibur cell analyzer.

Electrophoretic Mobility Shift Assay

HUVEC were pretreated with α-NF or β-NF for 16 h and then treated with DMSO or B[a]P (10 μM) for 4 h. To extract nuclear protein, cells were incubated with buffer A (10 mM HEPES pH 7.9, 10 mM KCl, 0.1 mM EDTA, 1 mM DTT, 0.5 mM PMSF) for 15 min on ice and then 10% NP-40 was added. After 90-95% of cells were lysed and centrifuged, nuclei were lysed by incubation and shaking for 5 min in buffer B (20 mM HEPES, 0.4 M NaCl, 1 mM EDTA, 1 mM DTT,

1 mM PMSF). Activator protein-1 (AP-1) DNA binding was measured by the Pierce LightShift Chemicluminescent EMSA Kit (Rockford, IL) as directed by manufacturer's protocol. Briefly, 3 µg nuclear protein incubated with 50 ng/µl Poly (dI•dC) and 20 fmol biotin end-labeled AP-1 DNA is separated on pre-run native polyacrylamide gel. The binding reaction is then transferred and cross-linked to nylon membrane. Finally, biotin-labeled DNA is detected via a Streptavidin-Horseradish Peroxidase Conjugate and Chemiluminescent substrate. Control reactions were conducted containing no protein extract or 200-fold molar excess of unlabeled DNA. AP-1 specificity was determined by a supershift of the band after addition of c-Jun antibody to the binding reaction.

siRNA Transfection

Double stranded small interfering RNA targeted to caveolin-1 and AhR were synthesized by Dharmacon Research (Lafayette, CO) as duplexed, 2'-unprotected, desalted, and purified siRNA as described previously [227, 228]. The sequences were as follows: Caveolin-1 5'-CCAGAAGGGACACACAGdTdT-3' and 5'-AACAUCUACAAGCCCAACAACdTdT-3'; Caveolin-1 control 5'-AGAGCGACUUUACACACdTdT-3'; AhR 5'-GUCGGUCUCUAUGCCGCdTdT-3'; and AhR mutated control 5'-CUCGGUCUCUAUGCCGC-3'. HUVEC were transfected with control or gene-targeted siRNA for 4 h using the GeneSilencer Reagent (Genlantis, San Diego, CA) and OptiMEM serum-free media (Invitrogen) at a final concentration of 120 nM (AhR) or 80 nM (caveolin). After 24 h, cells were pretreated with α-NF or β-NF for 16 h and then treated with DMSO or B[a]P (10 µM) for 24 h. Whole cell lysate was probed for ICAM-1, GAPDH, and caveolin-1 or AhR by immunoblot analysis.

Statistical Analysis

Values are reported as means ± SE of at least three independent groups. Comparisons between treatments were made by one-way or two-way analysis of variance followed by Tukey multiple comparison tests using GraphPad Prism 4.0 software (GraphPad Software, San Diego, CA). Statistical probability of $p<0.05$ was considered significant.

3.4 Results

B[a]P increases ICAM-1 and monocyte adhesion only after AhR activation

HUVEC were shown to have a responsive AhR by measuring activation of cytochrome P4501A1 after treatment with β-NF (Figure 3.1A). HUVEC were pre-treated with or without the AhR agonist β-NF and then treated with B[a]P or fluoranthene (FL) at 10-25 μM (Figure 3.1B and 3.1C). Exposure to B[a]P increased protein expression of ICAM-1 only after pre-treatment with β-NF (Figure 3.2B). These effects were specific because FL did not affect ICAM-1 protein levels regardless of pre-treatment with β-NF.

To verify the necessity of AhR in β-NF-induced ICAM-1 expression, the receptor was knocked down using gene silencing technology. Transfection with AhR siRNA resulted in over 90% reduction in AhR protein for 72 h (data not shown). These cells were then pre-treated with β-NF or the AhR antagonist, α-NF, and then treated with B[a]P or DMSO (Figure 3.2). In cells transfected with the control siRNA, exposure to B[a]P increased protein expression of ICAM-1 only after pre-treatment with β-NF, but not when pre-treated with α-NF. This response was eliminated when the cells were transfected with specific AhR siRNA, further signifying the requirement of this nuclear receptor.

A similar response pattern was seen after measurement of monocyte adhesion. B[a]P increased the adhesion of fluorescently labeled monocytes to the treated endothelium at 3-10 μM only in the groups pre-treated with β-NF (Figure 3.3). TNF-α was used as a positive control for monocyte adhesion.

B[a]P induced ICAM-1 is mediated by MEK/p38/AP-1

ICAM-1 expression has been shown to be stimulated by a number of signaling pathways including the MAPK cascades, AP-1, NF-κB, as well as a number of other proteins. HUVEC pretreated with β-NF and then treated with B[a]P significantly increased the phosphorylation, and thus the activation of MEK and p38-MAPK, while not changing the total protein levels of these kinases (Figure 3.4A and 3.4B). To confirm these findings, HUVEC were pretreated with β-NF and inhibitors of these kinases. Both SB203580 and PD98059, inhibitors of MEK and p38, respectively, decreased the induction of ICAM-1 protein elicited by β-NF/B[a]P treatment (Figure

3.4C). Phosphorylation of other MAPK family members, such as ERK1/2, was unaltered by treatment with β-NF/B[a]P (data not shown).

The activation of transcription factors downstream of the MAPK cascade was also investigated. Although treatment with B[a]P increased NF-κB DNA binding, this effect was not dependent upon β-NF pretreatment (data not shown), and thus was unlikely to be involved in B[a]P-induced stimulation of ICAM-1. On the other hand, HUVEC pretreated with β-NF but not α-NF (AhR antagonist), and then exposed to B[a]P increased the AP-1 DNA binding (Figure 3.5A). AP-1 is formed of homo- or heterodimers of Jun and Fos proteins. Phosphorylation of cJun proximal the transactivation domain is required for AP-1 containing cJun to be efficiently activated [140]. Therefore, to connect the activation of AP-1 with the activation of upstream MAPK cascades, cells were pretreated with the inhibitors to MEK (PD98059) and p38 (SB203580) and phosphorylation of cJun was measured. A 2 h exposure to βNF/B[a]P increased the phosphorylation of cJun and p38 and MEK inhibitors markedly blocked this effect (Figure 3.5B).

Caveolae are necessary for B[a]P induced ICAM-1

Caveolin-1, the main structural protein of caveolae, is able to concentrate signaling molecules together within caveolae microdomains and has been shown to be necessary for activation of p38-MAPK [142, 144]. Therefore, the role of caveolin-1 in B[a]P-mediated stimulation of ICAM-1 expression was also explored. HUVEC transfected with caveolin-1 siRNA were found to have 3% of the caveolin-1 protein compared to control transfected cells (Figure 3.6). Importantly, silencing of caveolin-1 by siRNA in HUVEC eliminated the ability of β-NF/B[a]P to induce ICAM-1 protein expression (Figure 3.6). Similar to the pattern observed in earlier experiments, ICAM-1 was only induced in cells that were pretreated with β-NF and then treated with B[a]P, whereas this was not the case in cells pretreated with α-NF. Treatment with β-NF/B[a]P did not change the protein levels or phosphorylation status of caveolin-1 (data not shown).

A

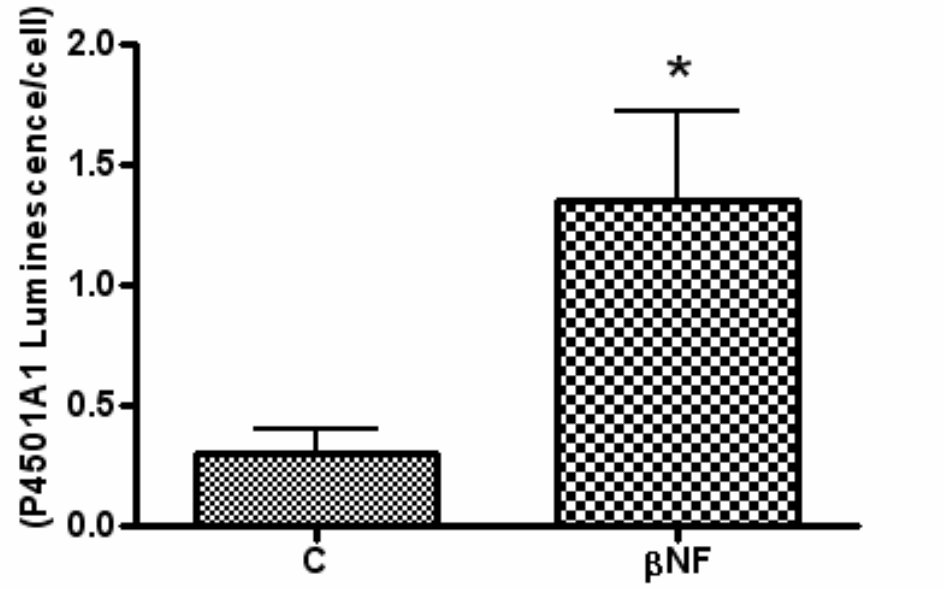
(P4501A1 Luminescence/cell)
2.0
1.5
1.0
0.5
0.0
*
C
βNF

B

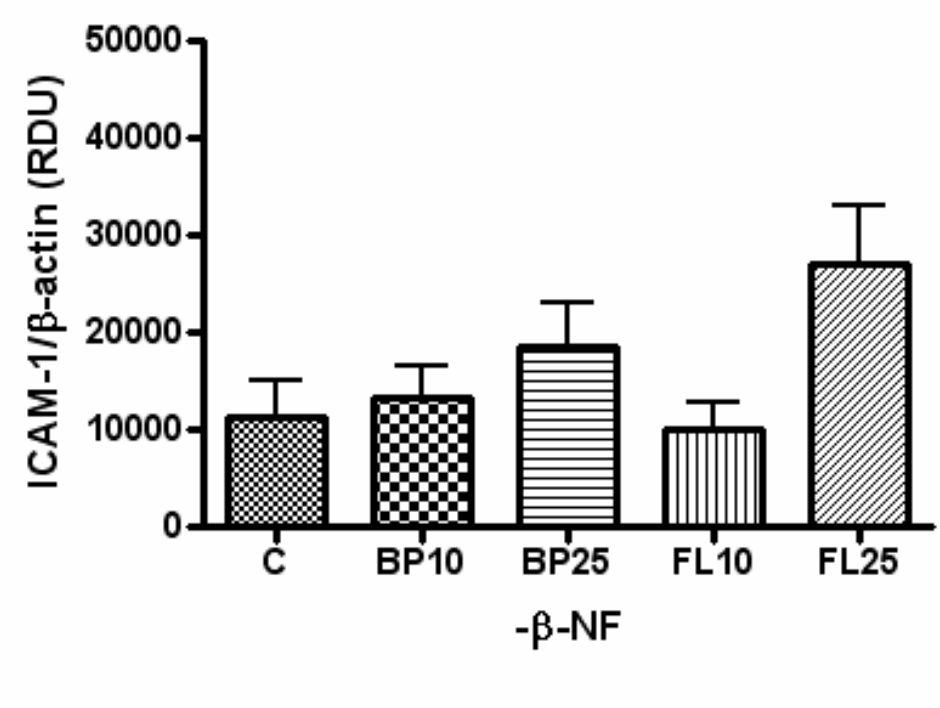
ICAM-1/β-actin (RDU)
50000
40000
30000
20000
10000
0
C
BP10
BP25
FL10
FL25
-β-NF

C

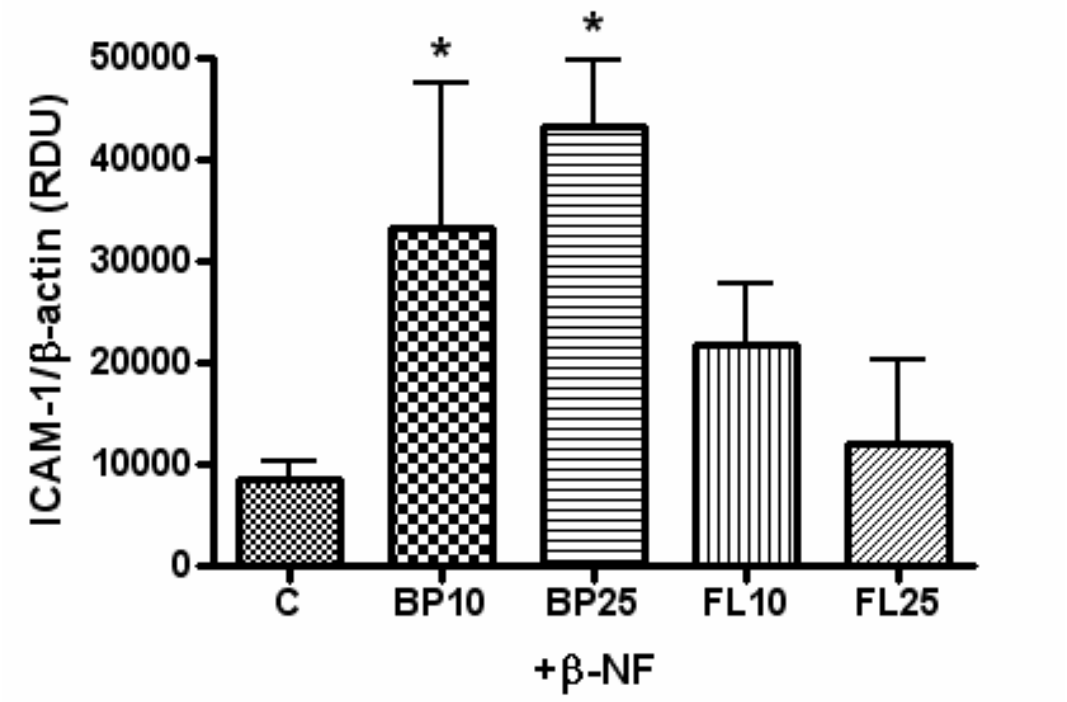

Figure 3.1: B[a]P induces intercellular adhesion molecule-1 only after aryl hydrocarbon receptor activation. HUVEC were treated with β–NF (1 μM) for 16 h and then measured for cytochrome P4501A1 activity by P450-Glo Assay. Cell number was measured by CellTiter-Glo Assay (A). Bars represent mean ± SEM of at least three independent experiments measuring P4501A1 Assay luminescence normalized to cell number. HUVEC were pretreated with DMSO (B) or 1 μM β-NF (C) for 16 h and then treated with either DMSO, B[a]P (BP), or fluoranthene (FL) at 10 and 25 μM for 24 h. Whole cell lysate was probed by immunoblot analysis for ICAM-1 and β-actin and measured by densitometry. Bars represent mean ± SE of at least three independent experiments.

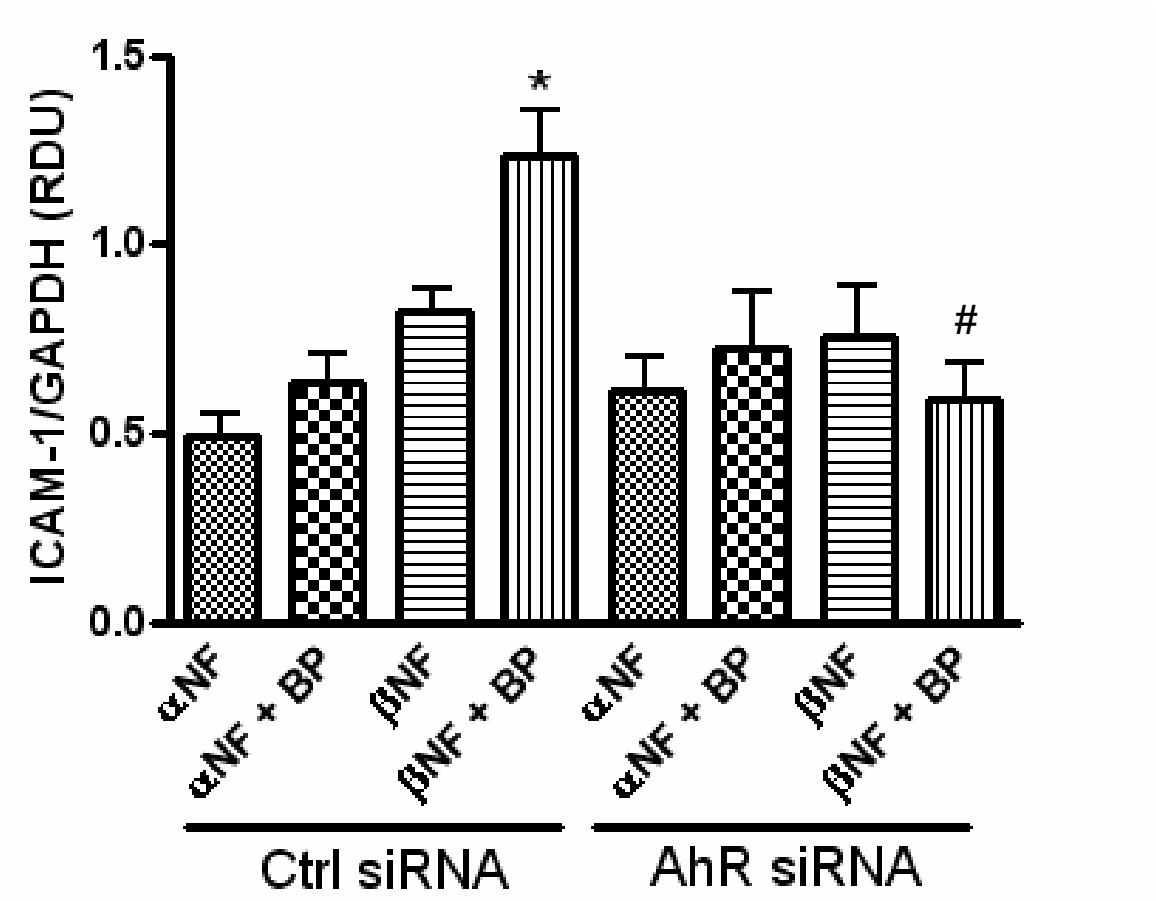

Figure 3.2: Absence of AhR reduces B[a]P-induced ICAM-1 expression. HUVEC were transfected with control siRNA or specific AhR siRNA using the GeneSilencer Transfection Kit, which knocked down AhR expression by 92%. After 24 h, cells were pretreated with α-NF or β-NF (1 μM) for 16 h and then treated with DMSO or B[a]P (10 μM) for 24 h. Whole cell lysate was probed for ICAM-1, GAPDH, and AhR by immunoblot analysis and measured by densitometry. Bars represent mean ± SE of at least three independent experiments. * $p<0.05$ compared to β-NF alone. # $p<0.05$ compared to same group transfected with AhR siRNA.

A

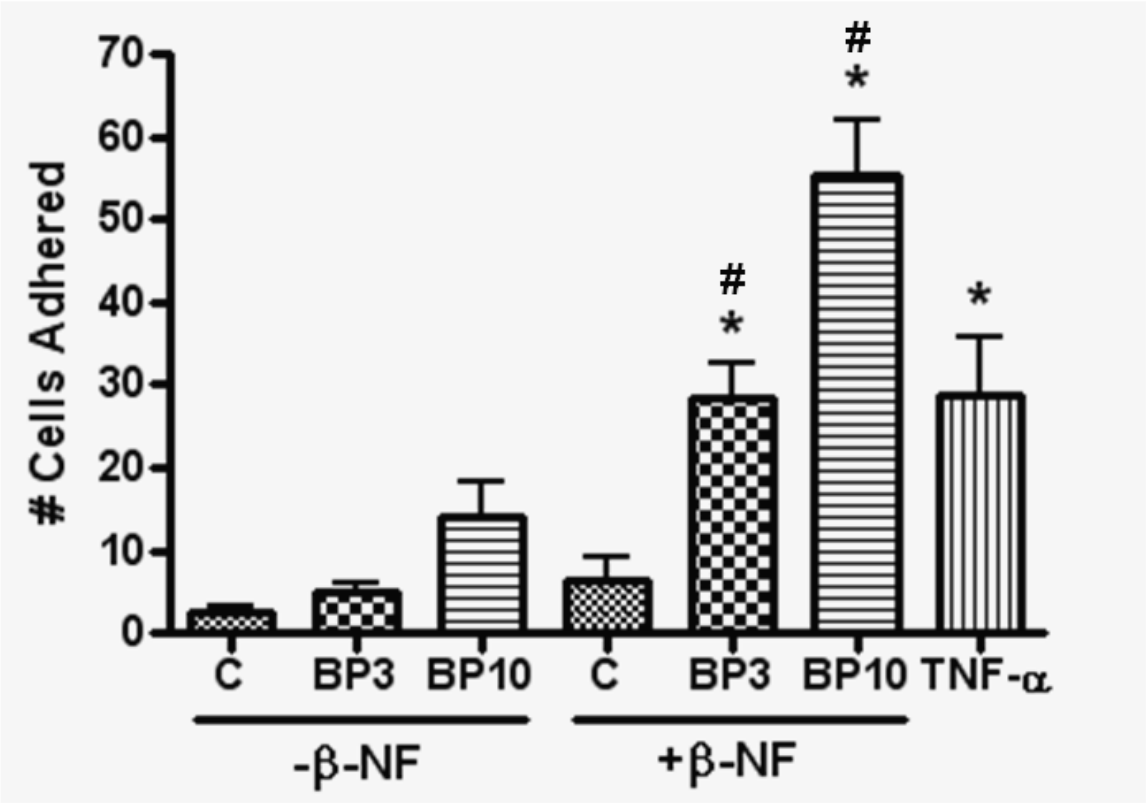

Figure 3.3: B[a]P induces monocyte adhesion only after AhR activation. HUVEC were pretreated with DMSO or β-NF (1 μM) for 16 h and then treated with DMSO or B[a]P (BP) at 3 and 10 μM for 24 h. THP-1 monocytes were activated by TNF-α treatment and then labeled with calcein. Monocytes were allowed to adhere to the treated HUVEC for 30 min and then unbound cells were washed off. Bound monocytes were visualized and counted by fluorescent microscopy (A). Bars represent mean ± SE of three independent experiments. Images are representative microscopic fields showing bound monocytes in white (B). * $p<0.05$ compared to control. # $p<0.05$ compared to same group treated with β-NF.

B

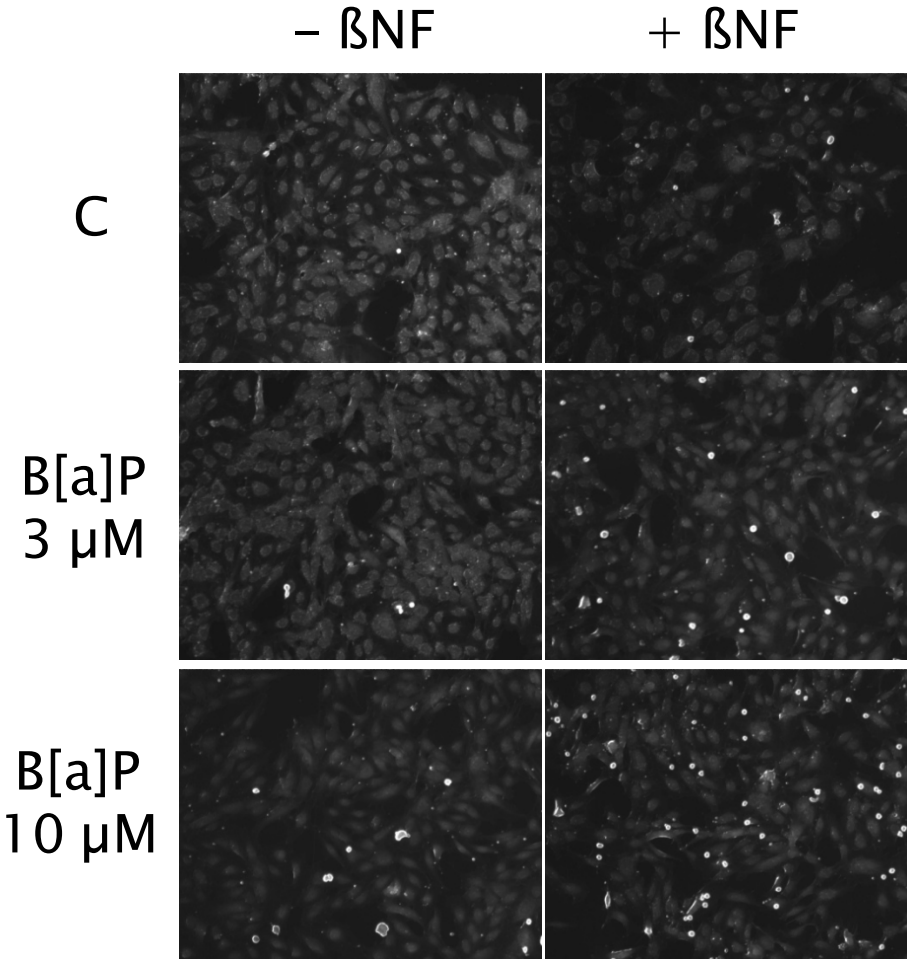

A

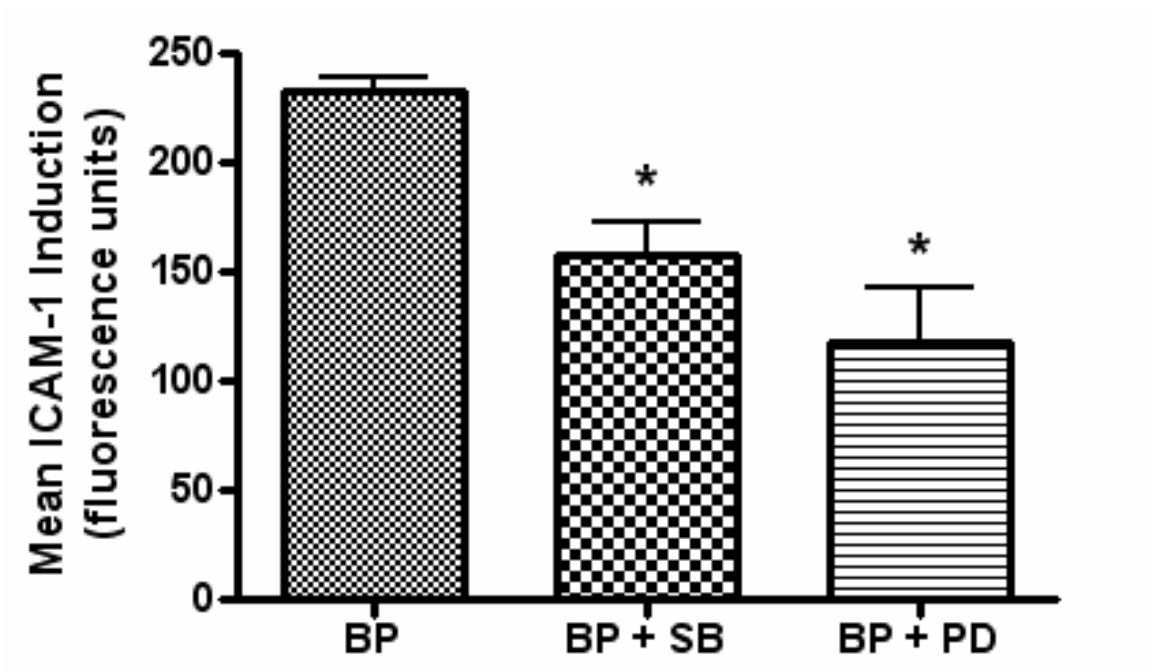
Mean ICAM-1 Induction (fluorescence units)
250
200
150
100
50
0
*
*
BP
BP + SB
BP + PD

B

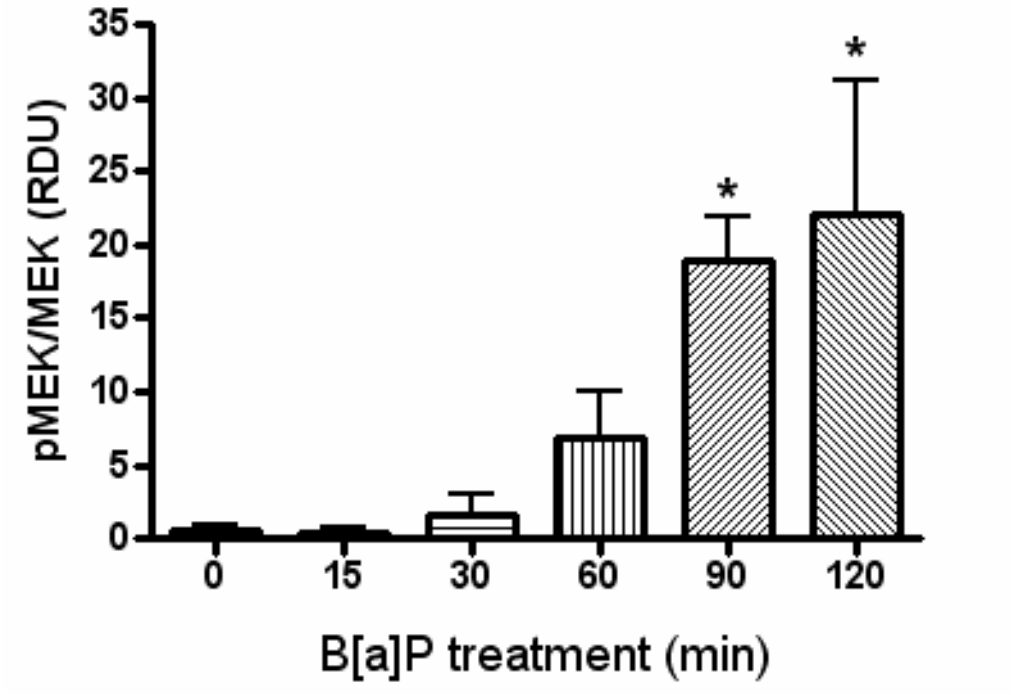
pMEK/MEK (RDU)
35
30
25
20
15
10
5
0
*
*
0
15
30
60
90
120
B[a]P treatment (min)

C

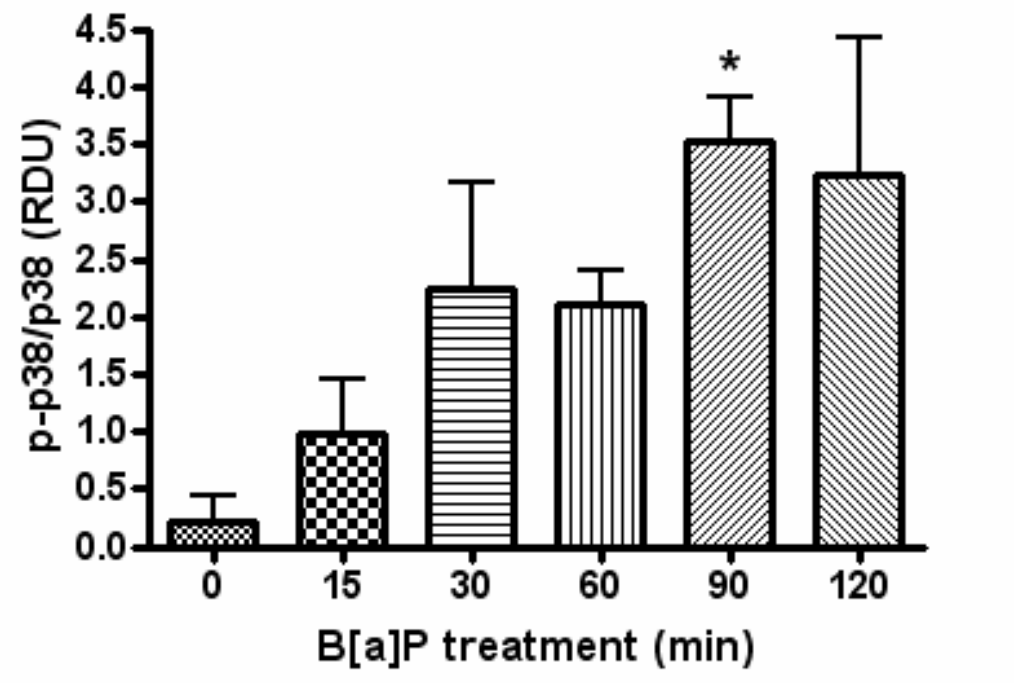

Figure 3.4: B[a]P activates MEK and p38. HUVEC were pretreated with β-NF (1 μM) for 16 h and then treated with DMSO or B[a]P (10 μM) for 15 – 120 min. Whole cell lysate extracts were probed by immunoblot analysis for phosphorylated MEK, total MEK (A), phosphorylated p38, and total p38 (B). Bars represent mean ± SEM of at least three independent experiments. HUVEC were pretreated with β-NF for 16 h and then pretreated with the inhibitors SB203580 (10 μM) or PD98059 (20 μM) for 1 h. Cells were then treated with DMSO or B[a]P (BP, 10 μM) for 24 h. ICAM-1 was measured by flow cytometry (C). Bars represent mean ± SE of the increase in ICAM-1 due to B[a]P treatment. * $p<0.05$ compared to control.

A

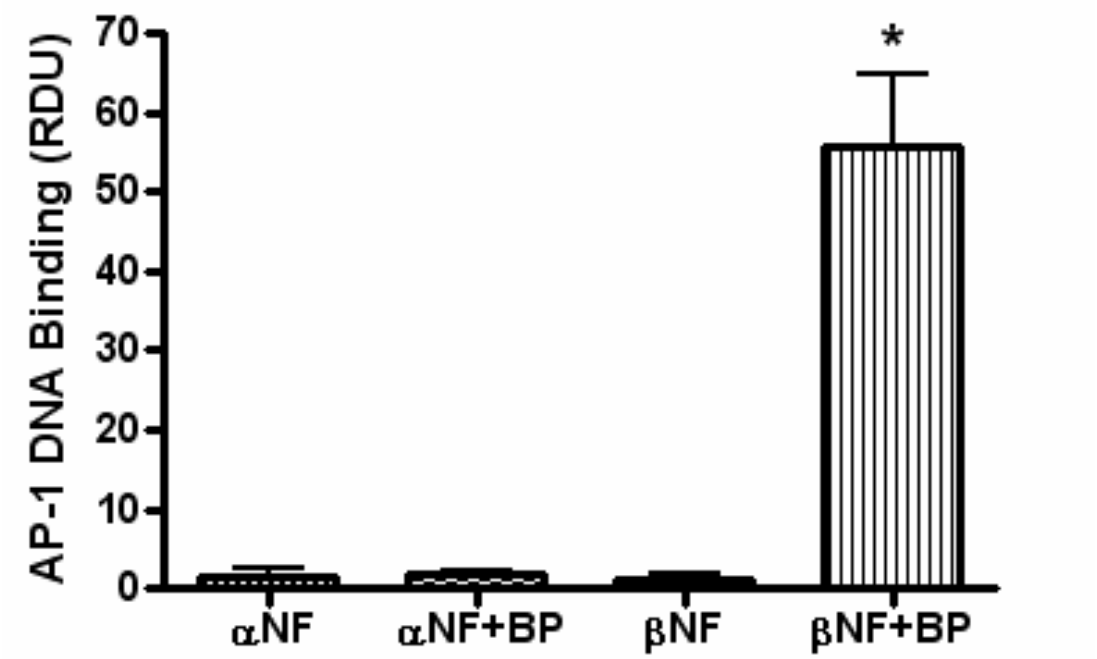

Figure 3.5: B[a]P activates activator protein-1 only after AhR activation and requires MEK and p38. HUVEC were pretreated with α-NF (AhR antagonist) or β-NF (AhR agonist) for 16 h and then treated with DMSO or B[a]P (10 μM) for 4 h. Nuclear extracts were probed for AP-1 DNA binding (A). HUVEC pretreated with βNF for 16 h were then pretreated with inhibitors to MEK (PD98059, 20 μM) or p38 (SB203580, 10 μM) for 1 h. After pretreatment, cells were treated with DMSO or B[a]P (10 μM) for 120 min. Whole cell lysate was probed by immunoblot analysis for phosphorylated cJun and total cJun and measured by densitometry (B). Bars represent mean ± SE of at least three independent experiments. * $p<0.05$ compared to control. # $p<0.05$ compared to BP treated group.

B

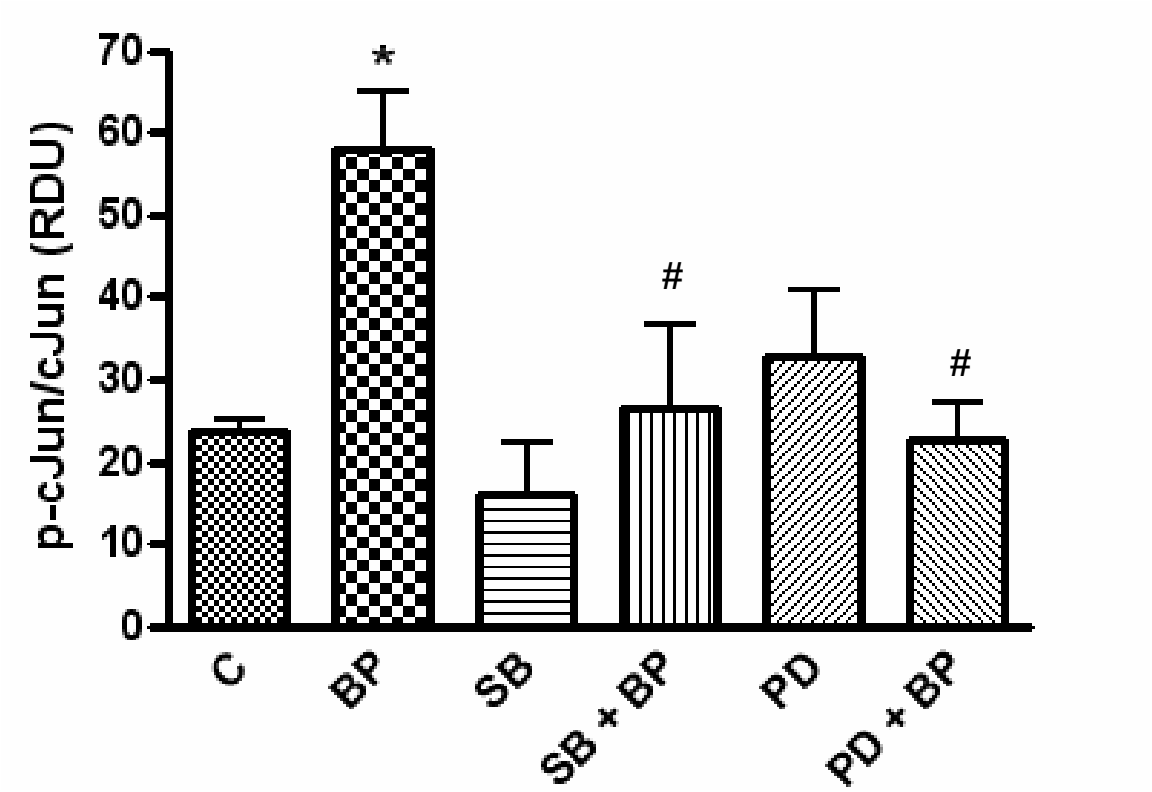

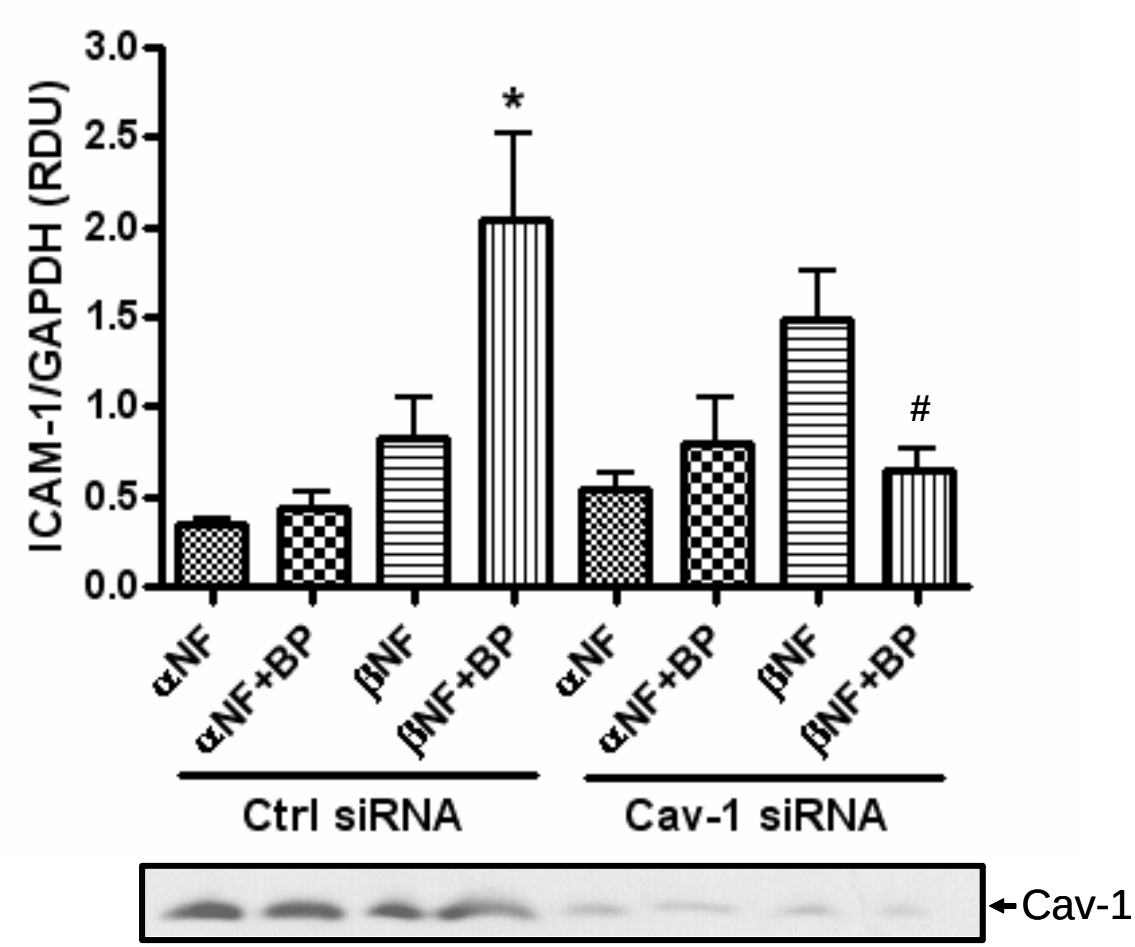

Figure 3.6: B[a]P does not induce ICAM-1 after caveolin-1 silencing. HUVEC were treated with control or caveolin-1 siRNA for 4 h using the GeneSilencer Transfection Kit. After 24 h, cells were pretreated with α-NF or β-NF for 16 h and then treated with DMSO or B[a]P (10 μM) for 24 h. Whole cell lysate was probed for ICAM-1, GAPDH, and caveolin-1 by immunoblot analysis and measured by densitometry. Bars represent mean ± SE of at least three independent experiments. The bands below are representative blots of caveolin-1. * $p<0.05$ compared to β-NF alone. # $p<0.05$ compared to same group transfected with Cav-1 siRNA.

3.5 Discussion

Much attention has been placed on the role of air pollution and the included organics in the development and progression of cardiovascular diseases such as atherosclerosis [53-56, 220]. B[a]P is a well studied carcinogen that has been shown to lead to atherosclerosis in animal models [120-122] and epidemiological data [119]. We suggest a mechanism by which B[a]P is contributing to atherosclerosis by increasing endothelial dysfunction and enhancing adhesiveness. The data clearly show that B[a]P is able to increase ICAM-1 in primary human endothelial cells and that these events require functional AhR and caveolin-1. The data also illustrate that β-NF/B[a]P induces ICAM-1 by signaling through MEK, p38 MAPK, and AP-1 leading to increased adhesion of monocytes to the activated endothelium.

PAHs are ubiquitous environmental contaminants. Humans are exposed through ingestion of contaminated foods and inhalation of polluted air. Both sources are a consequence of incomplete combustion processes. Animal studies have shown enhanced atherogenesis after PAH exposure for a number of years. More recently, hyperlipidemic mice treated with B[a]P have developed more severe atherosclerotic plaques [122, 123]. Interestingly, these plaques were characterized as having an increased content of inflammatory leukocytes such as macrophages and lymphocytes. Subsequent literature showed that B[a]P increased expression of MCP-1 in these mice, which was eliminated in vitro by AhR antagonist treatment [124]. MCP-1 plays a critical role in recruitment of leukocytes to the endothelium; however cellular adhesion molecules such as ICAM-1 are responsible for diapedesis of these inflammatory cells into the vessel intima. After adhesion molecules bind circulating leukocytes, they trans- or para-cellularly migrate through the endothelium, after which they can differentiate and take up oxidized lipid particles. The cells then transform into foam cells which create the plaque that is hallmark to atherosclerosis [7].

PAHs are a large class of organic compounds that vary by size and structure, for example the number and shape of rings [96]. Two PAHs were examined in this paper, B[a]P and FL. We show that B[a]P can significantly induce ICAM-1 after pretreatment with an AhR inducer, but not after pretreatment with an AhR antagonist or after AhR knockdown. However, FL was not able to increase ICAM-1 either with or without AhR activation. B[a]P is a ligand to AhR, enabling its own metabolism by AhR-controlled enzymes such as CYP1A1, CYP1A2, CYP1B1, glutathione S-

transferase, and UDP-glucuronyltransferase. B[a]P will induce the AhR enzymes CYP1A1 and CYP1B1, whereas FL is generally inactive or inhibitory to AhR [229, 230]. As expected, AhR activation did not enhance the ability of FL to induce pro-inflammatory mediators in HUVEC. We hypothesize that treatment with β-NF induce the AhR-controlled enzymes creating an existing metabolically active environment for when B[a]P is added to the culture. B[a]P may be able to induce ICAM-1 on it's own since it can induce its own metabolism, but this may require longer time points.

It is well understood that the carcinogenic nature of B[a]P is due to activation by P450s and epoxide hydrolases to the diol epoxide, (±)-anti-7β,8α-dihydroxy-9α,10α-epoxy7,8,9,10-tetrahydrobenzo[a]pyrene, however B[a]P can also be metabolically activated to radical cations, as well as reactive and redox active *o*-quinones [97]. Our data demonstrate that AhR is necessary for the induction of ICAM-1 protein, suggesting that B[a]P must be metabolically activated by AhR controlled enzymes. The data do not propose a specific metabolite as the active compound. B[a]P is atherogenic irrespective of its mutagenic properties [123], which may suggest that the diol epoxide is not the metabolite causing these effects. ICAM-1 transcription can be controlled by redox sensitive signaling pathways, of which the MAPK and AP-1 are examples. The B[a]P *o*-quinone can be formed by oxidation from a catechol, thus releasing H_2O_2 and O^{2}-, and can also undergo reduction to reform the catechol, thus establishing a futile redox cycle in which amplified reactive oxygen species (ROS) are produced [97]. It is possible that this increased oxidative stress is causing the induction of the inflammatory ICAM-1, making the *o*-quinone a potential atherogenic metabolite. The authors and others have shown that B[a]P produces more ROS after AhR activation (data not shown) [231]. The identity of the active metabolite is only speculative and requires further examination.

Interestingly, when HUVEC were pretreated with the CYP450 inhibitor SKF525-A, ICAM-1 induction was increased (data not shown). Similar phenomenon was seen in killifish treated with hydrocarbons [232, 233]. It was suggested that blocking CYP450 extended the normally relatively short half-life of B[a]P, prolonging the AhR agonism and presence of reactive intermediates. As was mentioned above, AhR is responsible for inducing a number of both Phase I and Phase II metabolizing enzymes. It is possible that B[a]P is metabolized by further monoxygenases to generate long-lived reactive metabolite(s). Thus, knockdown of AhR might

eliminate the secondary metabolizing enzymes that are able to create the active B[a]P derivative(s).

ICAM-1 expression has been linked with activation of the MAPK pathways [133, 234, 235]. In this study, we demonstrated that B[a]P induced ICAM-1 by activating MEK/p38-MAPK/AP-1. In contrast, neither ERK nor NF-κB seemed to contribute substantially to the ICAM-1 induction. B[a]P and its metabolites have been shown to induce MEK and p38 in other cellular systems [134-136, 236]. The inhibitors employed in the present study have been widely used as specific blockers for MEK and p38; however it has been suggested that they are somewhat ubiquitous and inhibit activation of other MAPK and enzymes [237]. For example, it has even been shown that SB203580 can block CYP1A1 induction by TCDD [238, 239]. For this reason, the inhibitors were used as secondary experiments with phosphorylation of the MAPK measured as well.

Caveolae are 50-100 nm nonclathrin-coated plasma membrane microdomains that are enriched in cholesterol and glycosphingolipids and constitute a well studied subset of lipid rafts. They are particularly abundant in endothelial cells [147] and play an important role in membrane traffic and cellular signal transduction. Caveolae have been reported to contain a number of proteins including receptors and signaling molecules like G-protein coupled receptors, tyrosine kinases, and serine/threonine kinases [147]. Disruption of these structures has been shown to lead to interruption of normal cellular signaling cascades, including the MAPK proteins. Disruption of caveolae by methyl-beta-cyclodextrin or by caveolin-1 knockout inhibits p38-MAPK nuclear translocation and activation [142, 144]. Caveolin-1 is the principal structural component of caveolae and drives caveolae formation by oligimerization with itself and other caveolins and interaction with cholesterol in the membrane [146, 150]. Deletion of caveolin-1 results in a complete loss of caveolae, and mice lacking this protein are protected against the development of atherosclerosis [151]. Our data demonstrate that the deletion of caveolin-1 disrupts the induction of ICAM-1 from B[a]P. Interestingly, it has been proposed that caveolin-1 could play a critical role in the adhesion process either as a signaling platform or as a structural participant in the building of the transcytotic channel [35, 154]. Adhesion molecules such as ICAM-1 once activated, redistribute and cluster into transmigratory cup structures which allow for trans-cellular and trans-endothelial migration of leukocytes from the lumen [34, 39,

156, 240]. It has been recognized that ICAM-1 is translocated to lipid rafts once activated [155, 156] and that caveolae play a direct role in the transcytosis process [35, 154].

In summary, data from the current experiments demonstrate that B[a]P is able to increase ICAM-1 in human endothelial cells after activation by AhR. In the same manner, B[a]P is able to increase monocyte adhesion to the treated endothelium only after AhR activation. The induction of ICAM-1 is through activation of the MEK/p38-MAPK/AP-1 signaling cascade and requires functional caveolae. These data provide a possible mechanism of increased endothelial adhesiveness to the body of literature showing that exposure to PAHs like B[a]P are a risk factor for cardiovascular diseases such as atherosclerosis.

Chapter Four. Flavonoids Protect Against Intercellular Adhesion Molecule-1 Induction by Benzo[a]pyrene

4.1 Synopsis

Dietary changes are an attractive means of protecting against environmental chemical exposure. Exposure to benzo[a]pyrene (B[a]P) is a risk factor for cardiovascular disease events. It has recently been shown that B[a]P can increase intercellular adhesion molecule-1 (ICAM-1) in endothelial cells, a probable means of promoting cardiovascular disease. This study investigated the ability of flavonoids to protect against B[a]P-induced ICAM-1. It was shown that only flavonoids that contain a 4' B-ring hydroxyl substitution and a 2-3 C-ring double bond were protective. These data suggest that selected bioactive compounds can decrease pro-inflammatory properties of environmental chemicals such as B[a]P.

4.2 Introduction

Air pollution is a complex mixture of particles, gases, and organics. The organic fraction is comprised in part by polycyclic aromatic hydrocarbons (PAHs) in which B[a]P is a member. B[a]P is a probable human carcinogen that has been linked to the progression of cardiovascular diseases, such as atherosclerosis in both humans and animal models [119-121, 123]. We have shown that B[a]P increases ICAM-1 expression in human endothelial cells through an aryl hydrocarbon receptor (AhR) and caveolae dependent mechanism (Chapter 3). ICAM-1 is an immunoglobulin type protein that plays a crucial role in the initiation of atherosclerosis by binding circulating immune cells and causing their migration into the intimal layer of the vessel, culminating in inflammatory foam cell formation [21, 23].

Treatment of environmental-contaminant induced toxicity is a complicated process. Diet has been suggested as a feasible and economical alternative as a preventative measure [241]. One such bioactive compound found extensively in fruits and vegetables is a class of polyphenolic compounds, namely flavonoids [242]. Flavonoids are divided into groups of compounds, among which are flavones, flavanones, and flavonols. Flavonoids are extensively studied for their antioxidant and anti-inflammatory abilities. However, various studies have shown that flavonoids can be cardioprotective as antioxidants, but also via antioxidant-

independent mechanisms [168, 185]. It was hypothesized that flavonoids would protect vascular endothelial cells against B[a]P-induced ICAM-1 induction.

4.3 Materials and Methods

Materials

Anti-ICAM-1antibody (clone RR1/1) and secondary AlexaFluor 488 conjugated anti-mouse were purchased from Invitrogen (Carlsbad, CA). B[a]P, beta-naphthoflavone (β-NF), kaempferol, apigenin, chrysin, naringenin, hesperetin, galangin, quercetin, luteolin, and propidium iodide were purchased from Sigma Aldrich (St. Louis, MO).

Cell Culture

Primary human umbilical vein endothelial cells (HUVEC) were used in these experiments as model for vascular inflammatory diseases. Cells were isolated from human umbilical cord veins as explained previously [195]. Human umbilical cords were obtained from the University of Kentucky Labor and Delivery unit and utilized until passage 5. HUVEC were cultured in M199 media (GIBCO Laboratories, Grant Island, NY) supplemented with FBS (Hyclone Laboratories, Logan, UT) as described previously [195].

Flow Cytometry

HUVEC were pre-treated with β-NF (1 μM) and either DMSO or the flavonoid (5 μM) for 16 h. After pretreatment, the cells were treated with DMSO or B[a]P (10 μM) for 24 h. HUVEC were washed with PBS, and then removed from culture plates with trypsin. Cells were centrifuged, washed, and then incubated in 3% bovine serum albumin containing the primary antibody for ICAM-1 (2μg/ml) for 30 min. Cells were then centrifuged, washed, and resuspended in AlexaFluor 488 labeled secondary antibody (3μg/ml) for 20 min. HUVEC were then washed and stained with propidium iodide (2 μg/ml) for 5 min in order to gate for live cells. Cells were then analyzed by the University of Kentucky Flow Cytometry Facility using a Becton-Dickinson FacsCalibur cell analyzer.

Antioxidant Capacity

Flavonoids were analyzed for their antioxidant capacity by the measurement of their ferric reducing ability as explained previously [172, 243]. Briefly, flavonoids dissolved in 10% FBS media were combined with a working reagent (1.66 mM $FeCl_3$, 0.83 mM tripyridyltriazine, 300 mM acetate buffer pH 3.6) and the change of absorbance at 593 nm was measured by micro-plate reader (Molecular Devices, SpectroMax M2).

Statistical Analysis

Values are reported as means ± SE of at least three independent groups. Comparisons between treatments were made by one-way analysis of variance followed by Tukey multiple comparison tests using GraphPad Prism 4.0 software (GraphPad Software, San Diego, CA). Statistical probability of $p<0.05$ was considered significant.

4.4 Results and Discussion

A number of epidemiological studies have shown that plant-rich diets are protective against chronic diseases, such as cardiovascular disease [157, 242]. It is also true that air pollution and the PAHs, such as B[a]P, that are contained within, lead to increases in cardiovascular disease events [54, 119]. The present study reveals that select flavonoids can protect against B[a]P-induced ICAM-1 induction (Figure 4.2), which has been shown to be a critical step in the development of cardiovascular diseases. Interestingly, two functional groups appear to be necessary to elicit the protective nature of the compounds, a 2-3 C-ring double bond and a 4' B-ring hydroxyl substitution. Flavonoids lacking either one of these functional groups were not protective, evidenced by hesperetin, chrysin, naringenin, and galangin (Figures 4.1 and 4.2). Past studies have been conducted on the protective role of flavonoids against cytokine induced adhesion molecule expression [172, 180]. Similarly, the 2-3 C-ring unsaturation was shown to be necessary and similarly apigenin was found to be a potent protector [172, 180]. However, most of these studies used high, physiologically irrelevant concentrations of flavonoids (up to 50 μM) and none of them have investigated other inducers of adhesion molecules such as environmental contamination.

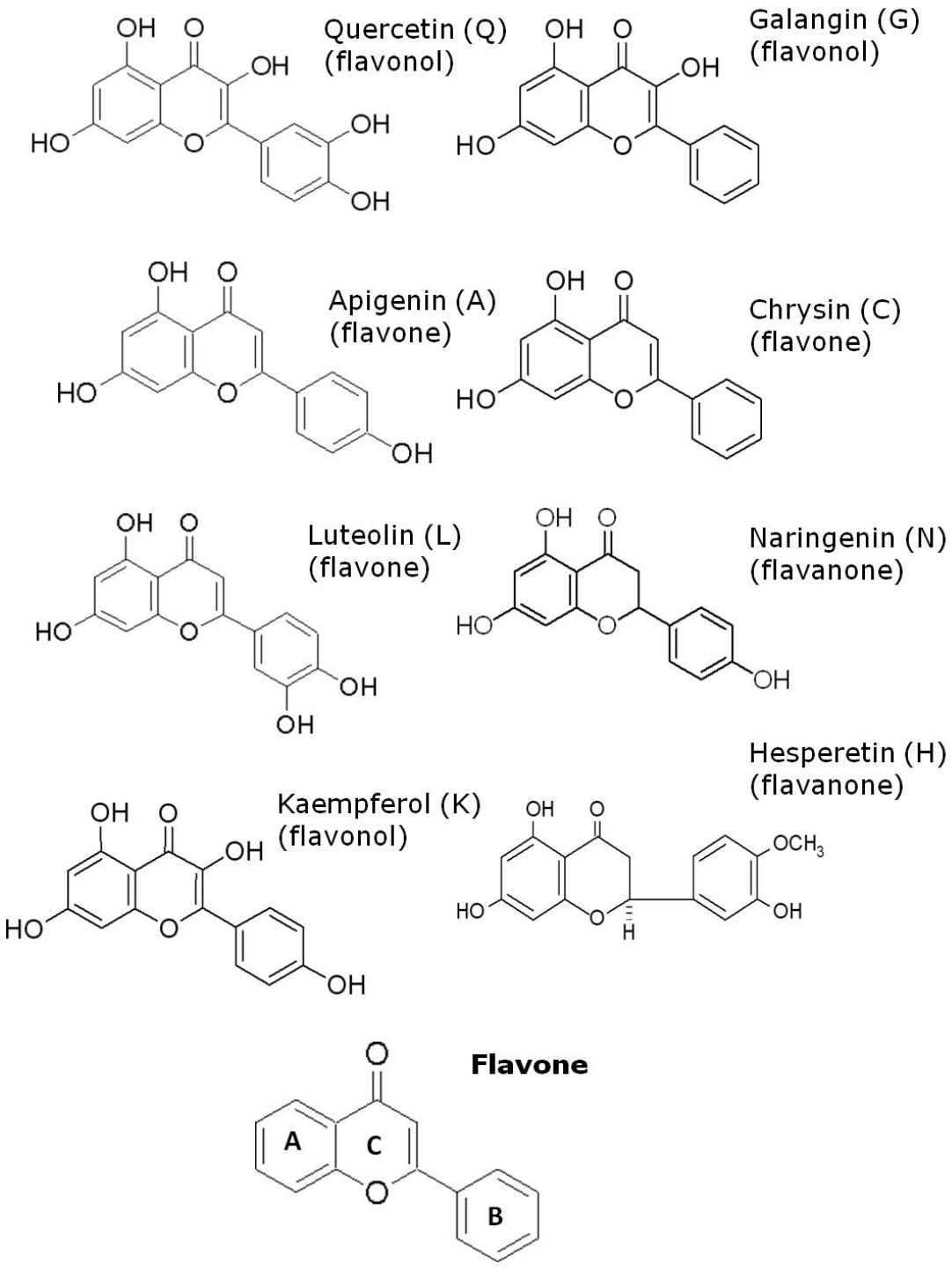

Figure 4.1: Structure of flavonoids used in these studies

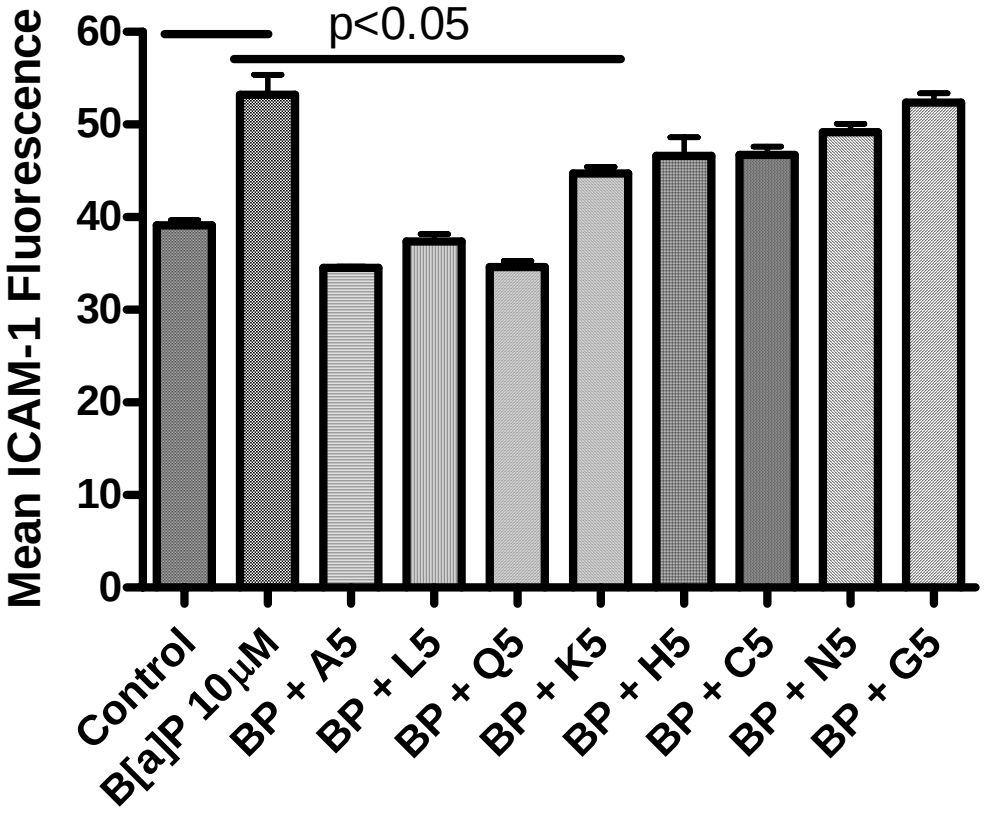

Figure 4.2: Select flavonoids protect against B[a]P-induced ICAM-1. HUVEC were pre-treated with 1 μM β-NF and 5 μM flavonoids (apigenin (A), luteolin (L), quercetin (Q), kaempferol (K), hesperetin (H), chrysin (C), naringenin (N), galangin (G)), followed by a 24 hour treatment with DMSO or B[a]P (10 μM). Cells were labeled with mouse anti-human ICAM-1 and AlexaFluor 488 antibodies. Positively labeled cells were analyzed by the flow cytometry. Bars represent mean ± SE of at least three independent experiments analyzed by one-way ANOVA followed by Tukey multiple comparison test.

One of the key characteristics of flavonoids that are heavily studied is the antioxidant ability of these compounds. Some studies have suggested that flavonoids elicit their protective effects through their antioxidant capability [157, 244], while others have suggested that the protection is independent of their antioxidant roles [168, 185]. We examined the ability of the eight flavonoids tested to reduce ferric iron and then compared the reducing capacity to their ability to protect against B[a]P-induced ICAM-1 (Figure 4.3). Apigenin was the least capable of reducing iron whereas luteolin was the strongest antioxidant tested. The antioxidant ability of each flavonoid did not correspond to it's ability to protect against B[a]P. For example, apigenin was the most protective flavonoid against B[a]P-induced ICAM-1, however apigenin had the least antioxidative properties. The reverse is true for hesperetin which showed a strong antioxidant ability but did not protect against B[a]P. It appears as though the flavonoids with numerous B-ring substitutions were more likely to be strong antioxidants (Figure 4.1). It has been suggested that the hydroxyl substitution on the C-ring is an important functional group for antioxidant capacity, however this was not true for this study [172] evidenced by the absence of this substiuent on both luteolin and hesperetin.

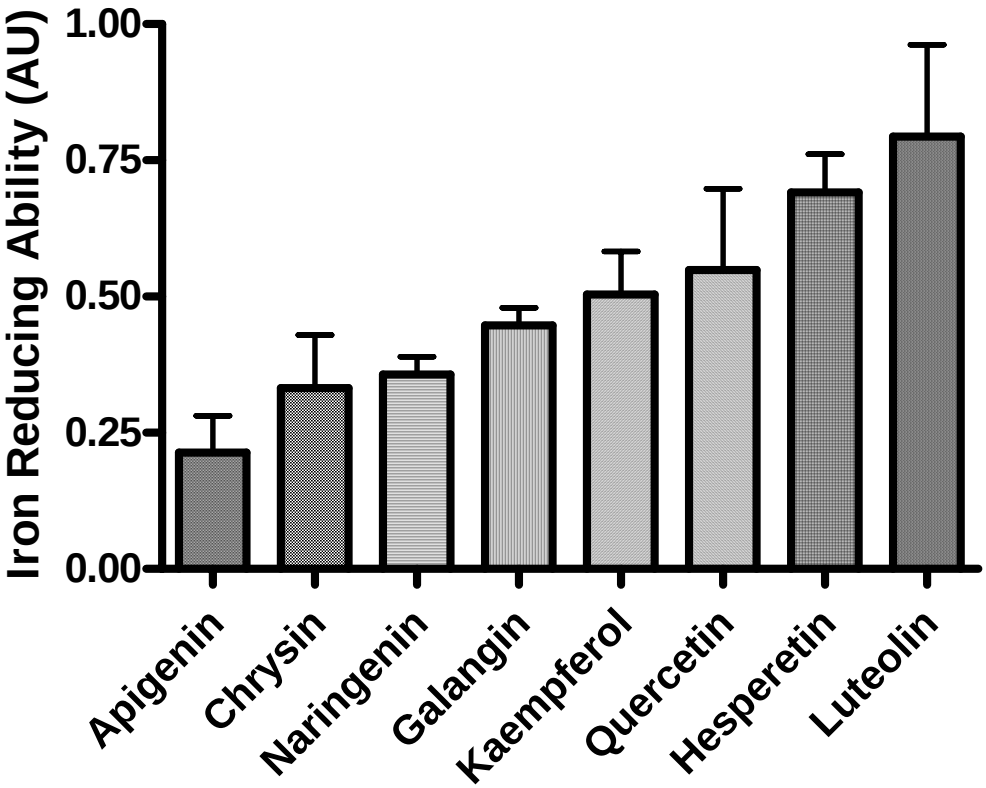

Figure 4.3: Antioxidant ability of flavonoids. Flavonoids (5 µM) were analyzed for their antioxidant capacity by the measurement of their ferric reducing ability. Results are expressed as mean ± SE of absorbance units (AU) of at least three independent experiments.

One possibility for the protective nature of the flavonoids is the antagonism of the aryl hydrocarbon receptor (AhR). Studies have suggested that the B-ring 4' substitution of the flavonoids is important for interaction with the AhR ligand binding site and that it could create a hydrogen bond between the compound and the AhR amino acids [183-185]. B[a]P is extensively metabolized by AhR-mediated xenobiotic metabolizing enzymes such as cytochrome P450 1A1 and epoxide hydrolase. It has been shown by our lab that B[a]P must be metabolized by AhR-responsive enzymes (cytochrome P450) to induce ICAM-1 (Chapter 3). It is possible that the flavonoids, acting as AhR antagonists, are able to minimize the metabolism of B[a]P to the metabolically active compounds, thus protecting the cells from these events. This study also showed the necessity of the 2-3 double bond of the flavonoids for protection. This functional group was also shown to be important in cytokine induced ICAM-1 studies suggesting that the double bond is more important to ICAM-1 induction and less to the specific inducer, whereas the 4' hydroxyl substitution is unique to AhR metabolized compounds such as B[a]P.

In summary, our data provide evidence that plant-derived flavonoids can down-regulate pro-inflammatory parameters induced by B[a]P. Furthermore, our data suggest that the protective properties of selected flavonoids initiate at the level of AhR, possibly by competing as ligands with B[a]P. Nutrition may be a sensible means of reducing health risks associated with exposure to environmental pollutants such as B[a]P.

Chapter Five. Discussion

5.1. Discussion

Endothelial cell dysfunction is an initiating step in the development of cardiovascular diseases, such as atherosclerosis. The current dissertation focuses on endothelial cell dysfunction in the sense of increased adhesion of circulating leukocytes and the induction of the adhesion molecules that perform this task. Adhesion molecules play an essential role in the recruitment and migration of leukocytes to and through the endothelial layer and into the vessel intima, where the immune cells can phagocytose lipid droplets and form foams cells and eventually a fatty plaque [5-7]. A number of risk factors exist for the development of atherosclerosis, among which are environmental factors, such as pollutant exposure and dietary habits. Two pollutants described within this dissertation were shown to induce an adhesive endothelial atmosphere: alumina nanoparticles and B{a]P. These pollutants differ in their form, creation, uses, and exposure scenarios, however both were able to similarly lead to a pro-inflammatory state.

The second chapter of the dissertation focuses on the description of newly studied alumina nanoparticles leading to upregulation of adhesion molecules in endothelial cells. The promise nanoparticles bring to the industrial and commercial world shadows concerns made for those exposed by the manufacture and use of these compounds. Studies must be conducted initially on the safety of these compounds at the nanoscale to avoid potential health and environmental dilemmas of the future. Data presented in chapter 2, indicate that alumina nanoparticles, but not polystyrene nanoparticles, cause increased adhesiveness shown by induction of VCAM-1, ICAM-1, and ELAM-1, as well as increased monocyte adhesion to vascular endothelial cells. These data suggest that exposure to certain nanoparticles may be a significant risk for the development of inflammatory diseases such as atherosclerosis. Similar phenomena have been observed elsewhere. Treatment with TiO_2 particles caused increased rolling and adhesion of polymorphonuclear leukocytes to the luminal surface of systemic venules in rats [84]. Also, other metal oxide nanoparticles, Y_2O_3 and ZnO, were able to induce the expression of ICAM-1, interleukin-8, or MCP-1 in human endothelial cells and these particles were shown to be internalized by the cells [83].

The third chapter of this dissertation focuses on a more heavily studied environmental pollutant, B[a]P. B[a]P was isolated from coal tar in 1930 and has been heavily studied due to the carcinogenicity of its P450 elicited reactive metabolites [98]. The data presented in chapter 3 indicate that not only does AhR controlled enzyme-mediated metabolism of this PAH lead to cancer; it also causes endothelial cell dysfunction. B[a]P was able to induce endothelial expression of ICAM-1 only after pretreatment with the AhR agonist β-NF, but not the AhR antagonist α-NF (Figure 5.1). In addition, silencing of AhR by siRNA attenuated the induction of ICAM-1 by B[a]P. Exposure to B[a]P has been shown to cause atherosclerosis in animal models but the mechanisms of action have remained unknown [120-123]. The hypothesis suggesting exposure to B[a]P creates a local inflammatory response that leads to atherosclerosis development [122], is supported by the data presented in this dissertation. These data coordinate well with published data showing that exposure to B[a]P increases expression of MCP-1 and that this event is also AhR dependent [124].

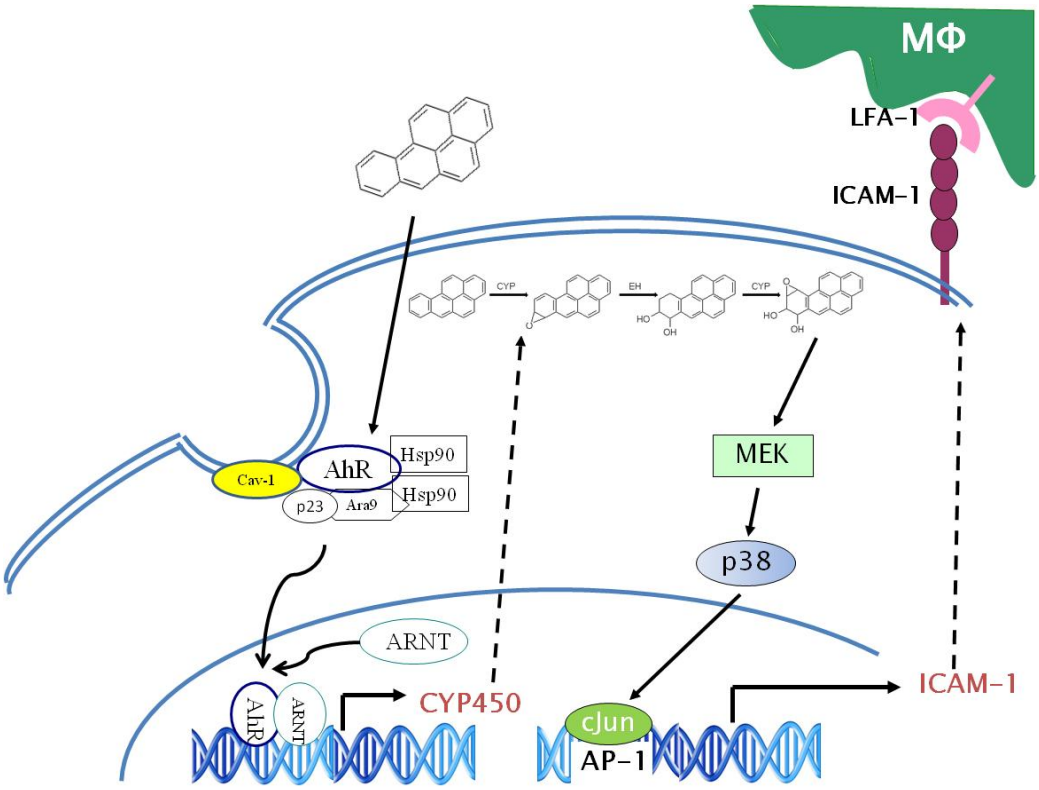

Figure 5.1: Proposed mechanism for B[a]P-induced ICAM-1

This dissertation, in chapter four, also considers the role of diet in protection against toxic endothelial events, namely ICAM-1 induction by B[a]P. Flavonoids are abundant in diets rich in fruits and vegetables [159]. These protective plant compounds act both as antioxidants and in antioxidant-independent pathways [168, 185]. The results submitted do not support a correlation between the antioxidant capacity of the flavonoids and the protection action against B[a]P-induced ICAM-1. Flavonoids also have the ability to bind to receptors such as AhR and act as potent agonists or antagonists of receptor-based processes [183, 185]. This dissertation allows room for much speculation of how flavonoids are protecting against B[a]P induced ICAM-1 in human endothelial cells. Literature reviews provide possible explanations, but further experimentation must be conducted on the exact mechanisms of action.

Interestingly, speculation as to how flavonoids may be exerting their protection leads to the possibility that AhR is also involved in this process. Past structure-function relationship studies conducted between AhR and flavonoids have implicated the 4' hydroxyl substitution of the B ring to be an important functional group for AhR antagonism. Interestingly, the data presented in chapter four also comes to this conclusion, that the 4' hydroxyl substitution is important for protection against B[a]P-induced ICAM-1. Logically, as AhR was shown to be necessary for the toxicity of B[a]P to the endothelium, antagonism of AhR by flavonoids would protect against ICAM-1 induction.

Another intriguing result, highlighted in chapter 3, is that B[a]P-induced ICAM-1 requires functional caveolae. The membrane microdomains called caveolae have been implicated in the development of cardiovascular diseases, namely atherosclerosis [151]. They are heavily involved in the organization of membrane localized signaling molecules and implicated in the compartmentalization and function of adhesion molecules [35, 145, 154, 155]. Data from our laboratory have suggested that AhR is one signaling molecule that is localized and controlled by caveolae (unpublished data). Immunoprecipitation studies have jointly pulled down AhR with caveolin-1 and caveolin-1 silencing decreased PCB77 induction of CYP1A1. However, AhR is not the only signaling molecule that has been linked with both caveolae and ICAM-1 induction. Results in this dissertation connect B[a]P-induced ICAM-1 with phosphorylation and activation of p38-MAPK and AP-1. Functional caveolae have been shown to be necessary for activation of p38-MAPK [142, 144]. This information helps to explain the need for functional caveolae for the AhR and p38 mediated process of induction of ICAM-1 by B[a]P.

Maintaining a physiologically relevant concentration is important for *in vitro* experiments. The flavonoids tested in this dissertation were used at 5 μM. For quercetin, this is a feasible plasma concentration as a compilation of pharmacokinetic bioavailability studies estimate levels around 4 μM, however plasma levels of 7 μM have been reported [245]. Naringenin received from grapefruit elicited plasma concentrations of 6 μM. Other flavonoids are less likely to reach this level in the plasma. Hesperidin averages less than 1 μM plasma concentrations [245].

Altogether, this dissertation describes how both newly recognized and heavily studied environmental contaminants can induce endothelial cell dysfunction through activation of adhesion molecule pathways. A possible mechanism for B[a]P induced atherosclerosis was proposed by which an AhR-mediated B[a]P metabolite elicits increased endothelial adhesiveness. Interestingly, this toxic event can be protected against by pretreatment with selective flavonoids containing both a 4' B-ring hydroxyl, which is possibly necessary for AhR antagonism, and a 2-3 double bond on the C-ring.

5.2. Further Directions

The scientific process constantly allows for continued questions that must be answered. The findings in this dissertation offer a number of new scientific questions to follow up on the conclusions and build upon the knowledge provided above.

The studies in this dissertation were conducted in cell culture. *In vitro* experiments provide a consistent environment that encloses a certain physiological system for in depth analysis. Conducting experiments *in vitro* allowed for elucidation of mechanisms of action of these compounds that would not be possible in animal models. However, animal models are necessary to look at the integrated biological system and confirm that what is seen *in vitro* also occurs *in vivo*. This is especially important since the action of B[a]P was shown to be dependent upon metabolism of the compound which could also occur in other cell types or tissues. Also, the endothelium is constantly under shear stress and flow conditions naturally, however in culture the cells are contained in a static environment. This could change the uptake and

dynamics of a number of cellular processes. Animal experiments should be conducted to confirm B[a]P-mediated increase of ICAM-1 in the endothelial vessel layer.

Further studies should also be conducted to understand the possible interaction between caveolae and AhR. Caveolae are important for macromolecule trafficking of the cell, as well as for concentration of signaling molecules. Results in this dissertation imply that both AhR and caveolae are important for B[a]P-induced signaling, however the reasons for this involvement are not elucidated. Experiments should be developed to differentiate between these functions of caveolae. Measurement of the uptake of B[a]P into the cell would help to determine if caveolae are playing a role in uptake of the pollutant, thus allowing for a stronger AhR contact. Studies have shown that MAPK proteins lead to AhR activation and proper AhR-dependent gene transcription [246]. The activation of AhR requires a number of cofactors, both for cytosolic ligand binding and transcription activation. It is possible that the disruption of caveolae has disrupted the proper cycling of the necessary AhR cofactors, leaving AhR unable to function as a transcription factor.

Metabolism and bioavailability is also important to consider when analyzing the protective actions of flavonoids. Bioavailability and absorption of flavonoids is difficult to estimate. The flavonoid content and form is variable among food sources [159]. For instance, quercetin in onions is mostly found as a quercetin glucoside and 52% has been shown to be absorbed into the blood, whereas quercetin found in apples is in the form of quercetin rutinoside and the same study reported 30% absorption of this form [247, 248]. The bound sugar moiety and food source also affects the half-life of elimination of the compounds. The half-life of plasma quercetin varied from 23 to 28 h from apples and onions, respectively. More interestingly, half-lives of this length could allow for accumulation in the blood with repeated consumption. Flavonoids are also extensively metabolized by the liver and gut as they undergo a first pass metabolism. Flavonoids are commonly found in the plasma as glucuronide and sulfate ester derivatives, which would likely influence the biological activity of the compounds. In fact, one study considered endothelial cells pretreated with hepatocyte conditioned flavonoids and the activation by TNF-α [172]. The flavonoids lost their protective properties when first incubated and metabolized by hepatocytes.

Further studies should also be conducted on the mechanism of protection of these flavonoids against B[a]P-induced ICAM-1. As mentioned before, it is speculated that flavonoids

containing a 4' hydroxyl substitution on the B-ring are potent antagonists to AhR and this is the reason for their protection. However, this should be confirmed experimentally. Also, it would be interesting to determine the mechanism leading to the necessity of the 2-3 double bond on the C-ring. It is possible that this functional group is less specific to the inducer, B[a]P, but instead is related to ICAM-1 induction. This double bond was also necessary for the protection against TNF-α induced ICAM-1 [172].

The experiments described in chapter two of this dissertation describe alumina nanoparticles increasing adhesion molecules in the endothelium. However, the studies do not provide a mechanism of action for these particles. Studies have shown that alumina nanoparticles can interact with phosphorylated proteins [249]. Unpublished data has also shown that alumina can bind strongly to p38α, the MAPK that is shown to be important for adhesion molecule expression in chapter 3 of this dissertation. It is possible that disruption of the ability of certain signaling cascades dependent on phosphorylation for activation can lead to altered cellular homeostasis. This could be a potential mechanism for alumina induced endothelial dysfunction, however this would have to be determined in further experiments.

It would also be interesting to understand how alumina particles enter the endothelial cells, thus allowing for the upregulation of adhesion molecules. Multiple studies have examined other nanoparticles and processes of endocytosis. Three main processes of endocytosis exist: clathrin-mediated uptake, caveolae-mediated uptake, and clathrin-and caveolae- independent internalization. One study showed that hydroxyapatite nanoparticles are internalized into liver cancer cells by a clathrin-mediated energy-dependent process [250]. However, it was shown that poly nanoparticles were internalized into epithelial cells independently of clathrin and caveolin-1-mediated processes [251]. Others have suggested that the surface charge of the nanoparticle determines the endocytic machinery involved [252]. Our group has found that alumina nanoparticles are able to increase caveolin-1 protein in endothelial cells and that alumina particles are internalized into vesicle like structures in these cells (data not shown). More data is needed to understand which endocytic pathways are being used and if caveolae play a role in this process.

This dissertation presents novel findings on the effects of two environmental pollutants on endothelial cell dysfunction, shown by increased endothelial adhesiveness. Nanoparticles are prevalent in today's manufacturing processes and uses of these compounds are growing

exponentially. Safety concerns warrant careful consideration as to the limits for exposed people. These studies provide evidence that vascular endothelial exposure to alumina nanoparticles causes an increased pro-inflammatory environment and cellular adhesion, which leads to the development of experimental atherosclerosis. Secondly, B[a]P, a component of air pollution, increased vascular adhesion by upregulating ICAM-1. This event occurs due to AhR controlled enzyme-mediated metabolism of B[a]P and signaling through MEK, p-38 MAPK, and AP-1. The membrane microdomains, caveolae, are also necessary for this response. These experiments provide a novel mechanism for the increases in risk for cardiovascular disease after air pollution and PAH exposure. Interestingly, select dietary flavonoids are able to ameliorate B[a]P-induced ICAM-1 and this protection does not correlate with the antioxidant capacity of these polyphenols, but does associate with the presence of certain functional groups. Proper diet may be a sensible means of providing a primary prevention strategy against diseases from environmental contaminants such as B[a]P.

Appendix A. Methods

1. Primary Endothelial Cell Isolation

a. Porcine Endothelial Cells

i. Establishing the Culture

Growth Media

M199 – total 400 mL
Penn-Strep – 4 mL
L-glutamine – 4 mL
Amino Acids – 4 mL
Fetal Bovine Serum (FBS) – 10%

Hanks

Water – 2 L autoclaved/filtered
KCL – 0.8 g
KH_2PO_4 – 0.12 g
NaCl – 16 g
$NaHCO_3$ – 0.7 g
Na_2HPO_4 * 7 H_2O – 0.18 g
D-glucose – 2 g
Phenol Red – 0.02 g

Porcine pulmonary arteries and aortas are obtained from University of Kentucky Agriculture Department.

ii. Freezing the Cells

- Trypsinize Cells
- Spin cells in 10mL of media in 15 mL conical tube @1200 rpm for 10 min
- Resuspend pellet in 2 mL freezing cocktail
- Split into 2 cyrovials (1 mL each)
- Cover with white foam
- -20° C overnight
- -80° C overnight
- Liquid nitrogen after that for long-term storage

Freezing Cocktail

FBS -2mL
M199 10% FBS (or 20%) – 13 mL
28% DMSO – 5 mL

- 1.75 mL DMSO + 4.5 mL M199

iii. Reviving the Cells

- Cells are frozen in high concentrations of DMSO so must be diluted immediately
- Fill a 15 mL tube with 9 mL of 37 °C medium (10% FBS)
- Take 0.5 to 1 mL of the M199 media and add to cryovial containing the frozen cells, pipet repeatedly and once some of the cells thaw, transfer to the 15 mL tube

- Continue until all thawed cells are in suspension
- Centrifuge for 10 min at 1200 rpm at 37 °C
- Discard supernatant, resuspend in fresh media, repeat centrifugation
- Seed to T75 flask
- Change media after 3 to 4 hours, again after 24 hours

b. Human Umbilical Vein Endothelial Cells

i. Establishing the Culture

Growth Media

M199 – total 400 mL
Penn-Strep – 4 mL
Antibiotic-Antimycotic – 4 mL
Sodium Pyruvate – 4 mL
Heparin – 120 mg (filtered 0.22µm)
HEPES – 2.4 g (filtered 0.22µm)
Endothelial Cell Growth Supplement – 3.2 mL
FBS – 20% (complete), 10% (experimental)

Dispase Solution

M199 – total 400 mL
Vitamins – 4 mL
Amino Acid – 4 mL
Antibiotic-Antimycotic – 4 mL
Sodium Pyruvate – 4 mL
Dispase – 800 mg
FBS – 20 mL (5%)
Aliquot 30 mL in tubes and freeze at -20 °C for 3 – 6 months

Cord Transport Media

M199 – total 400 mL
Penn-Strep – 12 mL
Heparin – 120 mg (filtered 0.22µm)
HEPES – 2.4 g (filtered 0.22µm)

Human umbilical cords (6-12 inch segments) are obtained from the University of Kentucky Labor & Delivery Department in sterile, plastic containers holding ~100 mL Cord Transport Media in Styrofoam cooler with ice packs. These can be refrigerated overnight.

- Collect instruments: 30 cc syringe, scalpel, surgical tape/cord, autoclaved 500 mL beaker, sterile specimen container, waste beaker, autoclaved surgical tools (2x canulas, 2x haemostatic forceps), warm dispase solution, cold Hanks media
- Sterile gauze was laid on the working area in hoop and dampened drop wise with Hanks
- The cord was laid flat on the gauze
- With sterile scalpel, ends were cut evenly

- Blood was wiped from ends with gauze and cord was always handled with gauze or clamps
- The canula was, with gentle force, placed in the vein of one side, avoiding direct contact with the non-sterile surface of the cord
- The ligature was tightly knotted behind the lip of the canula
- The syringe was placed into the tubing end of the canula and slowly Hanks was injected (30 mL) to rinse and remove blood.
- The second canula was inserted into the other end of the vein
- Hanks was further inserted to rinse away excess blood, One end of the cord was clamped and Hanks was injected until the vein was distended, then released
- Clamp one end of the cord
- Dispase was injected into the cord avoiding air bubbles
- The second canula was clamped and the syringe removed
- The clamped cord was placed in the beaker covered with Hanks and aluminum foil, and refrigerated for 18 hours

- Collect instruments: 30 cc syringe, specimen container, 50 mL centrifuge tube, T75 flask, cold Hanks
- Sterile gauze was laid on the working area in hoop and dampened drop wise with Hanks
- The clamped cord was laid flat on the gauze
- One canula was unclamped releasing the dispase and cells into a 50 mL tube
- Hanks was injected into the cord using the syringe, and rinsed, holding the cord and swirling it back and forth. Repeated 2-3 times and poured into a 50 mL tube
- Bring to 40 mL and centrifuge at 1000 rpm for 10 min at 37 °C
- Decant supernatant and resuspend pellet gently with growth media
- Seed the cells into T75 flask with growth media
- 8 hours later rinse cells with Hanks and change media
- Change media 24 hours later
- Leave until confluent

ii. Freezing the Cells

- Trypsinize Cells
- Spin cells in 10mL of media in 15 mL conical tube @1200 rpm for 10 min
- Resuspend pellet in 2 mL freezing cocktail
- Split into 2 cyrovials (1 mL each)
- Cover with white foam
- -20° C overnight
- -80° C overnight
- Liquid nitrogen after that for long-term storage

Freezing Cocktail

FBS -2mL

M199 10% FBS (or 20%) – 13 mL

28% DMSO – 5 mL

- 1.75 mL DMSO + 4.5 mL M199

c. THP-1 Monocytes

i. Reviving the Cells

Growth Media

RPMI – total 400 mL (Gibco 11875 with L-glutamine)
Glucose (2.5 g/L) – 4 mL of 0.25 g/mL stock
HEPES (10 mM) – 4 mL of 1 M stock
Sodium Pyruvate (1 mM) – 4 mL of 100 mM stock
Penn-Strep (1%) – 4 mL of 100x stock
FBS – 10%
β-mercaptoethanol (50 µM) – 1.75 µl of 14.3 M stock (add to aliquots, not to whole media stock)

2. Protein Isolation

a. Whole Cell Extraction

Lysis Buffer (whole cell lysate)

	100 mL		MW
Tris-HCl – 1 M (pH ~7.4)	2 ml	20 mM	121.14
Tris + H_2O up to 50 ml, stir, add HCl (2M), adjust pH, add rest of H_2O			
NaCl – 1 M	15 ml	150 mM	58.44
Triton X-100 – 10% (v/v)	5 ml	0.5%	liq
PMSF – 10 mg/ml (DMSO/EtOH)	1 ml	0.1 mg/ml	174.2
NP-40	500 ul	0.5%	liq
EDTA (0.1 M)	1 ml	1 mM	358.2
Leupeptin (1 mg/ml) DMSO	250 ul	2.5 ug/ml	
Pepstatin – 1 mg/ml DMSO	1 ml	10 ug/ml	
Na_3VO_4 (sodium orthovanadate)	500 ul	1 mM	
Protease inhibitor		200 mM	

****Make Lysis Buffer (-) then add proteinase inhibitors before using**

Lysis Buffer (-)

Tris-HCl	2 ml
NaCl	15 ml
Tr X-100	5 ml
EDTA	1 ml
dH_2O	73.75 ml

Lysis Buffer (+ proteinase inh) for 3 ml

NP-40	15 ul
PMSF	30 ul
Leupeptin	7.5 ul
Pepstatin	30 ul
Na_3VO_4	15 ul
Lys Buff (-)	2902.5 ul

If using Proteinase Inhibitor Cocktail (25 ul in 5 mL Lysis (-)) plus PMSF

Isolate Proteins

- Wash the monolayer with PBS (2 times at least)
- Add 3ml of PBS (ice-cold) and scrape the cells. Transfer to conical tube.
- Add 3ml more to the plate and collect the remaining cells
- Pellet it down 2500 rpm for 10 min at 4º
- Pour off supernatant
- Add PBS (ice-cold)

- Pellet for another 5 min
- Completely remove the PBS/ice-cold water (nanopure)
- Add 200-300 ul of lysis buffer and vortex it for 30 sec and put on ice for 2 min (5-8 times repeat) (60mm dishes 100ul)
- Keep on ice (incubate for at least 20-30 min)
- Vortex and then centrifuge at 12000/13000 rpm for 15 min at 4º C
- Take the supernatant out and make aliquots of it
- Quick freeze in dry ice then store at -80º C

b. Whole Cell Extraction by Sonication

Lysis Buffer
Water
Tris HCl (pH 7.5) 20 mM
NaCl 150 mM
EDTA 1 mM
EGTA 1 mM
Triton X-100 1%
Sodium pyrophosphate 2.5 mM
B-glycerophosphate 1 mM
To add just before:
Na_3VO_4 1 mM
Leupeptin 1 µg/mL
PMSF 1 mM

- Remove media and rinse with PBS
- Scrape cells in PBS into centrifuge tube on ice
- Centrifuge 2500 rpm 10 min at 4 °C
- Remove all PBS
- Add protease inhibitors to lysis buffer
- Add 100 µl to pellet, put in eppendorf tube
- Sonicate samples on ice 3x for 5 seconds at 65%/sec
- Microcentrifuge for 10 min at 14000 rpm at 4 °C
- Transfer supernatant to new tube, store at -80 °C

c. Nuclear Extraction

Buffer A
Water – total 10 mL
HEPES 10 mM pH 7.9
KCl 10 mM
EDTA 0.1 mM
DTT 1 mM
PMSF 0.5 mM

Buffer B
HEPES 20 mM
NaCl 0.4 M
EDTA 1 mM
DTT 1 mM
PMSF 1 mM

- Wash with ice cold PBS

- Harvest by scraping
- Centrifuge
- Resuspend in 400 µl of buffer A
- 15 min incubation on ice
- Add 25 µl 10% NP-40
- Wait ~5 min til 90-95% of cells are lysed
- Centrifuge 14,000 rpm for 1 min
- Resuspend with 25-50 µl of buffer B
- Nuclei lysed by shaking vigorously at 4 °C for 5 min
- Collect clear supernatant

3. Western Blot

SDS-page Running Buffer (no need to adjust pH)

	5x	10x
Tris Base	9 g	18 g
Glycine	43.2 g	86.4 g
SDS	3 g	6 g

- bring to 600 ml w/ dH_2O

5x Transfer Buffer

Tris Base	2.91 g	5.82 g
Glycine	1.46 g	2.92 g
Methanol	100 ml	200 ml
Adjust vol w/ dH_2O to:	500 ml	1000ml

Sample Loading Buffer → 2 ul + 8 ul sample (store at -70º C)

	5x	6x
H_2O	3.8 ml	2.96 ml
0.5M Tris-HCl	1 ml	1.2 ml
Glycerol (60%)	0.8 ml	0.96 ml
10% SDS	1.6 ml	1.92 ml
2-Mercaptoethanol	0.4 ml	0.48 ml
1% (w/v) Bromophenol blue (0.05 g in 5 ml)	0.4 ml	0.48 ml

TBS (pH 7.5) (keeps 3 months)

	1x	5x
Tris Base (50 mM)	6.05 g	30.25
NaCl (150 mM)	8.76 g	43.8

Adjust pH to 7.5 w/ approximately 9.5 ml 1M HCl
Add dH_2O to 1 L

TBST Buffer

1x TBS	500 ml
Tween 20	250 ul

Separation Gel

	5ml	10ml (10%)	20ml	30ml	for 30% Bis/Acryl
H_2O	2.3 ml	4.6	9.2	13.8	8
1.5 Tris-HCl (pH8.8) (27.23 g Tris adjust to 150 ml)	1.25 ml	2.5	5	7.5	5
Acrylamide/Bis (40%)	1.25 ml	2.5	5	7.5	6.8
10% SDS	50 ul	100 ul	200	300	200
10% Ammonium Persulfate (1ml dH_2O + 100 mg AP)	30 ul	60	120	180	100
TEMED	2.5 ul	5	10	15	20

Stacking Gel

					(10 ml)
H_2O	1.865 ml	3.73	7.46	11.2	6.1
0.5 Tris-HCl (pH6.8) (9.03 g Tris adjust to 150 ml)	1.25 ml	2.5	5	7.5	2.5
Acrylamide/Bis (40%)	0.28 ml	0.56	1.12	1.68	1.3
10% SDS	25 ul	50 ul	100	150	100
10% Ammonium Persulfate (1ml dH_2O + 100 mg AP)	12 ul	25	50	75	50
TEMED	3.5 ul	8	16	24	10

Preparing Sample

- Dilute sample with dI water to 1 ug/ul (20 ug/ul)
- Add 5 ul of sample loading buffer (contains DTT which is a reducing agent to break SH2 bonds) (400 ul 2x SSB and 100 ul DTT (1 M))
- Boil at 95-100º C for 5-7 min
- Put on ice until loading
- Load 5 ul of the marker and all 25 ul of sample

Preparing the Gel

1. Separation/Resolving Gel
   - to prepare 5 ml for thin or 10 ml for thick gel
   - prevent apparatus from leaking
   - after pouring, cover with ethanol/isopropanol
   - ~5 min to solidify
   - rinse with H_2O 2x, remove rest of H_2O with paper towel
2. Stacking gel
   - less than 5 ml/gel
   - fill up to glass, then insert comb (~1 cm between comb and separation gel)
   - 30 min to solidify
   - rinse with H_2O 2-3x

Running the Gel

- Prepare the running buffer (900 ml H_2O + 100 ml of 10x buffer)
- Put the gel in

- Load the samples (in each well something – marker, loading buffer)
- Run at 100 V until samples get to resolving buffer and then 90 V for 1.45 to 2 h

Transfer onto Membrane

- To prepare:
- Sponges, holders
- Transfer Buffer – ice cold
- Cut the filter paper and membrane – slightly smaller than the sponges
- In the dish, add transfer buffer
- **1.** sponge **2.** filter paper (soaked in buffer, roll with tube/pencil to remove air bubbles) **3.** gel (cut off stacking, rinse with water, cut side to tell orientation) **4.** membrane **5.** filter paper **6.** sponge (roll with tube/pencil)
- Close, put in apparatus (black on black/white on red)
- Add buffer
- Add the box with ice and cover with the whole thing
- Run at 100 V for 2 h

Blocking with Milk

- Dissolve 0.8 g of low-fat dry milk in 16 ml of TBST/box
    - (never let the membrane dry)
- After getting the membrane from apparatus, put it in the milk/TBST
- Shake 5 min at room temperature
- Leave overnight at 4º
- Shake 5 min at room temperature
- Rinse with 16 ml of TBST
- Shake in TBST for 1 hour

Binding of the Primary Antibody

- Dissolve 0.8 g BSA or milk in 32 ml (16 ml) of TBST
- Add certain amount of primary antibody
    - Ex. Caveolin-1: antibody- 1:2000 (8 ul into 16 ml) time- 2 h 15 min
- Shake for certain amount of time
- Wash 3x 15 min with 16 ml of TBST 1 box

Binding of the Secondary Antibody (anti-mouse)

- 5.4 ul into 16 ml TBST
- Shake for 1 h 15 min
- Wash 4 x 15 min with 16 ml TBST/box

Visualization

(all in darkroom under red light)

- Discard the TBST
- Mix ECL WB Detection Reagents (Amersham Biosci)
    - 1.5 ml of reagent A + 1.5 ml of reagent B
- Distribute the mixture evenly by pipette on the membrane
- Let sit for 1 minute (up to 5 minutes for a strong signal)
- Dry the membrane gently on a kim wipe
- Put the membrane into the plastic case in the cassette

- Put the film inside (Amersham- Hyperfilm) – cut the edge in the origin
- 1-5 min exposure
- develop the film

Stripping Buffer

- 50:50 H2O2 and water
- incubate with membrane for 30 min at room temperature shaking
- wash 3x 15 min with TBST, re-block, and start again

4. RNA Isolation

- Discard treatment media
- Add 800 µL Trizol to cells
- Scrape into microcentrifuge tube
- Incubate 5 min at 15 to 30 °C
- Add 0.2 mL chloroform
- Shake tubes vigorously by hand for 15 seconds and incubate them at 15 to 30 °C for 2 to 3 min
- Centrifuge at 12000 x g for 15 min at 4 °C
- Transfer aqueous phase to a fresh tube
- Add 0.5 mL isopropyl alcohol to precipitate RNA
- Incubate samples at 15 to 30 °C for 10 min
- Centrifuge at 12000 x g for 10 min at 4 °C
- Remove supernatant
- Add 1 mL 75% ethanol to pellet, vortex, centrifuge at 7500 x g for 5 min
- Remove ethanol, air dry for 5-10 min
- Dissolve RNA in RNase-free water (~20 µl)
- Boil at 55 °C for 10 min
- Freeze at -80 °C

5. Immunofluorescence

- Plate cells onto glass chamber slides leaving room for 3 extra controls (IgG, no 1°, no 1° or 2°), grow to confluence, serum starve overnight
- Remove media from wells
- Fix with 500 µL of 50:50 acetone/methanol solution for 30 minutes at RT (depends on antigen of interest, could use 4% paraformaldehyde, would need to quench with 0.3M glycine for 10 min if used)
- Wash with 1x PBS 3x for 5 minutes at 37°C shaking
- Depending on antigen, permealize with 0.5% Triton X 100 in 1x PBS for 10 min at 37°C shaking (could use less if unsure 0.01%)
- Wash with 1x PBS 3x for 5 minutes at 37°C shaking
- At this step you can put the slide in the fridge, wrapped in parafilm, before going on
- Heat slide back up if stopped.
- Block with 500 µL of a solution of 15 µL/mL of the serum of the secondary in 1% BSA in 1x PBS for ~45 minutes at 37°C shaking

- Without washing, put the respective primaries on the indicated wells diluted in 1x PBS. Add corresponding IgG to the control well allotted at the same concentration as your primary (ex. 5 μg/mL) for 30 minutes at 37°C shaking
- Wash the wells 2x in 1x PBS, then an additional 1x for 5 minutes at 37°C shaking
- **Avoiding light,** add the secondary antibody (ex. 1/200) diluted in 1x PBS for 15 minutes at 37°C shaking **covered in aluminum foil**. Have used AlexaFluor 488 and 546 donkey anti-mouse or goat IgG from Invitrogen.
- Wash the well 2x in 1x PBS, and then an additional 1x for 5 minutes at 37°C shaking
- Add Hoechst stain at a concentration of 1 ug/mL for 5-10 minutes at 37°C shaking
- Wash the wells 3x in 1x PBS, the pull of the sides of the wells, mount with VectaMount and store at 4°C in foil.

6. Flow Cytometry

- Wash with PBS 2x
- Remove cells with trypsin (0.25 mL for <2 min)
- Quench with 20% FBS media (1 mL)
- Centrifuge 150x g for 5 min at 4° C
- Wash with PBS 2x, centrifuge, vortex
- Resuspend in 1° Ab in 3% BSA-PBS (2 ug/mL for CD54)
  - (2ug/mL)*(0.25mL) = (0.5ug/ul)*(x) x=1uL
- Incubate 30 min at room temp
- Wash with PBS by centrifugation 150g 3x 5min 4°
- Resuspend in 2° Ab in 3% BSA-PBS (3 ug/mL for Alexa 488)
  - (3ug/mL)*(0.25mL) = (2mg/mL)*(x) x=0.375ul
- Incubate in dark for 20 min at room temp
- Wash 2x with PBS as before
- Stain with propidium iodide (if desired, to measure live/dead cells) 2ul/mL of 1mg/mL solution in PBS for 5 min
- Wash 3x with PBS
- Resuspend in 0.5 – 1mL PBS
- FACS Lab MN364

7. Cell Adhesion

- Treat cells 6-8 hrs with compound, TNF as a positive control (10 ng/mL)
- Activate THP-1 with TNF-a (10 ng/mL) for 10 min (wash 3x)
- Count 50,000 monocyte cells/well
- Resuspend in 1.0 mL 1% media
- Load cells with calcein (3ul/mL)
- Incubate 37º for 15 min
- Spin to get rid of excess calcein, wash with media
- Spin again, resuspend in 50 ul/well media (leave room for error ~5 wells)
- Aspirate off endothelial treatment media, add 1mL media
- Add 50 ul monocytes to each well (in absence of treatment)
- Incubate 37º for 30 min
- Gently wash unbound monocytes off with 1% media

- Add 200 ul 1% Glutaraldehyde (made with PBS containing Ca and Mg)
- Room Temp for 30 min
- Wash plate w/ PBS-B
- Count using confocal microscope

8. Small Interfering RNA (siRNA)

To begin, siRNA concentrations must be determined.

- Incubate the siRNA mix 5 min at RT
- Add 120 ul of GeneSilencer mixture to each diluted siRNA
- Incubate the Transfection Mix 5 min at RT
- Wash cells 2x with serum-free OptiMEM
- Add 3.8mL of serum-free OptiMEM to the Transfection Mix
- Add 1mL of the mixture to each well
- Add 1mL of 20% FBS OptiMEM to get final 10% FBS concentration 4 hours later

3 plates (extract at 24 h, 48 h, 72 h)

Ctrl siRNA	AhR (40nM)	AhR (60nM)
AhR (80nM)	AhR (100nM)	AhR (120nM)

Diluting siRNA: Control siRNA (in 15mL tube)		siRNA Diluent	24 x 4 = 96
		OptiMEM	15 x 4 = 60
		siRNA (80 uM)	1 x 4 = 4
	40 nM	siRNA Diluent	24 x 4 = 96
		OptiMEM	15 x 4 = 60
		siRNA (80 uM)	0.5 x 4 = 2
	60 nM	siRNA Diluent	24 x 4 = 96
		OptiMEM	15 x 4 = 60
		siRNA (80 uM)	0.75 x 4 = 3
	80 nM	siRNA Diluent	24 x 4 = 96
		OptiMEM	15 x 4 = 60
		siRNA (80 uM)	1 x 4 = 4
	100 nM	siRNA Diluent	24 x 4 = 96
		OptiMEM	15 x 4 = 60
		siRNA (80 uM)	1.25 x 4 = 5
	120 nM	siRNA Diluent	24 x 4 = 96
		OptiMEM	15 x 4 = 60
		siRNA (80 uM)	1.5 x 4 = 6
Diluting GeneSilencer:		GeneSilencer	5 x 25= 125
		OptiMEM	25 x 25 = 625

- Incubate the siRNA mix 5 min at RT (no vortex)
- Add 570 µl of GeneSilencer mixture to each diluted siRNA
- Incubate the Transfection Mix 5 min at RT

- Wash cells 2x with serum-free OptiMEM
- Add 17.67 mL of serum-free OptiMEM to the Transfection Mix
- Add 1mL of the mixture to each well
- Add 1mL of 20% FBS OptiMEM to get final 10% FBS concentration 4 hours later

Experimental Plates

C	BP10	C
Ctrl siRNA	Ctrl siRNA	Ctrl siRNA
AhR (120nM)	AhR (120nM)	AhR (120nM)

Diluting siRNA:	**Control siRNA**	siRNA Diluent	24 x 19 = 456
(in 15mL tube)		OptiMEM	15 x 19 = 285
		siRNA (80 uM)	1.5 x 19 = 28.5
	AhR siRNA	siRNA Diluent	24 x 19 = 456
		OptiMEM	15 x 19 = 285
		siRNA (80 uM)	1.5 x 19 = 28.5
Diluting GeneSilencer:		GeneSilencer	5 x 39 = 195
		OptiMEM	25 x 39 = 975

9. Cytochrome P450 Activity

To prepare:

- Detection Buffer and Glo Buffer to room temp.
- Thaw luminogenic substrate, store on ice, protect from light

Assay:

- Treat cells with test compound in 96 well white walled plate (leave some wells without cells)
- Remove culture medium, wash with PBS (warm)
- Replace with 60ul media containing luminogenic CYP450 substrate (Luciferin-CEE) (1:50 dilution), also add to empty wells
- Incubate for 3 hours
- Prepare Detection Reagent by transferring contents of P450-Glo Buffer to bottle containing Luciferin Detection Reagent, to room temp. (do not vortex, mix by swirling) (store <-15°C for 3 months, 4°C for 1 week)
- Transfer 50ul of medium from each well to 96-well white walled plate at RT, and combine with 50ul of Luciferin Detection Reagent
- Incubate 20 min at RT
- Read luminescence

CellTiter-Glo Assay

To prepare:

- Thaw CellTiter-Glo Buffer and bring to RT
- Bring lyophilized CellTiter-Glo Substrate to RT

- Transfer CellTiter-Glo Buffer into amber bottle containing Substrate, gently mix by vortexing, swirling, etc

Assay:

- 100ul of media in 96 well white-walled plate (including blank wells, no cells)
- Add 100ul CellTiter-Glo reagent
- Mix for 2 min on orbital shaker
- Allow to incubate at RT for 10 min
- Record luminescence

10. Antioxidant Capacity

Stock Solutions:

300 mmol/L acetate buffer pH3.6: 3.1 g $C_2H_3NaO_2 \cdot 3H_2O$, 16 mL $C_2H_4O_2$ in 1 L H_2O

10 mmol/L TPTZ in 40 mmol/L HCl: 25 mL total: 78.08 mg TPTZ, 83.33 µl HCL (12 M)

20 mmol/L $FeCl_3 \cdot 6H_2O$

Working Soln:

25 mL acetate buffer, 2.5 mL TPTZ soln, 2.5 mL $FeCl_3$ soln

- 300 µl fresh FRAP reagent warmed to 37 °C = blank reading
- 40 µl flavonoid containing media + 300 µl FRAP reagent in 96 well plate
- Incubate 15 min at 37 °C
- Read absorbance at 593 nm

Appendix B. Additional Data

The scientific process does not always allow for remarkable data. Appendix B holds experiments that were lost along the way. It includes mostly negative data but also those experiments that didn't quite fit anywhere yet.

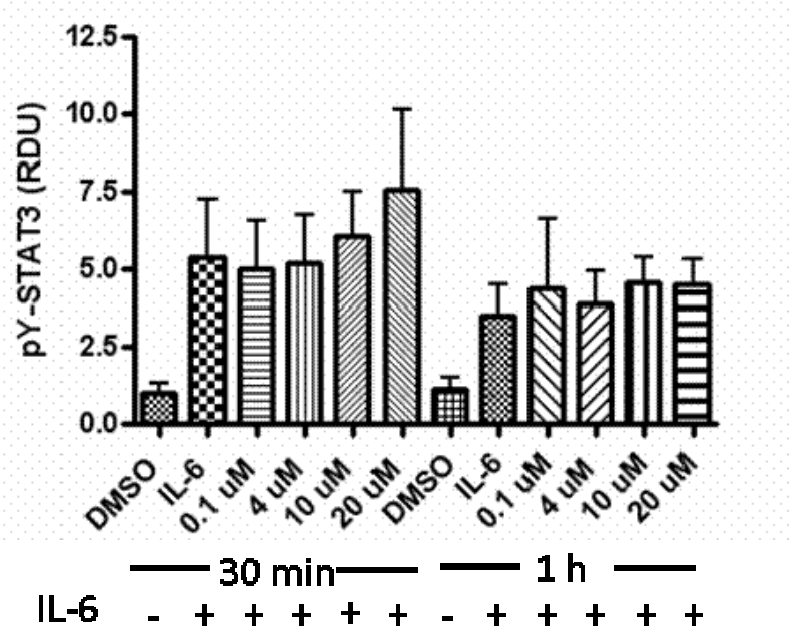

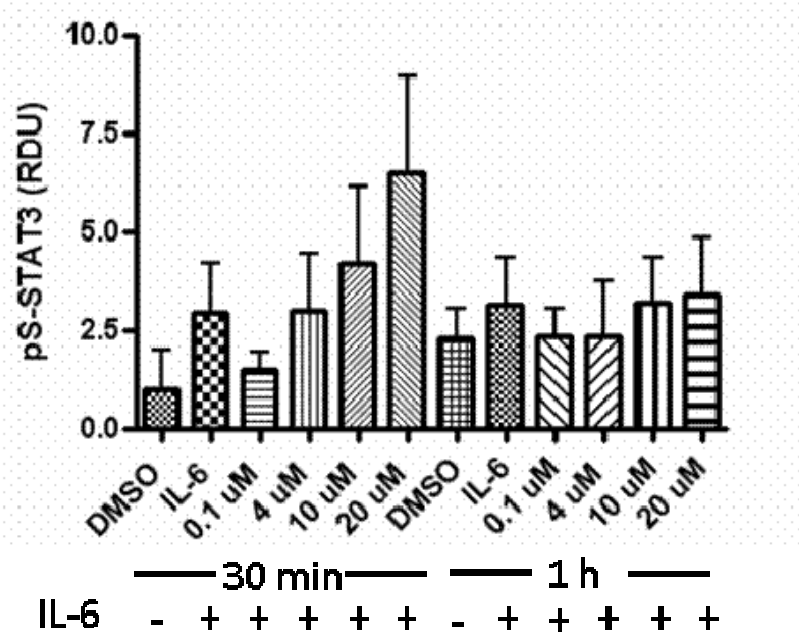

Figure I. PCB 153 in conjunction with IL-6 does not induce phosphorylation of STAT3 over IL-6 alone. EAhy926 endothelial cells were co-treated with IL-6 (1 µl/mL) and PCB153 (0.1 – 20 µM) for 30 or 60 m. Nuclear protein was extracted and probed by immunoblot for phosphorylated STAT3.

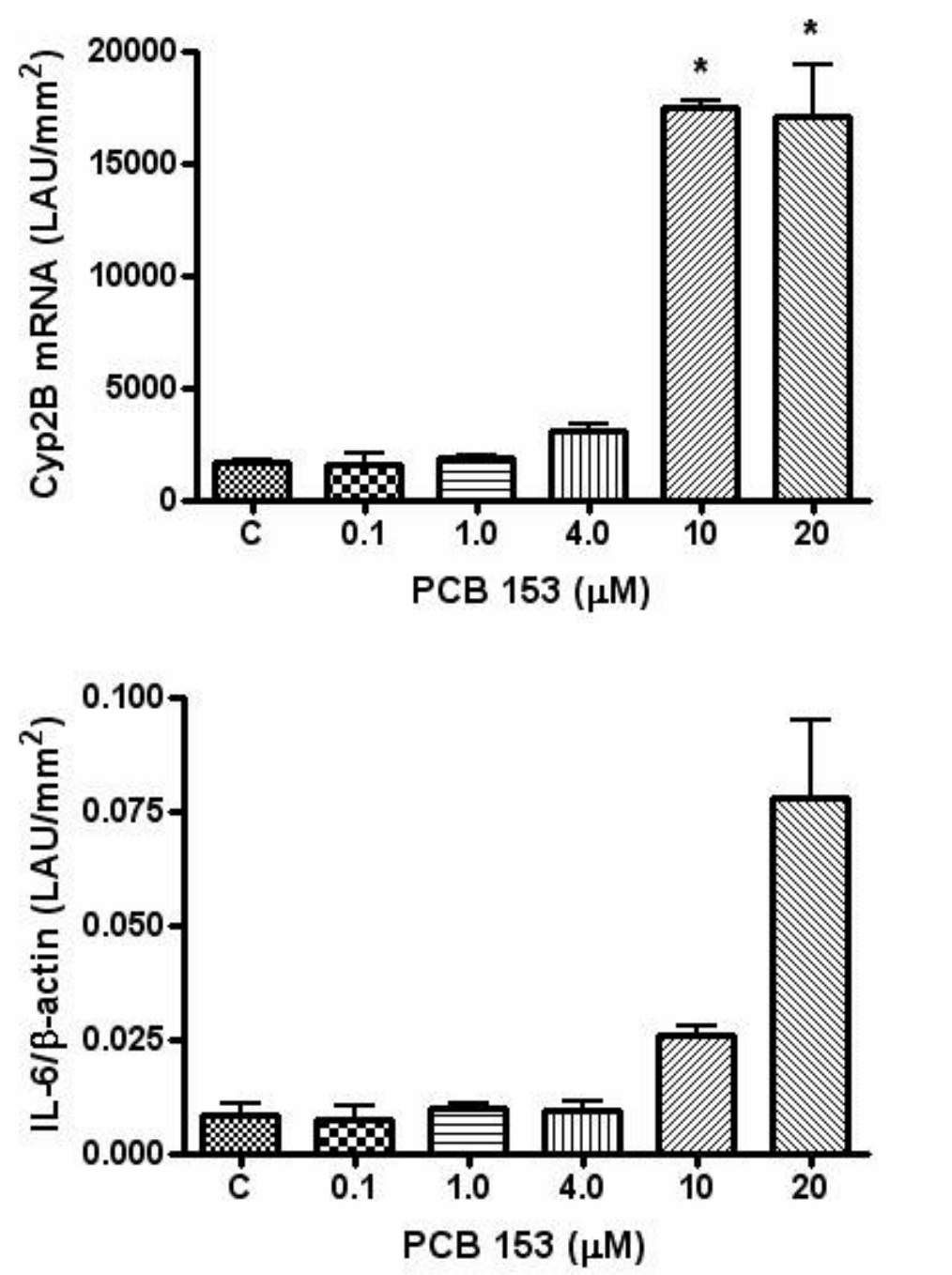

Figure II. PCB 153 increases CYP2B and IL-6 mRNA expression in EA human endothelial cells. EAhy926 endothelial cells were treated with PCB153 (0.1 – 20 μM) for 6 h. RNA was extracted and IL-6 and CYP2B gene expression was analyzed by RT-PCR.

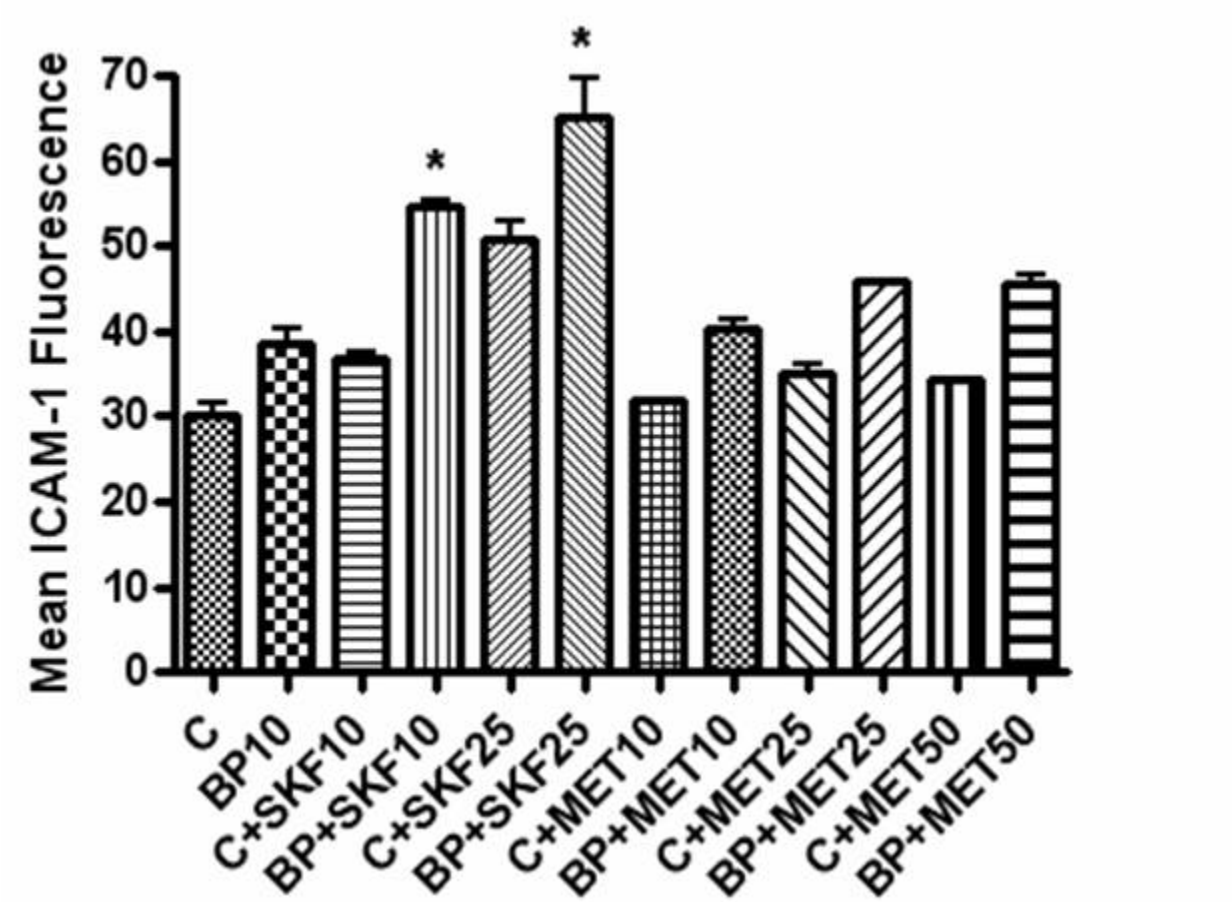

Figure III: Cytochrome P450 inhibitors increased ICAM-1-inducing effects of B[a]P. HUVEC were pre-treated with P450 inhibitors (SKF-525A, 10-25 µM; Metyrapone, 10-50 µM) for 30 m, then treated with DMSO (vehicle) or B[a]P (10 µM) for 24 h. ICAM-1 protein expression was measured by flow cytometry.

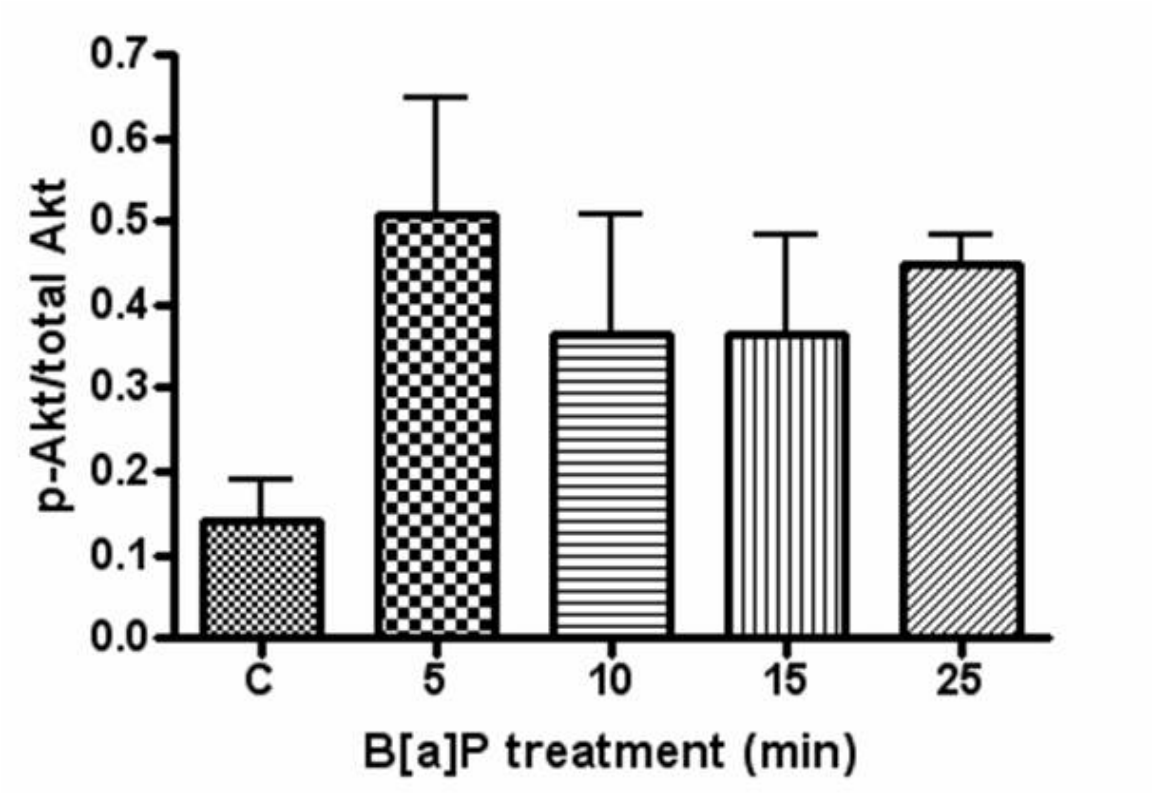

Figure IV. B[a]P pretreated with β -NF increase phosphorylation of Akt after 5 minutes. HUVEC were pre-treated with β –NF overnight, then treated with B[a]P (10 μM) for 5-25 m. Whole cell lysate was extracted and phosphorylated and total Akt was measured by immunoblot.

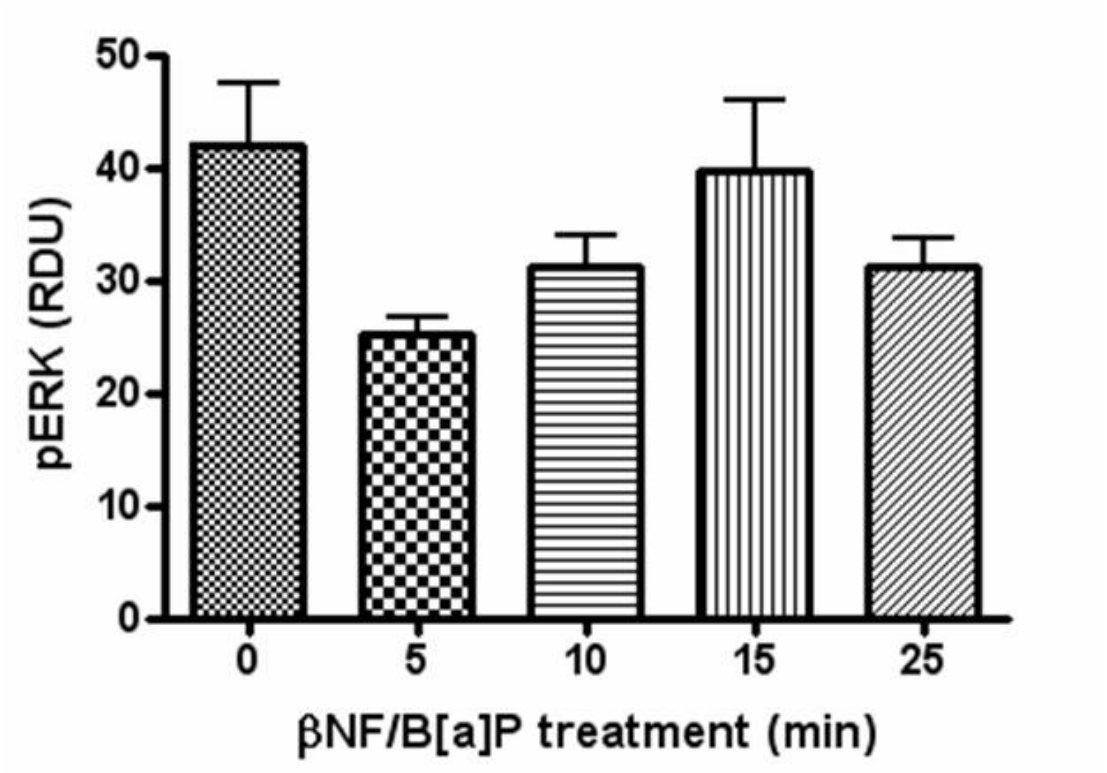

Figure V. B[a]P does not change phosphorylation of ERK after β-NF pretreatment. HUVEC were pre-treated with β –NF overnight, then treated with B[a]P (10 μM) for 5-25 m. Whole cell lysate was extracted and phosphorylated ERK was measured by immunoblot.

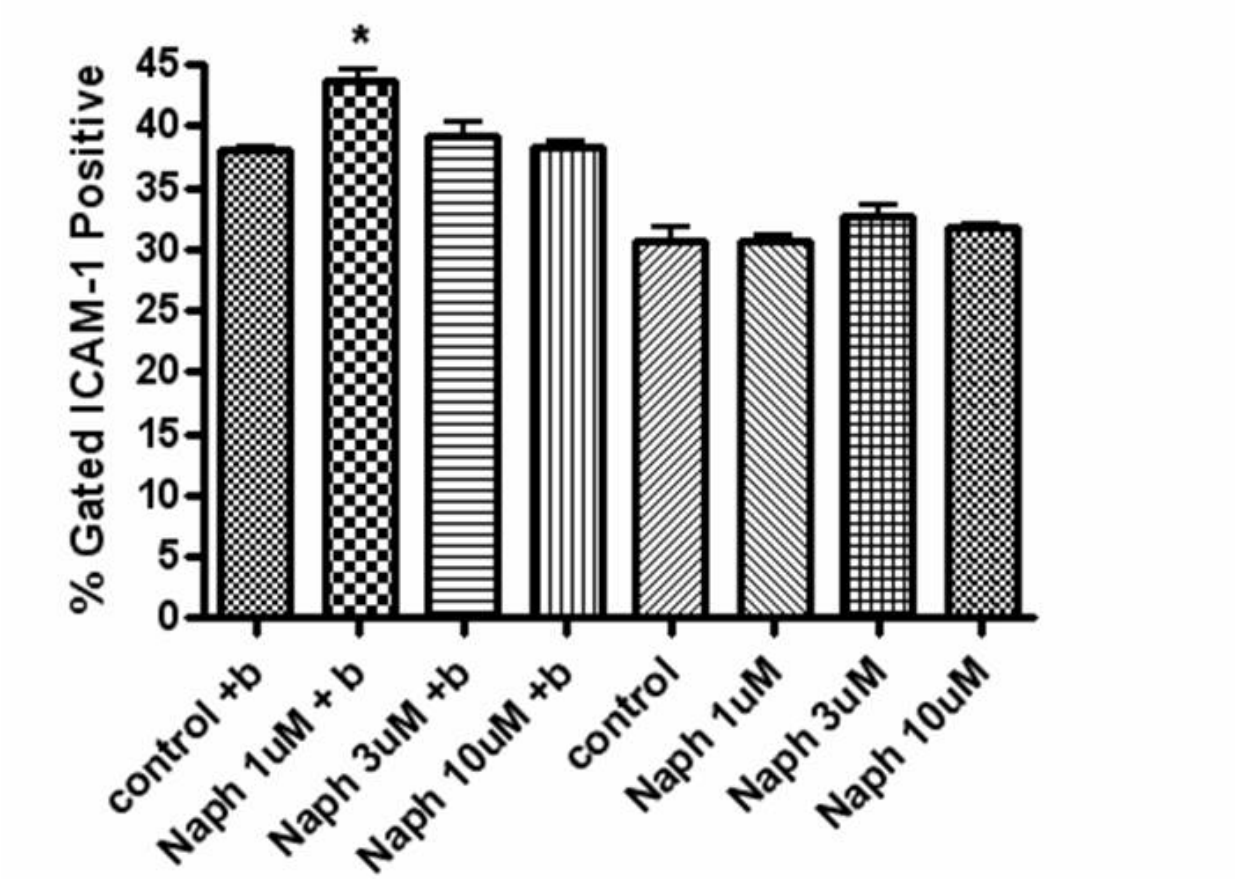

Figure VI. Naphthalene increases ICAM-1 slightly after pretreatment with β –NF. HUVEC were pre-treated with DMSO or β –NF overnight, and then treated with Naphthalene (1-10 μM) for 24 h. ICAM-1 protein expression was measured by flow cytometry.

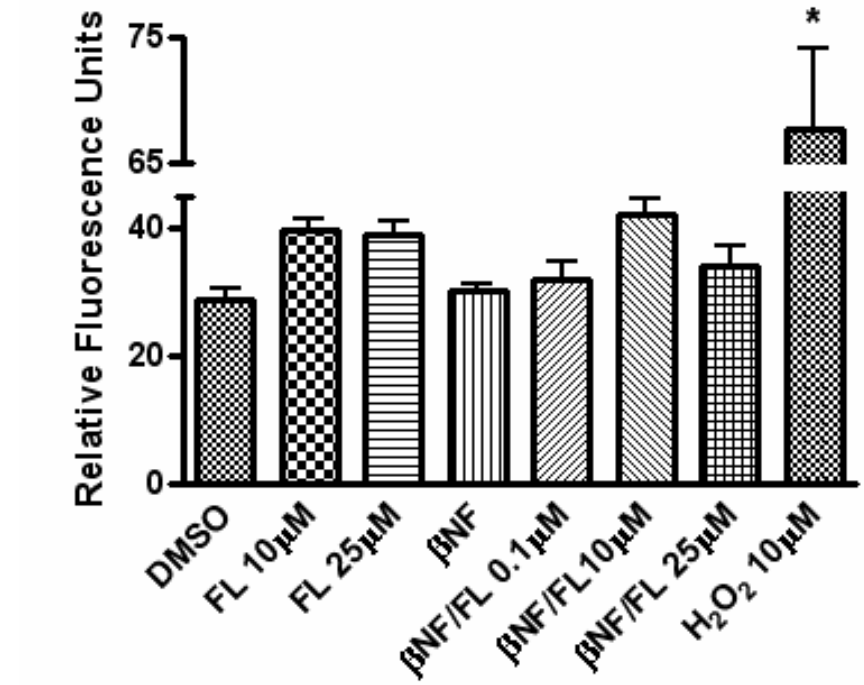
Relative Fluorescence Units
75
65
40
20
0
*
DMSO
FL 10μM
FL 25μM
βNF
βNF/FL 0.1μM
βNF/FL10μM
βNF/FL 25μM
H2O2 10μM

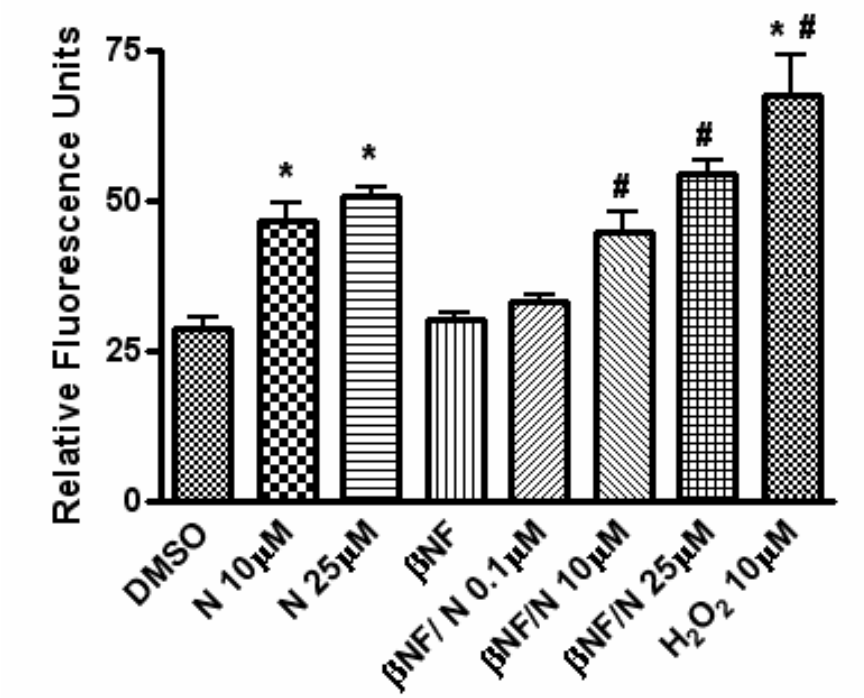
Relative Fluorescence Units
75
50
25
0
*
*
#
#
* #
DMSO
N 10μM
N 25μM
βNF
βNF/ N 0.1μM
βNF/N 10μM
βNF/N 25μM
H2O2 10μM

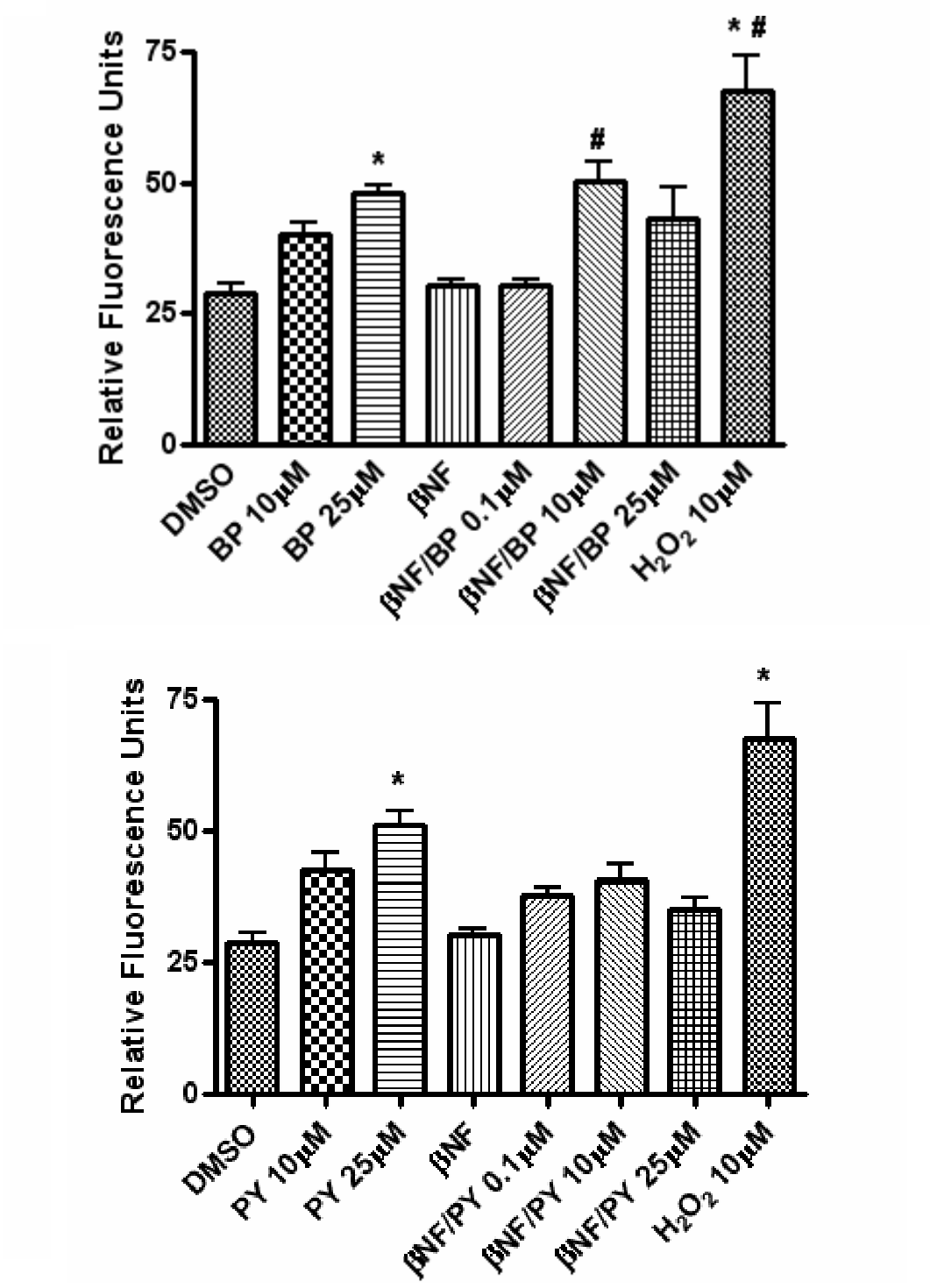

Figure VII. Oxidative Stress produced from PAH treatment. Porcine endothelial cells were pretreated with DMSO or β –NF overnight overnight, and then treated with B[a]P, Fluoranthene, Naphthalene, or Pyrene at 0.1-25 μM for 1 h. Oxidative stress was then measured by DCF fluorescence.

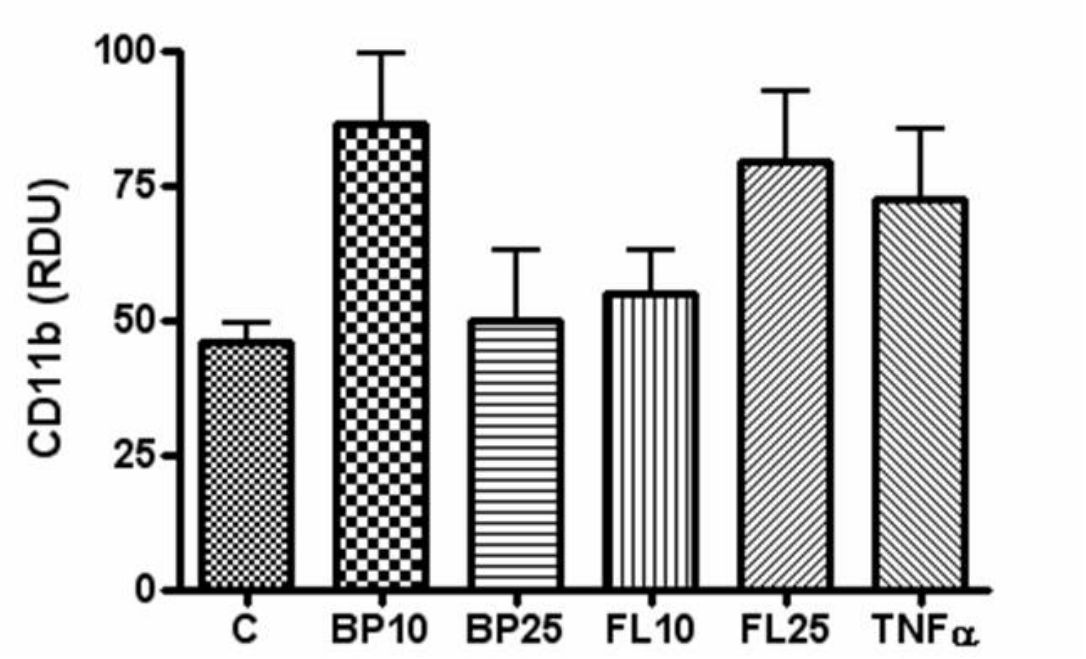

Figure VIII. B[a]P and Fluoranthene slightly increase CD11b in THP-1 monocytes. THP-1 monocytes were treated with TNF-α (1 µg/mL), B[a]P or FL (10-25 µM) for 24 h. Whole cell lysate was extracted and CD11b was measured by immunoblot.

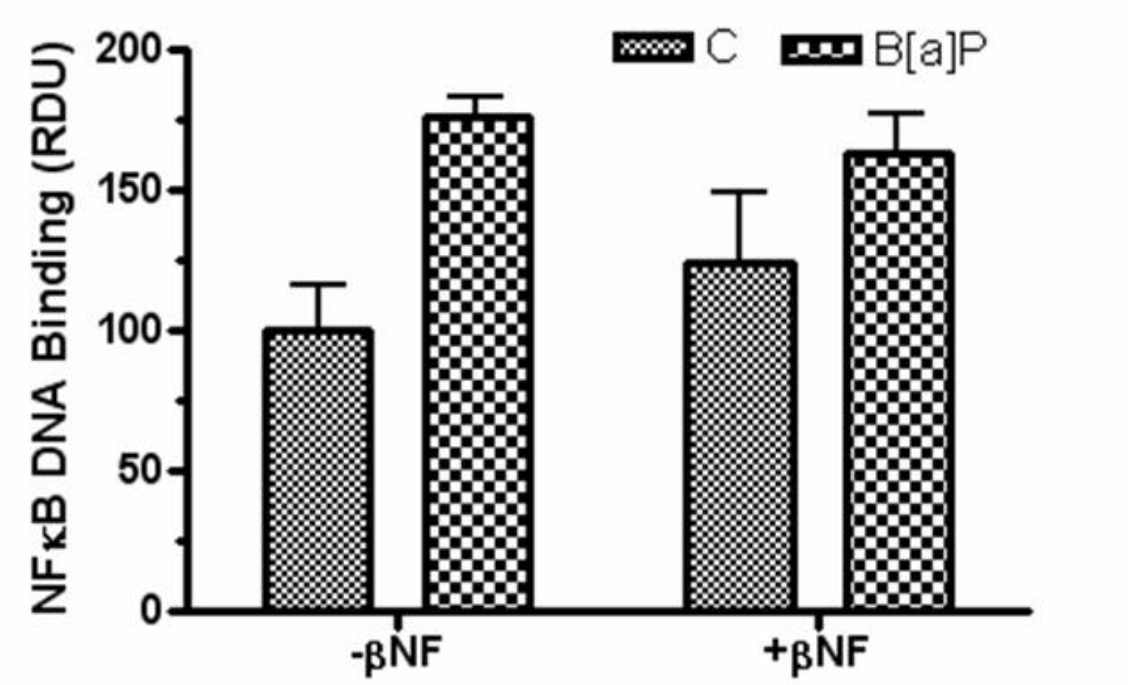

Figure IX. B[a]P pretreated with β –NF does not increase NF-κB more than B[a]P alone. HUVEC were pretreated with DMSO or β-NF for 16 h and then treated with DMSO or B[a]P (10 μM) for 4 h. Nuclear extracts were probed for NF-kB DNA binding by chemiluminescent EMSA.

References

1. Organization, W.H., *World Health Statistics 2008*. 2008, World Health Organization. p. 110.
2. Association, A.H., *Heart Disease and Stroke Statistics - 2005 Update*. 2005, American Heart Association: Dallas, Texas.
3. Pepine, C.J., *The effects of angiotensin-converting enzyme inhibition on endothelial dysfunction: potential role in myocardial ischemia.* Am J Cardiol, 1998. **82**(10A): p. 23S-27S.
4. Ross, R. and L. Harker, *Hyperlipidemia and atherosclerosis.* Science, 1976. **193**(4258): p. 1094-100.
5. Libby, P., *Inflammation in atherosclerosis.* Nature, 2002. **420**(6917): p. 868-74.
6. Mullenix, P.S., C.A. Andersen, and B.W. Starnes, *Atherosclerosis as inflammation.* Ann Vasc Surg, 2005. **19**(1): p. 130-8.
7. Glass, C.K. and J.L. Witztum, *Atherosclerosis. the road ahead.* Cell, 2001. **104**(4): p. 503-16.
8. Goligorsky, M.S., *Endothelial cell dysfunction: can't live with it, how to live without it.* Am J Physiol Renal Physiol, 2005. **288**(5): p. F871-80.
9. Rollins, B.J., et al., *Cytokine-activated human endothelial cells synthesize and secrete a monocyte chemoattractant, MCP-1/JE.* Am J Pathol, 1990. **136**(6): p. 1229-33.
10. Sica, A., et al., *Monocyte chemotactic and activating factor gene expression induced in endothelial cells by IL-1 and tumor necrosis factor.* J Immunol, 1990. **144**(8): p. 3034-8.
11. Yla-Herttuala, S., et al., *Expression of monocyte chemoattractant protein 1 in macrophage-rich areas of human and rabbit atherosclerotic lesions.* Proc Natl Acad Sci U S A, 1991. **88**(12): p. 5252-6.
12. Gosling, J., et al., *MCP-1 deficiency reduces susceptibility to atherosclerosis in mice that overexpress human apolipoprotein B.* J Clin Invest, 1999. **103**(6): p. 773-8.
13. Gu, L., et al., *Absence of monocyte chemoattractant protein-1 reduces atherosclerosis in low density lipoprotein receptor-deficient mice.* Mol Cell, 1998. **2**(2): p. 275-81.
14. Galkina, E. and K. Ley, *Vascular adhesion molecules in atherosclerosis.* Arterioscler Thromb Vasc Biol, 2007. **27**(11): p. 2292-301.
15. Leeuwenberg, J.F., G.M. Jeunhomme, and W.A. Buurman, *Adhesion of polymorphonuclear cells to human endothelial cells. Adhesion-molecule-dependent, and Fc receptor-mediated adhesion-molecule-independent mechanisms.* Clin Exp Immunol, 1990. **81**(3): p. 496-500.
16. Doukas, J. and J.S. Pober, *IFN-gamma enhances endothelial activation induced by tumor necrosis factor but not IL-1.* J Immunol, 1990. **145**(6): p. 1727-33.
17. Bevilacqua, M.P., et al., *Endothelial leukocyte adhesion molecule 1: an inducible receptor for neutrophils related to complement regulatory proteins and lectins.* Science, 1989. **243**(4895): p. 1160-5.
18. Davies, M.J., et al., *The expression of the adhesion molecules ICAM-1, VCAM-1, PECAM, and E-selectin in human atherosclerosis.* J Pathol, 1993. **171**(3): p. 223-9.
19. Dong, Z.M., et al., *The combined role of P- and E-selectins in atherosclerosis.* J Clin Invest, 1998. **102**(1): p. 145-52.
20. Wenzel, K., et al., *DNA polymorphisms in adhesion molecule genes--a new risk factor for early atherosclerosis.* Hum Genet, 1996. **97**(1): p. 15-20.
21. Nageh, M.F., et al., *Deficiency of inflammatory cell adhesion molecules protects against atherosclerosis in mice.* Arterioscler Thromb Vasc Biol, 1997. **17**(8): p. 1517-20.

22. Barringhaus, K.G., et al., *Alpha4beta1 integrin (VLA-4) blockade attenuates both early and late leukocyte recruitment and neointimal growth following carotid injury in apolipoprotein E (-/-) mice.* J Vasc Res, 2004. **41**(3): p. 252-60.
23. Patel, S.S., et al., *Inhibition of alpha4 integrin and ICAM-1 markedly attenuate macrophage homing to atherosclerotic plaques in ApoE-deficient mice.* Circulation, 1998. **97**(1): p. 75-81.
24. Diamond, M.S., et al., *ICAM-1 (CD54): a counter-receptor for Mac-1 (CD11b/CD18).* J Cell Biol, 1990. **111**(6 Pt 2): p. 3129-39.
25. Marlin, S.D. and T.A. Springer, *Purified intercellular adhesion molecule-1 (ICAM-1) is a ligand for lymphocyte function-associated antigen 1 (LFA-1).* Cell, 1987. **51**(5): p. 813-9.
26. Vonderheide, R.H. and T.A. Springer, *Lymphocyte adhesion through very late antigen 4: evidence for a novel binding site in the alternatively spliced domain of vascular cell adhesion molecule 1 and an additional alpha 4 integrin counter-receptor on stimulated endothelium.* J Exp Med, 1992. **175**(6): p. 1433-42.
27. Petruzzelli, L., M. Takami, and H.D. Humes, *Structure and function of cell adhesion molecules.* Am J Med, 1999. **106**(4): p. 467-76.
28. van de Stolpe, A. and P.T. van der Saag, *Intercellular adhesion molecule-1.* J Mol Med, 1996. **74**(1): p. 13-33.
29. Cybulsky, M.I. and M.A. Gimbrone, Jr., *Endothelial expression of a mononuclear leukocyte adhesion molecule during atherogenesis.* Science, 1991. **251**(4995): p. 788-91.
30. Cybulsky, M.I., et al., *A major role for VCAM-1, but not ICAM-1, in early atherosclerosis.* J Clin Invest, 2001. **107**(10): p. 1255-62.
31. Dansky, H.M., et al., *Adhesion of monocytes to arterial endothelium and initiation of atherosclerosis are critically dependent on vascular cell adhesion molecule-1 gene dosage.* Arterioscler Thromb Vasc Biol, 2001. **21**(10): p. 1662-7.
32. Huo, Y., A. Hafezi-Moghadam, and K. Ley, *Role of vascular cell adhesion molecule-1 and fibronectin connecting segment-1 in monocyte rolling and adhesion on early atherosclerotic lesions.* Circ Res, 2000. **87**(2): p. 153-9.
33. Feng, D., et al., *Neutrophils emigrate from venules by a transendothelial cell pathway in response to FMLP.* J Exp Med, 1998. **187**(6): p. 903-15.
34. Carman, C.V. and T.A. Springer, *A transmigratory cup in leukocyte diapedesis both through individual vascular endothelial cells and between them.* J Cell Biol, 2004. **167**(2): p. 377-88.
35. Millan, J., et al., *Lymphocyte transcellular migration occurs through recruitment of endothelial ICAM-1 to caveola- and F-actin-rich domains.* Nat Cell Biol, 2006. **8**(2): p. 113-23.
36. Butcher, E.C., *Leukocyte-endothelial cell recognition: three (or more) steps to specificity and diversity.* Cell, 1991. **67**(6): p. 1033-6.
37. Barreiro, O., et al., *Interactive protrusive structures during leukocyte adhesion and transendothelial migration.* Front Biosci, 2004. **9**: p. 1849-63.
38. Barreiro, O., et al., *Dynamic interaction of VCAM-1 and ICAM-1 with moesin and ezrin in a novel endothelial docking structure for adherent leukocytes.* J Cell Biol, 2002. **157**(7): p. 1233-45.
39. Shaw, S.K., et al., *Coordinated redistribution of leukocyte LFA-1 and endothelial cell ICAM-1 accompany neutrophil transmigration.* J Exp Med, 2004. **200**(12): p. 1571-80.
40. Hansson, G.K., *Immune mechanisms in atherosclerosis.* Arterioscler Thromb Vasc Biol, 2001. **21**(12): p. 1876-90.

41. Yamada, Y., et al., *Scavenger receptor family proteins: roles for atherosclerosis, host defence and disorders of the central nervous system.* Cell Mol Life Sci, 1998. **54**(7): p. 628-40.
42. Smith, J.D., et al., *Decreased atherosclerosis in mice deficient in both macrophage colony-stimulating factor (op) and apolipoprotein E.* Proc Natl Acad Sci U S A, 1995. **92**(18): p. 8264-8.
43. Suzuki, H., et al., *A role for macrophage scavenger receptors in atherosclerosis and susceptibility to infection.* Nature, 1997. **386**(6622): p. 292-6.
44. Febbraio, M., et al., *Targeted disruption of the class B scavenger receptor CD36 protects against atherosclerotic lesion development in mice.* J Clin Invest, 2000. **105**(8): p. 1049-56.
45. Frostegard, J., et al., *Platelet-activating factor and oxidized LDL induce immune activation by a common mechanism.* Arterioscler Thromb Vasc Biol, 1997. **17**(5): p. 963-8.
46. Brown, M.S., et al., *Reversible accumulation of cholesteryl esters in macrophages incubated with acetylated lipoproteins.* J Cell Biol, 1979. **82**(3): p. 597-613.
47. Gerrity, R.G., *The role of the monocyte in atherogenesis: I. Transition of blood-borne monocytes into foam cells in fatty lesions.* Am J Pathol, 1981. **103**(2): p. 181-90.
48. Gerrity, R.G. and H.K. Naito, *Ultrastructural identification of monocyte-derived foam cells in fatty streak lesions.* Artery, 1980. **8**(3): p. 208-14.
49. Ross, R. and J.A. Glomset, *Atherosclerosis and the arterial smooth muscle cell: Proliferation of smooth muscle is a key event in the genesis of the lesions of atherosclerosis.* Science, 1973. **180**(93): p. 1332-9.
50. Lee, R.T. and P. Libby, *The unstable atheroma.* Arterioscler Thromb Vasc Biol, 1997. **17**(10): p. 1859-67.
51. Organization, W.H., *WHO Air quality guidelines for particulate matter,ozone, nitrogen dioxide and sulfur dioxide - Global update 2005 - Summary of risk assessment*. 2005, World Health Organization. p. 22.
52. Pope, C.A., 3rd, *Air pollution and health - good news and bad.* N Engl J Med, 2004. **351**(11): p. 1132-4.
53. Pope, C.A., 3rd, et al., *Lung cancer, cardiopulmonary mortality, and long-term exposure to fine particulate air pollution.* Jama, 2002. **287**(9): p. 1132-41.
54. Pope, C.A., 3rd, et al., *Cardiovascular mortality and long-term exposure to particulate air pollution: epidemiological evidence of general pathophysiological pathways of disease.* Circulation, 2004. **109**(1): p. 71-7.
55. Pope, C.A., 3rd, et al., *Ischemic heart disease events triggered by short-term exposure to fine particulate air pollution.* Circulation, 2006. **114**(23): p. 2443-8.
56. Dockery, D.W., et al., *An association between air pollution and mortality in six U.S. cities.* N Engl J Med, 1993. **329**(24): p. 1753-9.
57. Daniels, M.J., et al., *Estimating particulate matter-mortality dose-response curves and threshold levels: an analysis of daily time-series for the 20 largest US cities.* Am J Epidemiol, 2000. **152**(5): p. 397-406.
58. Samet, J.M., et al., *Fine particulate air pollution and mortality in 20 U.S. cities, 1987-1994.* N Engl J Med, 2000. **343**(24): p. 1742-9.
59. Dockery, D.W., *Epidemiologic evidence of cardiovascular effects of particulate air pollution.* Environ Health Perspect, 2001. **109 Suppl 4**: p. 483-6.
60. Pope, C.A., 3rd, *Epidemiology of fine particulate air pollution and human health: biologic mechanisms and who's at risk?* Environ Health Perspect, 2000. **108 Suppl 4**: p. 713-23.

61. Dominici, F., et al., *Fine particulate air pollution and hospital admission for cardiovascular and respiratory diseases.* JAMA, 2006. **295**(10): p. 1127-34.
62. Koken, P.J., et al., *Temperature, air pollution, and hospitalization for cardiovascular diseases among elderly people in Denver.* Environ Health Perspect, 2003. **111**(10): p. 1312-7.
63. Schwartz, J., *Air pollution and hospital admissions for heart disease in eight U.S. counties.* Epidemiology, 1999. **10**(1): p. 17-22.
64. Krewski, D., et al., *Validation of the Harvard Six Cities Study of particulate air pollution and mortality.* N Engl J Med, 2004. **350**(2): p. 198-9.
65. Brook, R.D., et al., *Inhalation of fine particulate air pollution and ozone causes acute arterial vasoconstriction in healthy adults.* Circulation, 2002. **105**(13): p. 1534-6.
66. Peters, A., et al., *Particulate air pollution is associated with an acute phase response in men; results from the MONICA-Augsburg Study.* Eur Heart J, 2001. **22**(14): p. 1198-204.
67. Pope, C.A., 3rd, et al., *Ambient particulate air pollution, heart rate variability, and blood markers of inflammation in a panel of elderly subjects.* Environ Health Perspect, 2004. **112**(3): p. 339-45.
68. Riediker, M., et al., *Particulate matter exposure in cars is associated with cardiovascular effects in healthy young men.* Am J Respir Crit Care Med, 2004. **169**(8): p. 934-40.
69. Seaton, A., et al., *Particulate air pollution and the blood.* Thorax, 1999. **54**(11): p. 1027-32.
70. Salvi, S., et al., *Acute inflammatory responses in the airways and peripheral blood after short-term exposure to diesel exhaust in healthy human volunteers.* Am J Respir Crit Care Med, 1999. **159**(3): p. 702-9.
71. van Eeden, S.F., et al., *Cytokines involved in the systemic inflammatory response induced by exposure to particulate matter air pollutants (PM(10)).* Am J Respir Crit Care Med, 2001. **164**(5): p. 826-30.
72. Shi, J.P., et al., *Sources and concentration of nanoparticles (<10 nm diameter) in the urban atmosphere* Atmospheric Environment, 2001. **35**(7): p. 1193-1202.
73. Borm, P.J., et al., *The potential risks of nanomaterials: a review carried out for ECETOC.* Part Fibre Toxicol, 2006. **3**: p. 11.
74. Oberdorster, G., E. Oberdorster, and J. Oberdorster, *Nanotoxicology: an emerging discipline evolving from studies of ultrafine particles.* Environ Health Perspect, 2005. **113**(7): p. 823-39.
75. Kreyling, W.G., M. Semmler-Behnke, and W. Moller, *Ultrafine particle-lung interactions: does size matter?* J Aerosol Med, 2006. **19**(1): p. 74-83.
76. Nel, A., et al., *Toxic potential of materials at the nanolevel.* Science, 2006. **311**(5761): p. 622-7.
77. Maynard, A.D., *Nanotechnology: A Research Strategy for Addressing Risk*. 2006, Woodrow Wilson International Center for Scholars: Washington, DC.
78. Rittner, M.N., *Market analysis of nanostructured materials.* American Ceramic Society Bulletin, 2002. **81**: p. 33-36.
79. Thomas, K. and P. Sayre, *Research strategies for safety evaluation of nanomaterials, Part I: evaluating the human health implications of exposure to nanoscale materials.* Toxicol Sci, 2005. **87**(2): p. 316-21.
80. Maynard, A.D., *Nanotechnology: the next big thing, or much ado about nothing?* Ann Occup Hyg, 2007. **51**(1): p. 1-12.
81. Rodrigo, A., et al., *Alumina particles influence the interactions of cocultured osteoblasts and macrophages.* J Orthop Res, 2006. **24**(1): p. 46-54.

82. Yagil-Kelmer, E., et al., *Comparison of the response of primary human blood monocytes and the U937 human monocytic cell line to two different sizes of alumina ceramic particles.* J Orthop Res, 2004. **22**(4): p. 832-8.
83. Gojova, A., et al., *Induction of inflammation in vascular endothelial cells by metal oxide nanoparticles: effect of particle composition.* Environ Health Perspect, 2007. **115**(3): p. 403-9.
84. Nurkiewicz, T.R., et al., *Systemic microvascular dysfunction and inflammation after pulmonary particulate matter exposure.* Environ Health Perspect, 2006. **114**(3): p. 412-9.
85. Gerde, P., et al., *The rapid alveolar absorption of diesel soot-adsorbed benzo[a]pyrene: bioavailability, metabolism and dosimetry of an inhaled particle-borne carcinogen.* Carcinogenesis, 2001. **22**(5): p. 741-9.
86. Sun, J.D., et al., *Lung retention and metabolic fate of inhaled benzo(a)pyrene associated with diesel exhaust particles.* Toxicol Appl Pharmacol, 1984. **73**(1): p. 48-59.
87. Garry, S., et al., *Hematite (Fe2O3) acts by oxydative stress and potentiates benzo[a]pyrene genotoxicity.* Mutat Res, 2004. **563**(2): p. 117-29.
88. Henry, M.C., C.D. Port, and D.G. Kaufman, *Importance of physical properties of benzo(a)pyrene-ferric oxide mixtures in lung tumor induction.* Cancer Res, 1975. **35**(1): p. 207-17.
89. Bostrom, C.E., et al., *Cancer risk assessment, indicators, and guidelines for polycyclic aromatic hydrocarbons in the ambient air.* Environ Health Perspect, 2002. **110 Suppl 3**: p. 451-88.
90. Kamalakkannan, R., et al., *Chemical (polycyclic aromatic hydrocarbon and heavy metal) levels in contaminated stormwater and sediments from a motorway dry detention pond drainage system.* J Environ Monit, 2004. **6**(3): p. 175-81.
91. ATSDR, *Toxicological Profile for Polycyclic Aromatic Hydrocarbons (PAHs)*. 1995, Agency for Toxic Substances and Disease Registry, US Department of Health and Human Services. p. 487.
92. Izzotti, A., et al., *Cancer biomarkers in human atherosclerotic lesions: detection of DNA adducts.* Cancer Epidemiol Biomarkers Prev, 1995. **4**(2): p. 105-10.
93. Zhang, Y.J., et al., *Immunohistochemical detection of polycyclic aromatic hydrocarbon-DNA damage in human blood vessels of smokers and non-smokers.* Atherosclerosis, 1998. **140**(2): p. 325-31.
94. Miller, K.P. and K.S. Ramos, *Impact of cellular metabolism on the biological effects of benzo[a]pyrene and related hydrocarbons.* Drug Metab Rev, 2001. **33**(1): p. 1-35.
95. Ramos, K.S. and B. Moorthy, *Bioactivation of polycyclic aromatic hydrocarbon carcinogens within the vascular wall: implications for human atherogenesis.* Drug Metab Rev, 2005. **37**(4): p. 595-610.
96. Ramesh, A., et al., *Bioavailability and risk assessment of orally ingested polycyclic aromatic hydrocarbons.* Int J Toxicol, 2004. **23**(5): p. 301-33.
97. Penning, T.M., et al., *Dihydrodiol dehydrogenases and polycyclic aromatic hydrocarbon activation: generation of reactive and redox active o-quinones.* Chem Res Toxicol, 1999. **12**(1): p. 1-18.
98. Baird, W.M., L.A. Hooven, and B. Mahadevan, *Carcinogenic polycyclic aromatic hydrocarbon-DNA adducts and mechanism of action.* Environ Mol Mutagen, 2005. **45**(2-3): p. 106-14.
99. Pelkonen, O. and D.W. Nebert, *Metabolism of polycyclic aromatic hydrocarbons: etiologic role in carcinogenesis.* Pharmacol Rev, 1982. **34**(2): p. 189-222.

100. Otto, S., et al., *A novel adrenocorticotropin-inducible cytochrome P450 from rat adrenal microsomes catalyzes polycyclic aromatic hydrocarbon metabolism.* Endocrinology, 1991. **129**(2): p. 970-82.
101. Fujii-Kuriyama, Y. and J. Mimura, *Molecular mechanisms of AhR functions in the regulation of cytochrome P450 genes.* Biochem Biophys Res Commun, 2005. **338**(1): p. 311-7.
102. Korashy, H.M. and A.O. El-Kadi, *The role of aryl hydrocarbon receptor in the pathogenesis of cardiovascular diseases.* Drug Metab Rev, 2006. **38**(3): p. 411-50.
103. Hahn, M.E., *Aryl hydrocarbon receptors: diversity and evolution.* Chem Biol Interact, 2002. **141**(1-2): p. 131-60.
104. Heid, S.E., R.S. Pollenz, and H.I. Swanson, *Role of heat shock protein 90 dissociation in mediating agonist-induced activation of the aryl hydrocarbon receptor.* Mol Pharmacol, 2000. **57**(1): p. 82-92.
105. Kobayashi, A., K. Sogawa, and Y. Fujii-Kuriyama, *Cooperative interaction between AhR.Arnt and Sp1 for the drug-inducible expression of CYP1A1 gene.* J Biol Chem, 1996. **271**(21): p. 12310-6.
106. Kobayashi, A., et al., *CBP/p300 functions as a possible transcriptional coactivator of Ah receptor nuclear translocator (Arnt).* J Biochem, 1997. **122**(4): p. 703-10.
107. Dolwick, K.M., et al., *Cloning and expression of a human Ah receptor cDNA.* Mol Pharmacol, 1993. **44**(5): p. 911-7.
108. Mehrabi, M.R., et al., *The arylhydrocarbon receptor (AhR), but not the AhR-nuclear translocator (ARNT), is increased in hearts of patients with cardiomyopathy.* Virchows Arch, 2002. **441**(5): p. 481-9.
109. Stegeman, J.J., et al., *Induction of cytochrome P4501A1 by aryl hydrocarbon receptor agonists in porcine aorta endothelial cells in culture and cytochrome P4501A1 activity in intact cells.* Mol Pharmacol, 1995. **47**(2): p. 296-306.
110. Farin, F.M., T.H. Pohlman, and C.J. Omiecinski, *Expression of cytochrome P450s and microsomal epoxide hydrolase in primary cultures of human umbilical vein endothelial cells.* Toxicol Appl Pharmacol, 1994. **124**(1): p. 1-9.
111. Eskin, S.G., N.A. Turner, and L.V. McIntire, *Endothelial cell cytochrome P450 1A1 and 1B1: up-regulation by shear stress.* Endothelium, 2004. **11**(1): p. 1-10.
112. Thirman, M.J., et al., *Induction of cytochrome CYPIA1 and formation of toxic metabolites of benzo[a]pyrene by rat aorta: a possible role in atherogenesis.* Proc Natl Acad Sci U S A, 1994. **91**(12): p. 5397-401.
113. Theriault, G.P., C.G. Tremblay, and B.G. Armstrong, *Risk of ischemic heart disease among primary aluminum production workers.* Am J Ind Med, 1988. **13**(6): p. 659-66.
114. Gustavsson, P., A. Gustavsson, and C. Hogstedt, *Excess mortality among Swedish chimney sweeps.* Br J Ind Med, 1987. **44**(11): p. 738-43.
115. Hansen, E.S., *Mortality from cancer and ischemic heart disease in Danish chimney sweeps: a five-year follow-up.* Am J Epidemiol, 1983. **117**(2): p. 160-4.
116. Gustavsson, P., *Mortality among workers at a municipal waste incinerator.* Am J Ind Med, 1989. **15**(3): p. 245-53.
117. Erdogmus, B., et al., *Intima-media thickness of the common carotid artery in highway toll collectors.* J Clin Ultrasound, 2006. **34**(9): p. 430-3.
118. Maclaren, W.M. and J.F. Hurley, *Mortality of tar distillation workers.* Scand J Work Environ Health, 1987. **13**(5): p. 404-11.
119. Burstyn, I., et al., *Polycyclic aromatic hydrocarbons and fatal ischemic heart disease.* Epidemiology, 2005. **16**(6): p. 744-50.

120. Albert, R.E., et al., *Effect of carcinogens on chicken atherosclerosis.* Cancer Res, 1977. **37**(7 Pt 1): p. 2232-5.
121. Hough, J.L., et al., *Benzo(a)pyrene enhances atherosclerosis in White Carneau and Show Racer pigeons.* Arterioscler Thromb, 1993. **13**(12): p. 1721-7.
122. Curfs, D.M., et al., *Chronic exposure to the carcinogenic compound benzo[a]pyrene induces larger and phenotypically different atherosclerotic plaques in ApoE-knockout mice.* Am J Pathol, 2004. **164**(1): p. 101-8.
123. Curfs, D.M., et al., *Polycyclic aromatic hydrocarbons induce an inflammatory atherosclerotic plaque phenotype irrespective of their DNA binding properties.* Faseb J, 2005. **19**(10): p. 1290-2.
124. Knaapen, A.M., et al., *The environmental carcinogen benzo[a]pyrene induces expression of monocyte-chemoattractant protein-1 in vascular tissue: a possible role in atherogenesis.* Mutat Res, 2007. **621**(1-2): p. 31-41.
125. Gowdy, K., et al., *Modulation of pulmonary inflammatory responses and antimicrobial defenses in mice exposed to diesel exhaust.* Toxicol Appl Pharmacol, 2008.
126. Kalra, V.K., et al., *Mechanism of cigarette smoke condensate induced adhesion of human monocytes to cultured endothelial cells.* J Cell Physiol, 1994. **160**(1): p. 154-62.
127. O'Neill, M.S., et al., *Air pollution and inflammation in type 2 diabetes: a mechanism for susceptibility.* Occup Environ Med, 2007. **64**(6): p. 373-9.
128. Shen, Y., et al., *Cigarette smoke condensate-induced adhesion molecule expression and transendothelial migration of monocytes.* Am J Physiol, 1996. **270**(5 Pt 2): p. H1624-33.
129. Yatera, K., et al., *Particulate matter air pollution exposure promotes recruitment of monocytes into atherosclerotic plaques.* Am J Physiol Heart Circ Physiol, 2008. **294**(2): p. H944-53.
130. Torres, M. and H.J. Forman, *Redox signaling and the MAP kinase pathways.* Biofactors, 2003. **17**(1-4): p. 287-96.
131. Hoefen, R.J. and B.C. Berk, *The role of MAP kinases in endothelial activation.* Vascul Pharmacol, 2002. **38**(5): p. 271-3.
132. Ip, W.K., et al., *Interleukin-3, -5, and granulocyte macrophage colony-stimulating factor induce adhesion and chemotaxis of human eosinophils via p38 mitogen-activated protein kinase and nuclear factor kappaB.* Immunopharmacol Immunotoxicol, 2005. **27**(3): p. 371-93.
133. Yan, W., et al., *Role of p38 MAPK in ICAM-1 expression of vascular endothelial cells induced by lipopolysaccharide.* Shock, 2002. **17**(5): p. 433-8.
134. Chen, S., et al., *The role of the Ah receptor and p38 in benzo[a]pyrene-7,8-dihydrodiol and benzo[a]pyrene-7,8-dihydrodiol-9,10-epoxide-induced apoptosis.* J Biol Chem, 2003. **278**(21): p. 19526-33.
135. Mukherjee, J.J. and H.C. Sikka, *Attenuation of BPDE-induced p53 accumulation by TPA is associated with a decrease in stability and phosphorylation of p53 and downregulation of NFkappaB activation: role of p38 MAP kinase.* Carcinogenesis, 2006. **27**(3): p. 631-8.
136. Ouyang, W., et al., *Benzo[a]pyrene diol-epoxide (B[a]PDE) upregulates COX-2 expression through MAPKs/AP-1 and IKKbeta/NF-kappaB in mouse epidermal Cl41 cells.* Mol Carcinog, 2007. **46**(1): p. 32-41.
137. Yan, Z., et al., *Benzo[a]pyrene induces the transcription of cyclooxygenase-2 in vascular smooth muscle cells. Evidence for the involvement of extracellular signal-regulated kinase and NF-kappaB.* J Biol Chem, 2000. **275**(7): p. 4949-55.
138. Stade, B.G., et al., *Structural characteristics of the 5' region of the human ICAM-1 gene.* Immunobiology, 1990. **182**(1): p. 79-87.

139. Voraberger, G., R. Schafer, and C. Stratowa, *Cloning of the human gene for intercellular adhesion molecule 1 and analysis of its 5'-regulatory region. Induction by cytokines and phorbol ester.* J Immunol, 1991. **147**(8): p. 2777-86.
140. Pulverer, B.J., et al., *Phosphorylation of c-jun mediated by MAP kinases.* Nature, 1991. **353**(6345): p. 670-4.
141. Huang, C., et al., *Inhibition of benzo(a)pyrene diol-epoxide-induced transactivation of activated protein 1 and nuclear factor kappaB by black raspberry extracts.* Cancer Res, 2002. **62**(23): p. 6857-63.
142. Siddiqui, S.S., et al., *p38 MAPK activation coupled to endocytosis is a determinant of endothelial monolayer integrity.* Am J Physiol Lung Cell Mol Physiol, 2007. **292**(1): p. L114-24.
143. Wang, X.M., et al., *Caveolin-1: a critical regulator of lung fibrosis in idiopathic pulmonary fibrosis.* J Exp Med, 2006. **203**(13): p. 2895-906.
144. Zeidan, A., et al., *Leptin-induced cardiomyocyte hypertrophy involves selective caveolae and RhoA/ROCK-dependent p38 MAPK translocation to nuclei.* Cardiovasc Res, 2008. **77**(1): p. 64-72.
145. Lisanti, M.P., et al., *Characterization of caveolin-rich membrane domains isolated from an endothelial-rich source: implications for human disease.* J Cell Biol, 1994. **126**(1): p. 111-26.
146. Rothberg, K.G., et al., *Caveolin, a protein component of caveolae membrane coats.* Cell, 1992. **68**(4): p. 673-82.
147. Frank, P.G., et al., *Caveolin, caveolae, and endothelial cell function.* Arterioscler Thromb Vasc Biol, 2003. **23**(7): p. 1161-8.
148. Razani, B., S.E. Woodman, and M.P. Lisanti, *Caveolae: from cell biology to animal physiology.* Pharmacol Rev, 2002. **54**(3): p. 431-67.
149. Glenney, J.R., Jr., *Tyrosine phosphorylation of a 22-kDa protein is correlated with transformation by Rous sarcoma virus.* J Biol Chem, 1989. **264**(34): p. 20163-6.
150. Sargiacomo, M., et al., *Oligomeric structure of caveolin: implications for caveolae membrane organization.* Proc Natl Acad Sci U S A, 1995. **92**(20): p. 9407-11.
151. Frank, P.G., et al., *Genetic ablation of caveolin-1 confers protection against atherosclerosis.* Arterioscler Thromb Vasc Biol, 2004. **24**(1): p. 98-105.
152. Kim, M.J., J. Dawes, and W. Jessup, *Transendothelial transport of modified low-density lipoproteins.* Atherosclerosis, 1994. **108**(1): p. 5-17.
153. Frank, P.G., et al., *Stabilization of caveolin-1 by cellular cholesterol and scavenger receptor class B type I.* Biochemistry, 2002. **41**(39): p. 11931-40.
154. Bouzin, C., et al., *Effects of vascular endothelial growth factor on the lymphocyte-endothelium interactions: identification of caveolin-1 and nitric oxide as control points of endothelial cell anergy.* J Immunol, 2007. **178**(3): p. 1505-11.
155. Amos, C., et al., *Cross-linking of brain endothelial intercellular adhesion molecule (ICAM)-1 induces association of ICAM-1 with detergent-insoluble cytoskeletal fraction.* Arterioscler Thromb Vasc Biol, 2001. **21**(5): p. 810-6.
156. Tilghman, R.W. and R.L. Hoover, *E-selectin and ICAM-1 are incorporated into detergent-insoluble membrane domains following clustering in endothelial cells.* FEBS Lett, 2002. **525**(1-3): p. 83-7.
157. Dauchet, L., et al., *Fruit and vegetable consumption and risk of coronary heart disease: a meta-analysis of cohort studies.* J Nutr, 2006. **136**(10): p. 2588-93.
158. Rahman, I., S.K. Biswas, and P.A. Kirkham, *Regulation of inflammation and redox signaling by dietary polyphenols.* Biochem Pharmacol, 2006. **72**(11): p. 1439-52.

159. Ross, J.A. and C.M. Kasum, *Dietary flavonoids: bioavailability, metabolic effects, and safety.* Annu Rev Nutr, 2002. **22**: p. 19-34.
160. Hertog, M.G., et al., *Dietary antioxidant flavonoids and risk of coronary heart disease: the Zutphen Elderly Study.* Lancet, 1993. **342**(8878): p. 1007-11.
161. Hertog, M.G., et al., *Flavonoid intake and long-term risk of coronary heart disease and cancer in the seven countries study.* Arch Intern Med, 1995. **155**(4): p. 381-6.
162. Knekt, P., et al., *Flavonoid intake and coronary mortality in Finland: a cohort study.* BMJ, 1996. **312**(7029): p. 478-81.
163. Yochum, L., et al., *Dietary flavonoid intake and risk of cardiovascular disease in postmenopausal women.* Am J Epidemiol, 1999. **149**(10): p. 943-9.
164. Rimm, E.B., et al., *Relation between intake of flavonoids and risk for coronary heart disease in male health professionals.* Ann Intern Med, 1996. **125**(5): p. 384-9.
165. Hertog, M.G., E.J. Feskens, and D. Kromhout, *Antioxidant flavonols and coronary heart disease risk.* Lancet, 1997. **349**(9053): p. 699.
166. Manach, C., A. Mazur, and A. Scalbert, *Polyphenols and prevention of cardiovascular diseases.* Curr Opin Lipidol, 2005. **16**(1): p. 77-84.
167. Miura, Y., et al., *Tea catechins prevent the development of atherosclerosis in apoprotein E-deficient mice.* J Nutr, 2001. **131**(1): p. 27-32.
168. Waddington, E., I.B. Puddey, and K.D. Croft, *Red wine polyphenolic compounds inhibit atherosclerosis in apolipoprotein E-deficient mice independently of effects on lipid peroxidation.* Am J Clin Nutr, 2004. **79**(1): p. 54-61.
169. Arai, Y., et al., *Dietary intakes of flavonols, flavones and isoflavones by Japanese women and the inverse correlation between quercetin intake and plasma LDL cholesterol concentration.* J Nutr, 2000. **130**(9): p. 2243-50.
170. Jeong, Y.J., et al., *Differential inhibition of oxidized LDL-induced apoptosis in human endothelial cells treated with different flavonoids.* Br J Nutr, 2005. **93**(5): p. 581-91.
171. Kim, H.K., et al., *Lipid-lowering efficacy of hesperetin metabolites in high-cholesterol fed rats.* Clin Chim Acta, 2003. **327**(1-2): p. 129-37.
172. Lotito, S.B. and B. Frei, *Dietary flavonoids attenuate tumor necrosis factor alpha-induced adhesion molecule expression in human aortic endothelial cells. Structure-function relationships and activity after first pass metabolism.* J Biol Chem, 2006. **281**(48): p. 37102-10.
173. Lien, E.J., et al., *Quantitative structure-activity relationship analysis of phenolic antioxidants.* Free Radic Biol Med, 1999. **26**(3-4): p. 285-94.
174. Mira, L., et al., *Interactions of flavonoids with iron and copper ions: a mechanism for their antioxidant activity.* Free Radic Res, 2002. **36**(11): p. 1199-208.
175. Masella, R., et al., *Novel mechanisms of natural antioxidant compounds in biological systems: involvement of glutathione and glutathione-related enzymes.* J Nutr Biochem, 2005. **16**(10): p. 577-86.
176. Zhang, K. and N.P. Das, *Inhibitory effects of plant polyphenols on rat liver glutathione S-transferases.* Biochem Pharmacol, 1994. **47**(11): p. 2063-8.
177. Carluccio, M.A., et al., *Olive oil and red wine antioxidant polyphenols inhibit endothelial activation: antiatherogenic properties of Mediterranean diet phytochemicals.* Arterioscler Thromb Vasc Biol, 2003. **23**(4): p. 622-9.
178. Kim, J.D., et al., *Chemical structure of flavonols in relation to modulation of angiogenesis and immune-endothelial cell adhesion.* J Nutr Biochem, 2006. **17**(3): p. 165-76.

179. Koga, T. and M. Meydani, *Effect of plasma metabolites of (+)-catechin and quercetin on monocyte adhesion to human aortic endothelial cells.* Am J Clin Nutr, 2001. **73**(5): p. 941-8.
180. Gerritsen, M.E., et al., *Flavonoids inhibit cytokine-induced endothelial cell adhesion protein gene expression.* Am J Pathol, 1995. **147**(2): p. 278-92.
181. Chen, Z.H., et al., *Resveratrol inhibits TCDD-induced expression of CYP1A1 and CYP1B1 and catechol estrogen-mediated oxidative DNA damage in cultured human mammary epithelial cells.* Carcinogenesis, 2004. **25**(10): p. 2005-13.
182. Tsuji, P.A. and T. Walle, *Inhibition of benzo[a]pyrene-activating enzymes and DNA binding in human bronchial epithelial BEAS-2B cells by methoxylated flavonoids.* Carcinogenesis, 2006. **27**(8): p. 1579-85.
183. Puppala, D., C.G. Gairola, and H.I. Swanson, *Identification of kaempferol as an inhibitor of cigarette smoke-induced activation of the aryl hydrocarbon receptor and cell transformation.* Carcinogenesis, 2007. **28**(3): p. 639-47.
184. Gasiewicz, T.A., et al., *Analysis of structural requirements for Ah receptor antagonist activity: ellipticines, flavones, and related compounds.* Biochem Pharmacol, 1996. **52**(11): p. 1787-803.
185. Zhang, S., C. Qin, and S.H. Safe, *Flavonoids as aryl hydrocarbon receptor agonists/antagonists: effects of structure and cell context.* Environ Health Perspect, 2003. **111**(16): p. 1877-82.
186. Shimada, A., et al., *Translocation pathway of the intratracheally instilled ultrafine particles from the lung into the blood circulation in the mouse.* Toxicol Pathol, 2006. **34**(7): p. 949-57.
187. Nemmar, A., et al., *Passage of inhaled particles into the blood circulation in humans.* Circulation, 2002. **105**(4): p. 411-4.
188. Artelt, S., et al., *Bioavailability of fine dispersed platinum as emitted from automotive catalytic converters: a model study.* Sci Total Environ, 1999. **228**(2-3): p. 219-42.
189. Takenaka, S., et al., *Pulmonary and systemic distribution of inhaled ultrafine silver particles in rats.* Environ Health Perspect, 2001. **109 Suppl 4**: p. 547-51.
190. Nabel, E.G., *Biology of the impaired endothelium.* Am J Cardiol, 1991. **68**(12): p. 6C-8C.
191. Glass, C. and J. Witztum, *Atherosclerosis: The Road Ahead.* Cell, 2001. **104**(4): p. 503-516.
192. Collins, R.G., et al., *P-Selectin or intercellular adhesion molecule (ICAM)-1 deficiency substantially protects against atherosclerosis in apolipoprotein E-deficient mice.* J Exp Med, 2000. **191**(1): p. 189-94.
193. Hahn, A.F., *Intravenous immunoglobulin treatment in peripheral nerve disorders--indications, mechanisms of action and side-effects.* Curr Opin Neurol, 2000. **13**(5): p. 575-82.
194. Xie, L., et al., *Studies on the biomechanical properties of maturing reticulocytes.* J Biomech, 2006. **39**(3): p. 530-5.
195. Toborek, M., et al., *Measurement of inflammatory properties of fatty acids in human endothelial cells.* Methods Enzymol, 2002. **352**: p. 198-219.
196. Lanki, T., et al., *Associations of traffic related air pollutants with hospitalisation for first acute myocardial infarction: the HEAPSS study.* Occup Environ Med, 2006. **63**(12): p. 844-51.
197. Wichmann, H.E., et al., *Daily mortality and fine and ultrafine particles in Erfurt, Germany part I: role of particle number and particle mass.* Res Rep Health Eff Inst, 2000(98): p. 5-86; discussion 87-94.

198. Ibald-Mulli, A., et al., *Epidemiological evidence on health effects of ultrafine particles.* J Aerosol Med, 2002. **15**(2): p. 189-201.
199. Peters, A. and C.A. Pope, 3rd, *Cardiopulmonary mortality and air pollution.* Lancet, 2002. **360**(9341): p. 1184-5.
200. van Eeden, S.F., et al., *Systemic response to ambient particulate matter: relevance to chronic obstructive pulmonary disease.* Proc Am Thorac Soc, 2005. **2**(1): p. 61-7.
201. Hansen, C.S., et al., *Diesel exhaust particles induce endothelial dysfunction in apoE-/- mice.* Toxicol Appl Pharmacol, 2007. **219**(1): p. 24-32.
202. Xia, T., et al., *Comparison of the abilities of ambient and manufactured nanoparticles to induce cellular toxicity according to an oxidative stress paradigm.* Nano Lett, 2006. **6**(8): p. 1794-807.
203. Schubert, D., et al., *Cerium and yttrium oxide nanoparticles are neuroprotective.* Biochem Biophys Res Commun, 2006. **342**(1): p. 86-91.
204. Iademarco, M.F., et al., *Characterization of the promoter for vascular cell adhesion molecule-1 (VCAM-1).* J Biol Chem, 1992. **267**(23): p. 16323-9.
205. Schindler, U. and V.R. Baichwal, *Three NF-kappa B binding sites in the human E-selectin gene required for maximal tumor necrosis factor alpha-induced expression.* Mol Cell Biol, 1994. **14**(9): p. 5820-31.
206. Pierce, J.W., et al., *Novel inhibitors of cytokine-induced IkappaBalpha phosphorylation and endothelial cell adhesion molecule expression show anti-inflammatory effects in vivo.* J Biol Chem, 1997. **272**(34): p. 21096-103.
207. Neish, A.S., et al., *Sp1 is a component of the cytokine-inducible enhancer in the promoter of vascular cell adhesion molecule-1.* J Biol Chem, 1995. **270**(48): p. 28903-9.
208. Zhang, W.J. and B. Frei, *Intracellular metal ion chelators inhibit TNFalpha-induced SP-1 activation and adhesion molecule expression in human aortic endothelial cells.* Free Radic Biol Med, 2003. **34**(6): p. 674-82.
209. Verna, L., C. Ganda, and M.B. Stemerman, *In vivo low-density lipoprotein exposure induces intercellular adhesion molecule-1 and vascular cell adhesion molecule-1 correlated with activator protein-1 expression.* Arterioscler Thromb Vasc Biol, 2006. **26**(6): p. 1344-9.
210. Neish, A.S., et al., *Endothelial interferon regulatory factor 1 cooperates with NF-kappa B as a transcriptional activator of vascular cell adhesion molecule 1.* Mol Cell Biol, 1995. **15**(5): p. 2558-69.
211. Dagia, N.M., et al., *Phenyl methimazole inhibits TNF-alpha-induced VCAM-1 expression in an IFN regulatory factor-1-dependent manner and reduces monocytic cell adhesion to endothelial cells.* J Immunol, 2004. **173**(3): p. 2041-9.
212. Yamawaki, H. and N. Iwai, *Mechanisms underlying nano-sized air-pollution-mediated progression of atherosclerosis: carbon black causes cytotoxic injury/inflammation and inhibits cell growth in vascular endothelial cells.* Circ J, 2006. **70**(1): p. 129-40.
213. Wagner, A.J., et al., *Cellular interaction of different forms of aluminum nanoparticles in rat aveolar macrophages. .* J. Phys. Chem. B. , 2007. **111**: p. 7353-7359.
214. Liu, J. and J.I. Shapiro, *Endocytosis and signal transduction: basic science update.* Biol Res Nurs, 2003. **5**(2): p. 117-28.
215. Maynard, A.D. (2007) *Is Engineered Nanomaterial Exposure a Myth?* . www.safenano.org **Volume**,
216. Blackwell, J.E., et al., *Ligand coated nanosphere adhesion to E- and P-selectin under static and flow conditions.* Ann Biomed Eng, 2001. **29**(6): p. 523-33.

217. Nemmar, A., et al., *Passage of intratracheally instilled ultrafine particles from the lung into the systemic circulation in hamster.* Am J Respir Crit Care Med, 2001. **164**(9): p. 1665-8.
218. Oberdorster, G., et al., *Extrapulmonary translocation of ultrafine carbon particles following whole-body inhalation exposure of rats.* J Toxicol Environ Health A, 2002. **65**(20): p. 1531-43.
219. Geiser, M., et al., *Ultrafine particles cross cellular membranes by nonphagocytic mechanisms in lungs and in cultured cells.* Environ Health Perspect, 2005. **113**(11): p. 1555-60.
220. Auchincloss, A.H., et al., *Associations between Recent Exposure to Ambient Fine Particulate Matter and Blood Pressure in the Multi-Ethnic Study of Atherosclerosis (MESA).* Environ Health Perspect, 2008. **116**(4): p. 486-91.
221. Weintraub, W.S., *Cigarette smoking as a risk factor for coronary artery disease.* Adv Exp Med Biol, 1990. **273**: p. 27-37.
222. Davis, H.J., *Gas chromatographic determination of benzo(a)pyrene in cigarette smoke.* Anal Chem, 1968. **40**(10): p. 1583-5.
223. Liu, L.B., et al., *Determination of particle-associated polycyclic aromatic hydrocarbons in urban air of Beijing by GC/MS.* Anal Sci, 2007. **23**(6): p. 667-71.
224. Vincent, R., et al., *Acute pulmonary toxicity of urban particulate matter and ozone.* Am J Pathol, 1997. **151**(6): p. 1563-70.
225. Annas, A., A.L. Granberg, and E.B. Brittebo, *Differential response of cultured human umbilical vein and artery endothelial cells to Ah receptor agonist treatment: CYP-dependent activation of food and environmental mutagens.* Toxicol Appl Pharmacol, 2000. **169**(1): p. 94-101.
226. Merchant, M., V. Krishnan, and S. Safe, *Mechanism of action of alpha-naphthoflavone as an Ah receptor antagonist in MCF-7 human breast cancer cells.* Toxicol Appl Pharmacol, 1993. **120**(2): p. 179-85.
227. Cho, K.A., et al., *Senescent phenotype can be reversed by reduction of caveolin status.* J Biol Chem, 2003. **278**(30): p. 27789-95.
228. N'Diaye, M., et al., *Aryl hydrocarbon receptor- and calcium-dependent induction of the chemokine CCL1 by the environmental contaminant benzo[a]pyrene.* J Biol Chem, 2006. **281**(29): p. 19906-15.
229. Shimada, T., et al., *Arylhydrocarbon receptor-dependent induction of liver and lung cytochromes P450 1A1, 1A2, and 1B1 by polycyclic aromatic hydrocarbons and polychlorinated biphenyls in genetically engineered C57BL/6J mice.* Carcinogenesis, 2002. **23**(7): p. 1199-207.
230. Willett, K.L., et al., *In vivo and in vitro inhibition of CYP1A-dependent activity in Fundulus heteroclitus by the polynuclear aromatic hydrocarbon fluoranthene.* Toxicol Appl Pharmacol, 2001. **177**(3): p. 264-71.
231. Elbekai, R.H., et al., *Benzo[a]pyrene, 3-methylcholanthrene and beta-naphthoflavone induce oxidative stress in hepatoma hepa 1c1c7 Cells by an AHR-dependent pathway.* Free Radic Res, 2004. **38**(11): p. 1191-200.
232. Wassenberg, D.M. and R.T. Di Giulio, *Synergistic embryotoxicity of polycyclic aromatic hydrocarbon aryl hydrocarbon receptor agonists with cytochrome P4501A inhibitors in Fundulus heteroclitus.* Environ Health Perspect, 2004. **112**(17): p. 1658-64.
233. Wassenberg, D.M. and R.T. Di Giulio, *Teratogenesis in Fundulus heteroclitus embryos exposed to a creosote-contaminated sediment extract and CYP1A inhibitors.* Mar Environ Res, 2004. **58**(2-5): p. 163-8.

234. Gao, F., et al., *p38 MAPK inhibition reduces myocardial reperfusion injury via inhibition of endothelial adhesion molecule expression and blockade of PMN accumulation.* Cardiovasc Res, 2002. **53**(2): p. 414-22.
235. Tamura, D.Y., et al., *p38 mitogen-activated protein kinase inhibition attenuates intercellular adhesion molecule-1 up-regulation on human pulmonary microvascular endothelial cells.* Surgery, 1998. **124**(2): p. 403-7; discussion 408.
236. Patten Hitt, E., M.J. DeLong, and A.H. Merrill, Jr., *Benzo(a)pyrene activates extracellular signal-related and p38 mitogen-activated protein kinases in HT29 colon adenocarcinoma cells: involvement in NAD(P)H:quinone reductase activity and cell proliferation.* Toxicol Appl Pharmacol, 2002. **183**(3): p. 160-7.
237. Birkenkamp, K.U., et al., *The p38 MAP kinase inhibitor SB203580 enhances nuclear factor-kappa B transcriptional activity by a non-specific effect upon the ERK pathway.* Br J Pharmacol, 2000. **131**(1): p. 99-107.
238. Shibazaki, M., et al., *Suppression by p38 MAP kinase inhibitors (pyridinyl imidazole compounds) of Ah receptor target gene activation by 2,3,7,8-tetrachlorodibenzo-p-dioxin and the possible mechanism.* J Biol Chem, 2004. **279**(5): p. 3869-76.
239. Shibazaki, M., et al., *Blockade by SB203580 of Cyp1a1 induction by 2,3,7,8-tetrachlorodibenzo-p-dioxin, and the possible mechanism: possible involvement of the p38 mitogen-activated protein kinase pathway in shuttling of Ah receptor overexpressed in COS-7 cells.* Ann N Y Acad Sci, 2004. **1030**: p. 275-81.
240. Yang, L., et al., *Endothelial cell cortactin coordinates intercellular adhesion molecule-1 clustering and actin cytoskeleton remodeling during polymorphonuclear leukocyte adhesion and transmigration.* J Immunol, 2006. **177**(9): p. 6440-9.
241. Hennig, B., et al., *Modification of environmental toxicity by nutrients: implications in atherosclerosis.* Cardiovasc Toxicol, 2005. **5**(2): p. 153-60.
242. Manach, C., et al., *Polyphenols: food sources and bioavailability.* Am J Clin Nutr, 2004. **79**(5): p. 727-47.
243. Benzie, I.F. and J.J. Strain, *The ferric reducing ability of plasma (FRAP) as a measure of "antioxidant power": the FRAP assay.* Anal Biochem, 1996. **239**(1): p. 70-6.
244. Kris-Etherton, P.M., et al., *Bioactive compounds in nutrition and health-research methodologies for establishing biological function: the antioxidant and anti-inflammatory effects of flavonoids on atherosclerosis.* Annu Rev Nutr, 2004. **24**: p. 511-38.
245. Manach, C., et al., *Bioavailability and bioefficacy of polyphenols in humans. I. Review of 97 bioavailability studies.* Am J Clin Nutr, 2005. **81**(1 Suppl): p. 230S-242S.
246. Tan, Z., et al., *Activation of mitogen-activated protein kinases (MAPKs) by aromatic hydrocarbons: role in the regulation of aryl hydrocarbon receptor (AHR) function.* Biochem Pharmacol, 2002. **64**(5-6): p. 771-80.
247. Hollman, P.C., et al., *Absorption of dietary quercetin glycosides and quercetin in healthy ileostomy volunteers.* Am J Clin Nutr, 1995. **62**(6): p. 1276-82.
248. Hollman, P.C., et al., *Bioavailability of the dietary antioxidant flavonol quercetin in man.* Cancer Lett, 1997. **114**(1-2): p. 139-40.
249. Li, J., et al., *Alumina-Pepsin Hybrid Nanoparticles with Orientation-Specific Enzyme Coupling.* Nano Letters, 2003. **3**: p. 55-58.
250. Bauer, I.W., et al., *Internalization of hydroxyapatite nanoparticles in liver cancer cells.* J Mater Sci Mater Med, 2008. **19**(3): p. 1091-5.

251. Qaddoumi, M.G., et al., *Clathrin and caveolin-1 expression in primary pigmented rabbit conjunctival epithelial cells: role in PLGA nanoparticle endocytosis.* Mol Vis, 2003. **9**: p. 559-68.
252. Harush-Frenkel, O., et al., *Surface charge of nanoparticles determines their endocytic and transcytotic pathway in polarized MDCK cells.* Biomacromolecules, 2008. **9**(2): p. 435-43.

Vita

ELIZABETH OESTERLING

Birthplace: Williamsburg, Virginia, USA
May 6, 1981

EDUCATION

B.S. Cell Biology/Biochemistry, Bucknell University, Lewisburg, Pennsylvania, May 2003

PROFESSIONAL BACKGROUND AND EXPERIENCE

9/01 – 5/03	Bucknell University: Teaching Assistant for Introduction to Molecules and Cells Laboratory Major Professor: Professor Karin Knisely
9/00 – 5/03	Bucknell University: Environmental Toxicology and Chemistry Research Assistant Major Professor: Dr. Alison Draper
5/01- 9/01	Community outreach and environmental lobbying research for Clean Water Action Supervisor: Pamela Irvine
5/99- 9/00	Virginia Institute of Marine Science: Aquaculture Genetics and Breeding Technology Center Summer Aide Major Professor: Dr. Stan Allen
6/98- 8/98	Virginia Institute of Marine Science: Organic Chemistry Laboratory FIRST (Female Initiation into Research Science and Technology) Funded by NSF. Major Professors: Dr. Elizabeth Canuel and Dr. Rebecca Dickhut
10/96-5/98	Virginia Institute of Marine Science, College of William and Mary: Environmental Chemistry Laboratory Major Professor: Dr. Rob Hale

GRANTS AND FUNDING

7/06-7/08	Awarded American Heart Association Pre-doctoral Fellowship, 2 years at $21,000: “Polycyclic Aromatic Hydrocarbon-Mediated STAT Signaling: Implications in Vascular Inflammation” (0615216B)
7/03-7/06	Ruth L. Kirschstein National Research Service Award and Training Grant Recipient (ES-07266)

AWARDS AND HONORS

4/08	Poster Award at 2008 Toxicology and Risk Assessment Conference in Cincinnati, OH
3/08	Burroughs Welcome Fund Travel Award to 2008 Society of Toxicology Meeting in Seattle, WA
12/07	Poster Award at 20th Annual Superfund Basic Research Program Meeting in Durham, NC
4/07	Poster Award at 2007 Toxicology and Risk Assessment Conference in Cincinnati, OH
3/07	UK Graduate School Travel Award to 2007 Society of Toxicology Meeting
10/06	Poster Award at 2006 Central and Eastern European Conference on Health and Environment (CEECHE) in Bratislava, Slovak Republic

10/06	Session Co-chair for Student Priority Session on Risk Assessment and Remediation at 2006 Central and Eastern European Conference on Environment and Health in Bratislava, Slovak Republic
10/06	Travel Award Recipient to CEECHE 2006 to Bratislava, Slovak Republic
4/06	UK Graduate School Travel Award to 2006 EPA Science Forum
10/04	Poster Award at 2004 Central and Eastern European Environmental Health Conference: Health Sciences Solving Common International Problems in Prague, Czech Republic
10/04	UK Graduate School Travel Award to 2004 CEEHC
05/02-09/02	Katherine Mabis McKenna Summer Environmental Internship Program Awardee, Bucknell University, Major Professor: Dr. Alison Draper

PROFESSIONAL ACTIVITIES

2008	Attended Workshop at Toxicology and Risk Assessment Conference in Cincinnati, OH entitled: "Toxicogenomics in Risk Assessment"
2008	Attended Workshop at 2008 SOT Meeting in Seattle, WA entitled: "Introduction to Pathology for Toxicologists and Study Directors"
2007	Invited and hosted UK Graduate Center for Toxicology Seminar Speaker and Lecturer Dr. John Lipscomb, US EPA, "Application of Quantitative Toxicokinetic Data in Chemical Risk Assessment"
2007	Attended Workshops at Toxicology and Risk Assessment Conference in Cincinnati, OH entitled: "Intermediate Topics in Health Risk Assessment of Chemical Mixtures" and "Epidemiologic Fundamentals for Risk Assessment Applications"
2007	Environmental Science Judge for Regional Public School Science Fair
2007	Certified in Hazardous Waste Operations and Emergency Response (HAZWOPER) standard training by Environmental Response Training Program, U.S. EPA
2006 – Present	Internal Advisory Board Member for UK Superfund Basic Research Program
2005 – 2006	President of Toxicology Student Forum, Graduate Center for Toxicology, UK
2004 – 2005	VP of Toxicology Student Forum, Graduate Center for Toxicology, UK

PUBLICATIONS

Elizabeth Oesterling, Michal Toborek, Bernhard Hennig. (Submitted) Benzo[a]pyrene induces intercellular adhesion molecule-1 in an aryl hydrocarbon receptor and caveolae dependent manner via MEK/p38/AP-1 pathway in human vascular endothelial cells. **Toxicology and Applied Pharmacology**

Elizabeth Oesterling, Michal Toborek, Bernhard Hennig, (Submitted) Flavonoids protect against intercellular adhesion molecule-1 induction by benzo[a]pyrene. **Bulletins of Environmental Contamination and Toxicology**

Huiyun Shen, Elizabeth Oesterling, Arnold Stromberg, Michal Toborek, Ruth MacDonald, Bernhard Hennig. (In Press) Zinc deficiency induces vascular pro-inflammatory parameters associated with NF-κB and PPAR signaling. **Journal of American College of Nutrition.**

Elizabeth Oesterling, Nitin Chopra, Vasileios Gavalas, Xabier Arzuaga, Eun Jin Lim, Rukhsana Sultana, D. Allan Butterfield, Leonidas Bachas, Bernhard Hennig. Alumina nanoparticles induce expression of endothelial cell adhesion molecules. (2008) **Toxicology Letters**: 178(3): 160-166.

Hong Lu, Debra L. Rateri, David L. Feldman, Richard J. Charnigo Jr., Akiyoshi Fukamizu, Junji Ishida, Elizabeth G. Oesterling, Lisa A. Cassis, Alan Daugherty. Renin inhibition reduces hypercholesterolemia-induced atherosclerosis. (2008) **Journal of Clinical Investigation**: 118(3): 989-993.

Zuzana Majkova, Elizabeth Oesterling, Michal Toborek, Bernhard Hennig. Impact of nutrition on PCB toxicity. (2008) **Environmental Toxicology and Pharmacology**: 25(2): 192-196.

Bernhard Hennig, Elizabeth Oesterling, Michal Toborek. Environmental toxicity, nutrition, and gene interactions in the development of atherosclerosis. (2007) **Nutrition, Metabolism & Cardiovascular Diseases**: 17: 162-129.

Bernhard Hennig, Gudrun Reiterer, Zuzana Majkova, Elizabeth Oesterling, Purushothaman Meerarani, Michal Toborek. Modification of Environmental Toxicity by Nutrients: Implications in Atherosclerosis. (2005) **Cardiovascular Toxicology**: 5(2): 153-160.

PRESENTATIONS

E. Oesterling, N. Chopra, V. Gavalas, X. Arzuaga, E.J. Lim, L. Bachas, B. Hennig, 'Nanoparticle Induced Inflammation of Vascular Endothelial Cells', 2008 Toxicology and Risk Assessment Conference, Cincinnati, OH, April 14-17, 2008.

E. Oesterling, M. Toborek, B. Hennig, 'Benzo[a]pyrene-Induced Vascular Endothelial Adhesion Molecule Expression Can Be Reduced By Selective Flavonoid Treatment', 47th Annual Society of Toxicology Meeting, Seattle, WA, United States, March 16-20, 2008.

E. Oesterling, M. Toborek, B. Hennig, 'Benzo[a]pyrene-Induced Vascular Endothelial Adhesion Molecule Expression Can Be Reduced By Selective Flavonoid Treatment', 20th Annual Superfund Basic Research Program Meeting, Durham, NC, United States, December 3-5, 2007.

E. Oesterling, B. Hennig, 'University of Kentucky Superfund Basic Research Program Overview', 2007 Kentucky Research Consortium for Energy and the Environment Scientific and Technical Symposium, Lexington, KY, October 30-31, 2007.

E. Oesterling, M. Toborek, B. Hennig, 'Benzo[a]pyrene-Induced Vascular Endothelial Adhesion Molecule Expression Can Be Disrupted By Selective Flavonoid Treatment', 10th Annual Linda and Jack Gill Heart Institute Cardiovascular Research Day, Lexington, KY, United States, October 19, 2007.

E. Oesterling, N. Chopra, V. Gavalas, X. Arzuaga, E.J. Lim, L. Bachas, B. Hennig, 'Nanoparticle Induced Inflammation of Vascular Endothelial Cells', 16th International Symposium on Microencapsulation in Lexington, KY, September 9-12, 2007.

E. Oesterling, M. Toborek, B. Hennig, 'Benzo[a]pyrene-Induced Vascular Endothelial Adhesion Molecule Expression Can Be Disrupted By Flavonoid Treatment: Implications in Cardiovascular Disease', 2007 Toxicology and Risk Assessment Conference, Cincinnati, OH, April 23-26, 2007.

E. Oesterling, X. Arzuaga, E.J. Lim, V. Gavalas, L. Bachas, M. Toborek, B. Hennig 'Manufactured Nano-Sized Alumina Particles Induce Endothelial Cell Dysfunction: Implications in Vascular Disease', 46th Annual Society of Toxicology Meeting in Charlotte, NC, March 25-29, 2007.

E. Oesterling, X. Arzuaga, E.J. Lim, V. Gavalas, L. Bachas, M. Toborek, B. Hennig 'Manufactured Nano-Sized Alumina Particles Induce Endothelial Cell Dysfunction: Implications in Vascular Disease', 2006 Superfund Basic Research Program Annual Meeting, La Jolla, CA, December, 2006.

E. Oesterling, X. Arzuaga, Z. Majkova, E.J. Lim, G. Reiterer, M. Toborek, B. Hennig, 'PCB-Induced Endothelial Cell Dysfunction: Implications in Atherosclerosis', 2nd Central and Eastern

European Conference on Environment and Health, Bratislava, Slovak Republic, October 22-25, 2006.

E. Oesterling, X. Arzuaga, E.J. Lim, M. Toborek, B. Hennig, 'Manufactured Nano-sized Alumina Particles Induce Endothelial Cell Dysfunction: Implications in Vascular Disease', 2006 Linda and Jack Gill Heart Institute Cardiovascular Research Day, Lexington, KY, October, 2006.

B. Hennig, X. Arzuaga, Z. Majkova, E.J. Lim, E. Oesterling, E. Smart, M. Toborek, 'Endothelial Cell Dysfunction: Environmental Contaminants and Nutritional Implications', XIV International Symposium on Atherosclerosis, Rome, Italy, June, 2006.

E. Oesterling, X. Arzuaga, G. Reiterer, M. Toborek, and B. Hennig, 'Persistent Organic Pollutants and Endothelial Cell Dysfunction: Implications in Vascular Disease', 2006 UK Clinical and Translational Science Meeting, Lexington, KY, June 2006.

E. Oesterling, X. Arzuaga, Z. Majkova, G. Reiterer, M. Toborek, B. Hennig, 'Persistent Organic Pollutants and Endothelial Cell Dysfunction: Implications in Vascular Disease', 2006 EPA Science Forum, Washington, DC, May 2006.

E. Oesterling, Z. Majkova, G. Reiterer, H. Guo, M. Toborek, B. Hennig, 'PCB-mediated inflammatory signaling: implications in atherosclerosis', 2004 Central and Eastern European Environmental Health Conference: Health Sciences Solving Common International Problems in Prague, Czech Republic, October 2004.

L. Wang, E. Oesterling, G. Reiterer, M. Toborek, B. Hennig, 'Nutrient-Mediated Protection of PCB Toxicity in Endothelial Cells', 2004 PCB Workshop, University of Illinois, Champaign, IL, June 2004.

PROFESSIONAL SOCIETIES

2007-Present Society of Toxicology
- Women in Toxicology